ISTANBUL TECHNICAL UNIVERSITY ★ GRADUATE SCHOOL OF SCIENCE ENGINEERING AND TECHNOLOGY

GEOLOGICAL, GEOCHEMICAL INVESTIGATION AND SUBSURFACE MODELING OF PORPHYRY COPPER-MOLYBDENUM DEPOSIT IN TEPEOBA-HAVRAN,BALIKESIR (NW TURKEY)

M.Sc. THESIS

Torkan TAHERI BONAB

Department of Geology Engineering

Applied Geology Programme

JUNE 2013

ISTANBUL TECHNICAL UNIVERSITY ★ GRADUATE SCHOOL OF SCIENCE ENGINEERING AND TECHNOLOGY

GEOLOGICAL, GEOCHEMICAL INVESTIGATION AND SUBSURFACE MODELING OF PORPHYRY COPPER-MOLYBDENUM DEPOSIT IN TEPEOBA-HAVRAN,BALIKESIR (NW TURKEY)

M.Sc. THESIS

Torkan TAHERI BONAB
505111321

Department of Geology Engineering

Applied Geology Programme

Thesis Advisor: Doç. Dr. Mustafa KUMRAL

JUNE 2013

İSTANBUL TEKNİK ÜNİVERSİTESİ ★ FEN BİLİMLERİ ENSTİTÜSÜ

TEPEOBA-HAVRAN, BALIKESİR İN PORFİR BAKIR-MOLİBDEN YATAĞININ JEOLOJİ, JEOKİMYA VE YERALTI MODELLEME İNCELENMESİ

YÜKSEK LİSANS TEZİ

Torkan TAHERI BONAB
505111321

Anabilim Dalı : JEOLOJİ MÜHENDİSLİĞİ

Programı : UYGULAMALI JEOLOJİ

Tez Danışmanı: Prof. Dr. Mustafa KURAL

HAZİRAN 2013

Torkan TAHERI BONAB, a **M.Sc.** student of ITU **Gratuade school of science and engineering and technology** student ID 505111321, successfully defended the **thesis** entitled "**GEOLOGICAL, GEOCHEMICAL INVESTIGATION AND SUBSURFACE MODELING OF PORPHYRY COPPER-MOLYBDENUM DEPOSIT IN TEPEOBA-HAVRAN,BALIKESIR (NW TURKEY)**", which she prepared after fulfilling the requirements specified in the associated legislations, before the jury whose signatures are below.

Thesis Advisor :	**Doç. Dr. Mustafa KUMRAL** İstanbul Technical University	....
Jury Members :	**Doç.Dr. Mustafa KUMRAL** İstanbul Teknik Üniversitesi	....
	Doç.Dr. Emin Çiftçi İstanbul Teknik Üniversitesi	....
	Yrd.Doç.Dr. Mustafa Selman Aydoğan Balıkesir Üniversitesi	....

Date of Submission : 2 May 2013
Date of Defense : 4 June 2013

To my Family and my Husband,

FOREWORD

First of all, I am grateful to the God for establishing me to completed this thesis.
I wish to express my sincere thanks to my advisor, Doç.Dr. Mustafa KUMRAL. I thank him for presenting me with an amazing research opportunity in Turkey, and for your constant guidance and support. I would also like to thank to geochemisty research group at ITU and my co-thesis researcher Ayse Kubra AKAY.
I should also thank to Mr. Hosein YASROBI Manager of Company P.O.Rahvar Consulting Engineers and Dr.Ebrahim ASGHARI and Mr.Mehdi ZARGHANI from department of rahvar Company in IRAN-Tehran and my special thanks to Mahsa SAFAEE from ITU architecture faculty, all of your help and kind words are greatly appreciated.
Most importantly, I should thank my family and friends. Thank you to my mother, her spirit shines in every moment of my life and my brother who have always believed in my dreams no matter how big or small. I also place on record, my sense of gratitude to my father, his courage, wisdom and passion inspires me to be a better person every day, and one and all who directly, have lent his helping hand in this venture.
I also extend my heartfelt thanks to my husband Tohid and his family, who has always been there for me and I ‘m very thankful for his practical and emotional support as I added the roles of wife, to competing demands of business, study, work and personal development.
I am truly blessed to share life with all of you.

JUNE 2013 Torkan TAHERIBONAB
(Geology Engineer)

TABLE OF CONTENTS

Page

ABBREVIATIONS

N : North
S : South
E : East
W : West
Cm3 : Centimeter Cubic
Km : Kilometer
Km^2 : Square kilometer
XRF : X-ray fluorescence
ppm : Parts per million (10^6)
ppb : Part per bilion
Py : Pyrite
Cp : Calcopyrite
Qtz : Quartz
Cal : Calcite
Bt : Biotit
Amp : Amphibolite
Ms : Muscovite
Spn : Sphene
Opq : Opaque
Plg : Plagioclase
Ser : Sericite
Ep : Epidote
Afs : Alkalifeldspar
Fsp : Feldspar
Mol : Molybdenite
Au : Gold
Cu : Copper
Zn : Zinc
Ag : Silver
Pb : Lead
TAS : Total Alkali Silica
Wt% : Weight percent

LIST OF TABLES

LIST OF FIGURES

Page

INVESTIGATION OF GEOLOGY, GEOCHEMİSTRY AND SUBSURFACE MODELING OF PORPHYRY COPPER-MOLYBDENUM DEPOSIT IN TEPEOBA-HAVRAN,BALIKESİR

SUMMARY

The Biga Peninsula contains a very rich zone in terms of metallic ores. There are many known sulphur mineralizations (bornite, pyrit, chalcopyrite, molybdenite, etc.) which are observed in the study area. Currently discovered Tepeoba is the largest porphyry Cu–Mo–Au deposit with known resources in the Biga Peninsula. Porphyry deposits are the world's highly significant source of Cu and Mo, and also the source for Au, Ag, and Sn; significant byproduct metals include Re, W, In, Pt, Pd, and Se.

Study area approximately located in 10 km to the north of the town of Havran in the Balikesir Province is examined in detail. The pre-Jurassic basis of the field consists one of the tectono-stratigraphic units that were juxtaposed during the late Triassic: the pre-Karakaya units including Torasan Formation, the sub-group of Kalabak Formation and metasedimentary and metabasite rocks which form Early-Triassic Karakaya Complex. The composition of Eybak Granite and Granodiorite and acidic and basic rock veins have been aged as Tertiary era. At the study area, Eybak Granotoid has imposed contact metamorphism to meta-sedimentary and metabasite rocks and turned them to andalusite- biotite schist.

This study indicated the low-to medium grade Cu-Mo deposits and purpose of this study was to identify the amounts of copper, molybdenum and Gold, with data of geochemical analysis for each borehole samples and applied them to rockworks software for modeling underground potential zones between different layers in depth to simplify the research and increase the rate of probable economical reserves of deposit for the future exploitation.

Aslo several analysis done on granite samples was prepared beside subsurface modeling like XRF for detecting major elements and mineralogical study about each formation to better understand geology and the structural of those formations on investigation area. Major element compositions of pre-mineralization, mineralized, and post mineralization rocks have been determined for many individual porphyry copper deposits and districts. The results of TAS diagram shows us copper molybdenum deposit are mostly granite, and also shows the range between monzonite and quartz monzonite and siyenite. The result of Harker diagram that all major elements against Sio_2 display patterns consistent with fractional crystallization common in granites. Mineralogical results represent the main lithologic units start with basic volcanics, greywacke, sandstone, and lenticular limestones and contain different-sized Permo Carboniferous limestone blocks in the interior part. The oldest tectonic unit that consist: calc schist, phyllite and existance of marble between this units, represents Torasan formation is subgroup of kalabak unit. At the top of this unit, marble lenses, spilite and metatuffites took place in metabasic member represents lower karakaya complex. Metasedimentar rocks represents the upper karakaya complex that consising Arkosic metasandstone, phyllites and schist, meta conglomerates, sandstone. Both metasedimentary and metabasite rocks are form Early-Triassic Karakaya complex. The composition of Eybak Granite and Granodiorite and acidic and basic rock veins have been aged as Tertiary era. At the study area, Eybak Granitoid, has imposed contact metamorphism to meta-sedimentary and metabasite rocks and turned them to andalusite- Biotite schist.

Keywords: Copper, Molybdenum,Gold, Geology , Geochemistry, Havran,Tepeoba , Subsurface modeling, Minerology.

TEPEOBA-HAVRAN, BALIKESİR İN PORFİR BAKIR-MOLİBDEN YATAĞININ JEOLOJİ, JEOKİMYA VE YERALTI MODELLEME İNCELENMESİ

ÖZET

Türkiye'nin demir cevheri yataklarının büyük bir kısmı, oluşum bakımından farklı jeolojik devirlere ait çeşitli mağmatik kayaçlarla ilgilidir. Ekserisi kontakt pnâmatoltık tipte olan bu yataklar, Anadolu'nun farklı bölgelerinde ortaya çıkmaktadır. Mağmatik kokenli demir zuhurlarını NW-Anadolu'da Biga yarımadası üzerindeki varistik orojenezin sial mağmatizmasının granit-granodioritik intruzyonlarına bağlı kontakt yataklar (Ayazmant, Şamlı, Eğrigöz masifi zuhurları) ile tersiyer orojenezindeki andezitik-dasitik final volkanizmasma ilişkin eksalâtif yataklar oluşmuştur.

Türkiye'nin bakır yatakları çoğunlukla magmatik kökenlidir. Bağlı oldukları magma cinslerine göre bakır zuhurlarını üç ana grup altında toplamak mümkündür :

1. Ofiolitik magmatizmaya bağlı zuhurlar,

2. Asitik plutonizmaya bağlı zuhurlar,

3. Andezitik - dasitik volkanizmaya bağlı zuhurlar,

Her üç magma tipine bağlı olarak, farklı jenezde bakır yatakları oluşmuştur. Cu-Pb-Zn minerallerinden oluşan metazomatik ve hidrotermal - filoniyen tipteki zuhurlar sayıca en fazla bulunmakla beraber, rezerv yönünden ekselatif - hidrotermal tipi karekterize eden (Murgul, Çayeli, Lahanos, Ergani ve Küre gibi) zuhurlar çok daha fazla önem kazanmaktadır. Geleceğin bakır aramalarında ise ekselatif - hidrotermal tipler yanında, bilhassa Tersier devri asitik plutonlarına bağlı porfiri tipi yataklar önem kazanacaktır.

Türkiye bakır anomali hartasının küçültülmüş ve dolayısiyle genelleştirilmiş halini inceliyerek, yoğunluğu ve uzanım istikametlerine bakarak Türkiye'de bakır aramaları için önemli bölgelerden biri Biga yarımadasıdır. Ve bu bölgeni daha detaylı araştırmak icin önem taşımaktadır.

Çalışma alanının içinde yer aldığı Biga Yarımadası, metalik cevherler bakımından oldukça zengin bir bölgedir. Biga Yarımadasın'da çok sayıda sülfürlü mineralizasyonun (kalkopirit, molibdenit, antimonit, vb.) varlığı bilinmektedir. Biga Yarımadası'nda Karakaya öncesi birimler, Edremit ve Havran'ın kuzeyinde yüzeyleyen metasedimanter kayaçlar (Kalabak Formasyonu) ile intrüzif bir granodiyorittir (Çamlık Metagranodiyoriti). Metasedimanter kayaçlar Triyas öncesi düşük dereceli metamorfizma geçirmiş olup, doğuda Geç Triyas yaşlı Çamlık Metagranodiyoriti, batıda ise Oligo-Miyosen yaşlı Eybek Granodiyoriti tarafından kesilmişlerdir. Metasedimanter kayaçlar Epimetamorfik kayaçlar olarak adlandırılmış olup, Kazdağı'ndaki yüksek dereceli metamorfik kayaçların epizonal örtüsü olarak yorumlanmıştır

Tepeoba Cu-Mo-Au cevherleşmesi, Balıkesir ili Havran ilçesinin yaklaşık 10 km kadar kuzeyinde yer almaktadır. Tepeoba sahasında, Alt Triyas yaşlı metasedimanter ve metabazik kayaçlar (Karakaya Formasyonu) ile Oligo-Miyosen yaşlı Eybek granitoyiti yer almaktadır. Granitoyit çalışma alanında, granit, granodiyorit, asidik damar kayaçları ve bazik damar kayaçlarından oluşmakta olup, metasedimanter ve metabazik kayaçları kontak metamorfizmaya uğratmıştır.

Cu-Mo-Au cevherleşmesi kontakt metamorfik kayaçlar ile granit içinde, breşik, ağsal damar-damarcık ve dissemine olarak görülmektedir. jeolojik ve jeokimyasal çalışmalar sonucunda belirlenmiş ve sondajlarla derinlik devamı ortaya çıkartılmış, KD-GB uzanımlı, yaklaşık 800 m uzunluğunda, yer yer 150 m genişliğinde, cevherli-breşik bir zon bulunmaktadır.

Cevherli zon KD-GB uzanımlı olmasına karşın, cevherleşme sırasında (sin-tektonik) veya cevherleşme sonrasındaki (post-tektonik) eğim atımlı bir ters fay ile kesikliğe uğramış ve haritadaki yanıltıcı görüntü (K-G doğrultulu) ortaya çıkmıştır. Çalışma alanında özellikle cevherli bölgede çok sayıda irili ufaklı fay mevcuttur. Bunlardan en belirgin olan yaklaşık D-B doğrultulu ve 70° G'ye eğimli dört adet eğim atımlı normal fay, ve yine yaklaşık K-G doğrultulu ve 70° B'ya eğimli iki adet eğim atımlı ters fay cevherleşmeyi etkilemiş ve atıma uğratmıştır.

Sahadaki cevher mineralleri, kalkopirit, molibdenit, altın, pirit, aikinit, emplektit, manyetit, ilmenit, ilmeno-manyetit, rutil, limonit, sfen, siderit, pirotin, anataz, lökoksen, malahit, azurit, olup, gang mineralleri, kuvars, feldspat, biyotit, flogobit, turmalin, klorit, muskovit, epidot ve kalsittir. Çok evreli intrüzyon ve mineral parajenezi nedeniyle sahadaki Cu-Mo-Au cevherleşmesi porfiri sistemlere dahil edilmiştir.

Çalışma alanında, detay jeoloji ve jeokimya çalışmaları, yapılmıştır. Bu analizler bölgenin jeolojisini ve jeokimyasini detaylı incelemek icin veriler elde edilmiştir. Detay çalışmalar sırasında sahanın 1/25000 ölçekli detay jeoloji, haritası yapılmış, litolojik birimler, formasiyonlar ayırtlanmıştır. Çalışmalar sırasında sahadan 60 adet jeokimyasal kayaç XRF örneği, major elementleri elde etmek icin alınmıştır , 40 adet kayaç numunesi mineraloji-petrografi incelemesi icin ince kesit alınmıştır. Numunelerin major elementleriyle, TAS ve Haker diagramlari çizilmiş ve bölgenin kayaç türleri belirlenmiş ve numunelerin ince kesitlerini yorumlayarak, bolgenin jeolojisini daha iyi ortaya çıkarmak icin incelenmiştir. Harker ve TAS diagramın elde edilen sonuçlarda örnekler genelde granit olarak sınıflandırılmakla beraber monzonit, kuvars monzonit, siyenit alanına düşen örnekler de görülmektedir.

Petrografi, mineraloji incelemesi sonucunda, Biga Yarımadası'nın(KB Türkiye) Tepeoba sahasının Bölgesinde Cu-Mo-Au oluşumları, Ust paleozoik yaşlı kalabak birimini temsil eden kalkşist, fillit ve bunların aralarında yeralan mermer mercekleri, Torasan formasiyonuna aitdir. Alt Triyas yaşlı metasedimanter ve metabazik kayaçlar mega mermer mercekleri, spilit ve metatüflerden oluşan metabasite üyesi yer alır. Arkozik metakumtaşları, fillit ve şistlerden oluşan meta sedimentar kayaçların alttaki birimler ile tektonik dokanaklı olarak üste yer alır. Granit-granodiyorit bileşimli Eybek Granitoyiti ile onun asidik ve bazik damar kayaçları Tersiyer yaşlıdır. Eybek Granitoyiti, çalışma sahasında Karakaya Formasyonuna ait metasedimanter ve metabazik kayaçları kontakt metamorfizmaya uğratmış, ve onları andaluzit-biyotit felslere dönüştürmüştür.

Çalışma alanı icin yapılan yeraltı modellemesi, madencilik sektöründede yer alan 3D modelleme çalışmalarının asıl amacı yer altındaki karmaşık jeolojik, mineralojik ve yapısal etmenleri çözmek ve cevher zon/zonlarını tespit etmektir. Bu karmaşayı çözmek için nitelikli veri (örn. geniş bir alanda düzenli aralıklarla yer alan sondajlar) kullanmak gereklidir. Ancak bu durum, yoğun bitki örtüsü, yüksek eğimli araziler ve bazı ekonomik kısıtlamalar sebebiyle her zaman mümkün olamamaktadır. Aynı zamanda, bilgisayar teknolojisinin gelişmesiyle, kullanılmayan ve/veya yeteri derecede dikkate alınmayan verilerin bir araya getirilmesi ve yeniden gözden geçirilmesi gerekmektedir. Bu değerlendirme belki de yeni potansiyel alan/alanların tespit edilmesine ve/veya yapılabilecek gereksiz harcamaların da önüne geçilmesine neden olacaktır. Bu çalışmada, yetersiz sayıda ve kullanılmayan verilere sahip bir çalışma alanı seçilerek, veriler mümkün olduğunca etkin olarak kullanılmaya çalışılmıştır.

Üç boyutlu model, herhangi bir objenin veya objelerin mümkün olduğu kadar gerçeğine yakın görünümlerinin bilgisayar ortamında oluşturulması ve bu görünümlerin görselleştirilmesi olarak tanımlanabilir. Yaşadığımız dünyanın üç boyutlu olması, anlatım ve iletişimde kolaylık sağlaması, sunum ve görselleştirme açısından bilgisayar ortamında da üçüncü boyutun kullanılmasını ve bu sayede modelleme yapılması gereğini doğurmuştur. Özellikle yerin iç yapısı ve yeryüzündeki nesnelerin üç boyutlu modellenmesi ve içerisinde sanal olarak dolaşma olanağına sahip olunmasıyla planlama, projelendirme, sunum ve görselleştirme ve bu yolla coğrafi tabanlı bilgi sistemlerine altlık oluşturma açısından önemli bir yol kat edilmiştir.

üç boyutlu modellenmesinin sağlayacağı yararlardan bazıları aşağıdaki başlıklarda toplanabilir:

• Harita bilgilerinin ve haritaların daha kolay güncelleştirilebilmesi,

• Harita yapımına esas olan bilgilerden veri tabanının oluşturulması,

• Toplanılan istatiksel bilgilerin analizi ve yorumlanması,

• Çalışma ortamlarının fiziksel açıdan daha doğru ve gerçeğe yakın modellemelerinin yapılabilmesi,

• Topoğrafik yapı ile jeolojik yapının deha doğru bir biçimde ilişkilendirilmesi,

• Yeraltı ile ilgili havalandırma, emniyet, nakliyat gibi konularla ilgili etüt ve projelendirme çalışmalarının daha kolay, hızlı ve doğru yapılabilmesi,

• İşletmenin, ocağın çalışılan ve terk edilen bölümlerinin plan, perspektif, kesit gibi grafiklerle kolaylıka görselleştirilebilmesi.

Bu çalışmada bölgenin orta dereceli Cu-Mo reserving söz konusudur. Yeraltı modellemesinin amacı bölgenin yeraltı potansielinin sondaj verileri kullanılarak Rockworks2006® yazılımı ile bölgenin 3D olarak yer altı modeli oluşturmaya çalışılmış ve amacı porfır sahasında Bakır, Molibden ve Altın miktarini belirlemek ve ilerde muhtemel ekonomik reserve oranını yüksek olduna dahil datalar elde edilmiştir. Tepeoba-Havran bölgesinde uygulanan yeratlı modellemesıyle ilerdeki yeni cevher zonları, önemli unsurları tespit ederek, gereksiz maliyetlerin onu alına bilir. Bu uygalama boglenin ekonomik açısından büyük onem taşıdığını sağlamaktadır.

Anahtar kelemeler: Havran-Tepeoba- bakır-molibden-altin- jeolojisi-jeokimyası- yeraltı modelleme uygulaması.

1. INTRODUCTION

1.1 Purpose

This master thesis was process and completed with three steps; working about
1) field study, 2) laboratory studies and 3) office studies. The most necessary item for these steps was literature review about formation of porphyry copper and molybdenum for related area. This thesis is reporting geology, geochemistry and subsurface modeling of investigation area to better understand the nature of extension of the Biga Peninsula, (NW Turkey).

1.2 Method and Approach

1.2.1 Field study

The fieldwork was conducted over 4 weeks in the summer and one week in the fall 2012. Most of field work was focused on the Cu-Mo deposit. The field area is in active exploration site, owned and operated by Özdoğu private company. Access to the site form 15km- yenice road, Edremit-Balikesir.
My field study was covered around 50 km of copper and molybdenum mining in Tepeoba-Havran. The place was skimmed and planned for studying to solve the general formations and geology and potential of Cu-Mo-Au in area.

1.2.2 Laboratory works

From investigated area 60 Samples are collected with their locations form field study. Samples were spent various steps for preparing to analyze. For this reason, at first they are moved to ITU geo-chemical research laboratory and they crushed for 3 or 4 pieces for different missions. Form one pieces of every sample was grind to make powder of rocks and prepare tablets for XRF to detect major element of samples. 40 of same samples are moved to make thin section and polishing for studying the mineralogy and petrography of rocks. I observe all of thin section with instrument, which is called polarizing microscope to study and analyze the collected samples to determine mineral textures. A thin section is made by grinding down a slice of rock which has been glued to a glass slide until it reaches a thickness of about 0.03mm (30 microns). At this thickness most minerals become more or less transparent and can therefore be studied by a microscope using transmitted light. Thin section samples are study and imaged and edited in Adobe Photoshop. Samples were collected from different formation of field study to show and describe them with their photos.

Bulk major element geochemical analyses from the field study are listed in Table B.1 and B.2 . Images of thin sections and field view from each formations are displayed in Figures (4.4 up to 4.16) so that visual differences between different formation of field sites can be seen. The geochemical data were plotted in a series of diagrams to distinguish chemical differences in source magmas.

1.2.3 Office works

The main structural of this thesis are office studies. Drawing map is to simplify the overview of site. Prepared map of field study with scale of 1/25000 and Fix up all the geochemical data results that exported from laboratory and imported them to excel. Data were collect to provide information regarding the geochemical relationships of the formation in the region to better understand the extensional evolution of western Turkey. The most important part of my thesis is subsurface modeling and majority of this chapter was need office work and used Rockworks software, added all borehole data to export the deposit's depth image with its detail to figure out the potential of deposit for future exploitation. (All borehole geochemistry datas are at appendix-C)

1.3 Turkey and World Copper Production

Turkey is a Eurasian country straddling the south-eastern Balkan region of Europe and the Anatolian peninsula in western Asia. Turkey's geology is extremely complex and this complexity is reflected in the diversity of its mineral deposits. Copper and chromite are the most significant minerals in the metals sector.

Turkey has a long mining history going back at least 9,000 years; copper, gold, iron, lead, mercury, silver, tin, and other metals have been mined since ancient times. Archaeologists believe bronze, an alloy of copper and tin, was first made in Turkey. The first iron was refined there. The fabled wealth of Croesus, the king of Lydia in

6th century, B.C., came from the placer mining of gold in western Turkey. The island of Cyprus, from which the word "cupros" or copper is derived, lies 32 km south of Turkey and was the source of copper for many Mediterranean cultures. The historic name of Turkey and the peninsula that forms the Asian part of Turkey is known as Anatolia, "Anadolu" in Turkish, which means several things including "the mother lode."

Turkey's proven copper reserves are about 3.7 million tons metal copper, total reserves are 15.8 million tons. Turkey has three important copper reserves; the East Black Sea, Southeast Anatolia and Thrace. Rods, profiles and cables are the most important export products in the sector. Turkey's copper ore exports were US$284 million in 2009. The main buyers were China, Finland, Sweden and India(USGS2009).

International Copper Study Group projected that global refined copper demand in 2011 would exceed refined copper production by about 200,000 tons, continuing the production deficit experienced in 2010, as operational problems and labor unrest, including strikes in Chile and Indonesia, continued to constrain world copper mine output. Global consumption and production of refined copper were projected to increase by 1.5% and 2.3%, respectively, in 2011.

U.S. mine production rose slightly in 2011 as restorations of mine cutbacks instituted at yearend 2008 were mostly offset by lower ore grades at a major producer. Electrolytic refinery production declined owing to the 2010 closure of a refinery that treated imported anode and to lower domestic smelter output, the latter resulting in increased concentrate exports. U.S. copper mine production was expected to rise by more than 100,000 tons in 2012, primarily owing to continued restoration of cutbacks. Domestic consumption of refined copper was nearly unchanged in 2011. After Chile, Peru is second place gives it slightly less than 14% of the market with all other countries away from that top seven combining for over 41% of total world production. As this decade develops, Peru will likely consolidate its position as worlds second place in the list with large mine developments in the pipeline.

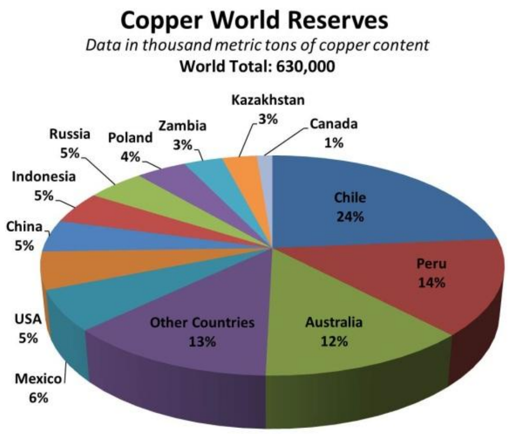

Figure 1.1 : Copper world reserves (modified from USGS).

MAJOR PRODUCER OF COPPER IN 2011

COUNTRY	PRODUCTION (THOUSAND METRIC TONNES)
Chile	5420
Peru	1220
China	1190
United States	1120
Australia	940
Zambia	715
Russia	710
Indonesia	625
Canada	550
Congo	440
Poland	425
Mexico	365
Kazakhstan	360
Other countries	2000

Figure 1.2 : Major producer of copper in 2011(modified from USGS).

1.4 Brief Description of Porphyry Copper Deposits

Porphyry deposits are the world's highly important source of Cu and Mo, and are major origins of Au, Ag, and Sn; significant byproduct metals include Re, W, In, Pt, Pd, and Se. They account for about 50 to 60% of world Cu production and more than 95% of world Mo production. Porphyry deposits are large, low- to medium-grade deposits in which primary (hypogene) ore minerals are mainly structurally controlled and which are genetically associated with felsic to intermediate porphyritic intrusions (Kirkham,1972). They are categorized from other granite-related deposits such as mantos and skarns by their large size and structural control, mainly stockworks, veins, vein sets, fractures, and breccias. Porphyry deposits usually contain hundreds of millions of tonnes of ore, eventhough they range in size from tens of millions to billions of tonnes; grades for the different metals vary considerably but generally average less than 1%. In porphyry Cu deposits, for example, Cu grades range from 0.2% to more than 1% Cu(Byron and others,2008).

A porphyry copper deposit is defined as follows:

1. One wherein copper-bearing sulfides are localized in a network of fracture-controlled stockwork veinlets and as disseminated grains in the adjacent altered rock matrix;
2. Alteration and ore mineralization at 1–4-km depth are genetically related to magma reservoirs emplaced into the shallow crust (6–8+ km), predominantly intermediate to silicic in composition, in magmatic arcs above subduction zones;
3. Intrusive rock complexes that are emplaced immediately before porphyry deposit formation and that host the deposits are predominantly in the form of upright-vertical cylindrical stocks and(or) complexes of dikes;
4. Zones of phyllic-argillic and marginal propylitic alteration overlap or surround a potassic alteration assemblage.

Copper may also be introduced during overprinting phyllic-argillic alteration events

1.4.1 Associated commodities and porphyry deposit types

A variety of deposit types are spatially, if not genetically, related to porphyry copper mineralization, including skarns, polymetallic veins and replacements, and epithermal veins. Copper skarn deposits occur near many porphyry copper host intrusions that intruded carbonate-bearing units Einaudi and others(1981), and skarn mineral zoning patterns may be useful in the targeting of a potentially associated porphyry copper deposit (Meinert and others, 2005). Typically, the garnet/pyroxene ratio increases toward the causative skarn-forming pluton with the distal pyroxene zones containing more iron and manganese-rich pyroxenes than proximal zones (Meinert and others, 2005). In some districts (for example, Christmas, Arizona, and Battle Mountain, Nevada), more copper is recovered from calc-silicate rocks than from the associated intrusive rocks.

Polymetallic replacement deposits occur in carbonate-bearing units peripheral to porphyry-style mineralization. At Bingham, Utah Babcock and others (1995), and Bisbee, Arizona Bryant and Metz (1966), polymetallic replacement deposits surround the intrusive complexes with offshoots appearing to radiate outward from the stocks. Vein deposits occur peripheral to many porphyry copper deposits (for example, Bingham, Utah), as well as crosscutting porphyry-style mineralization (for example, Valea Morii, Romania).

Porphyry copper deposits are mined primarily for copper, although molybdenum and gold are co-products in some deposits, and with silver a by-product in many deposits. Rhenium, tellurium, platinum group elements, arsenic, and zinc are recovered from a few deposits. With increasing molybdenum/copper, porphyry copper deposits are transitional to low fluorine (quartz monzonite type) porphyry molybdenum deposits, and with increasing gold/copper, they are transitional to porphyry gold deposits.

A variety of mineral deposits may be genetically associated with porphyry copper deposits, including:

- Skarns (including copper, iron, gold, zinc types)
- Polymetallic replacement (silver, lead, zinc, copper, gold)
- Polymetallic veins (gold, silver, copper, lead, zinc, manganese, arsenic)
- Distal disseminated gold-silver (gold, silver)
- Epithermal vein (intermediate/low sulfidation gold-silver)
- High sulfidation epithermal (gold, silver, copper, arsenic)

Copper is the primary commodity of economic interest in most porphyry copper deposits, although some deposits with low to very low copper grades are mined principally for their gold (for example, Çopler, Turkey) and (or) molybdenum (for example, Sierrita, Arizona; Continental [Butte], Montana resources.

By-Product Commodities: Molybdenum, gold, and silver are the economically most important by-products.

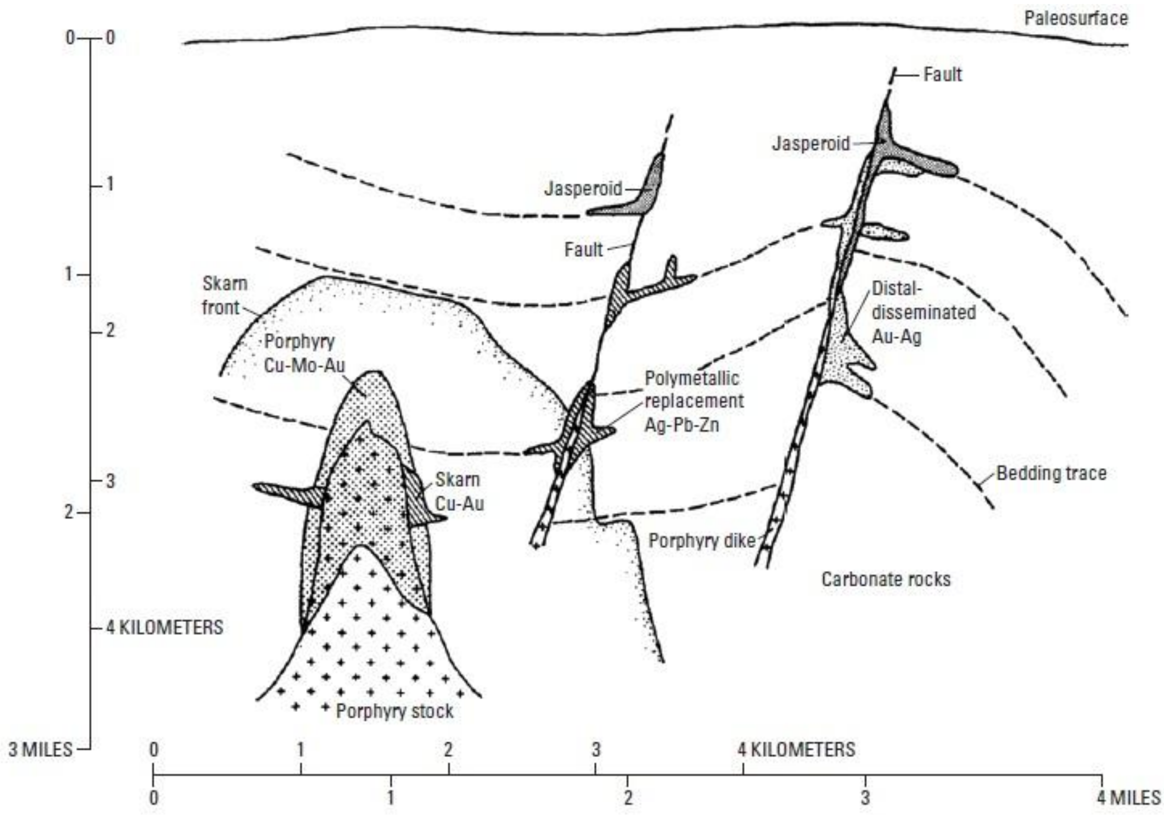

Figure 1.3 : General setting of porphyry copper and associated deposit types (modified from Sillitoe and Bonham, 1990).

1.4.2 Trace constituents of porphyry copper deposits

Rhenium and platinum-group metals are recovered from some deposits. Augé and others (2005) reported the occurrence of platinum-group-metal-bearing tellurides and arsenides in an assemblage of magnetite, chalcopyrite, and bornite in the porphyry deposit at Elatsite, Bulgaria. Tin has been reported from some deposits. Jambor and Owens (1987) found complex tin-bearing sulfide minerals in late-stage veins in the Maggie deposit in British Columbia (Canada), together with a polymetallic assemblage of copper, zinc, lead, and silver-bearing sulfide minerals.

1.4.3 Regional and geotectonic environment of porphyry copper deposits

Porphyry copper deposits form in continental magmatic arcs along convergent plate-margin boundaries or in island-arc environments. The deposits are associated with subduction-related volcanic centers, although in some examples, they thought to be associated with post collisional volcanism. Permissive magmatic-arc environments may be transpressional or transtensional.

Deformation of magmatic arcs can be exceedingly complex owing to the large variety of mechanisms by which strains can partitioned in the postmagmatic geologic history of a terrane. Despite the complexity, however, Hindle and Kley (2002) found in the Andes that different scales of analysis elucidate different tectonic effects. For example, near the surface, multitudes of small displacement structures may be typical; yet, at depth, the structures merge and transfer their displacements to large basement faults. Thus, the localization of volcanic centers and their spatial histories may reflect local manifestations of tectonic strains, while chains of volcanic centers may reflect more regional-scale strains. Such issues are important when trying to interpret the localization of porphyry copper deposits within extensive magmatic arcs. It accepted that porphyry copper deposits are structurally controlled, but opinions vary as to the relative importance of regional compared to local fault systems. The vertical extent of ore is dependent upon the lower copper cutoff grade, which will vary with the price of copper and local mining costs. At Dos Pobres, Arizona, from the top of the orebody to the 0.2 percent copper cutoff at its deepest points is approximately 1–1.2 km (Langton and Williams, 1982).

1.4.4 Host rocks of porphyry copper deposits

Most porphyry copper deposits are associated with shallow intermediate to silicic intrusive complexes composed of small plutons and dikes; some are associated wholly with dikes. Ore is sometimes hosted in volcanic and sedimentary rocks into which the shallow intrusive rocks were emplaced.

1.5 Earlier Studies

Earlier studies were focusing to generalize geology detail to make map for the investigated area and nearby vicinity. They are Konvenko(1940), Kadeen (1957, 1959), Philipson (1958,1967), Tchihatchef (1967).

Earlier studies are started for investigated area and nearby vicinity during the 1960s. Gümüş (1964) during the research for Tepeoba-kalabak-Eymir, they found fillates with black marbles and schists that are belongs to silurian-devonian aged near kalabak. Late Devonian serpantinize spilites and Carbonifer aged felsic fillates are contains marble near Tepeoba. These units are cutting by eybek granodiorites that are belongs to orogenized hercynian compact zone named as syntectonic granodiorites.

And also described the upper side of these units are covered by three incompatible units like arcoz, shale and sandstone trias-dogger aged. Aslaner (1965) he reffered to the karakaya complex with whole metamorphic units must be included in Kazdağ massive. He interpreted that gnays and amphibolites were creates the lower zone sequences, green schists, marble facies, spilites, fillat and metasandstones are created othe upper zones. He identified the Eybek granodiorites and Çamlık metagranodiorites are only as a granite and the product of compatible zone after hercynian, Permian aged and it cuts the today's kazdağ groups and karakaya complex. The name Karakaya Formation was introduced in 1975 Bingöl et al. (1975); however, pre-Jurassic clastic rocks with exotic limestone blocks were known earlier from Anatolia.Bailey & McCallien (1950, 1953) and Erol 1956) mapped and described a deformed greywacke series with exotic Permian and Carboniferous limestone blocks, which formed part of the famous Ankara mélange (for a detailed story of the discovery of the Ankara mélange see fiengör 2003).Brinkmann (1971) described olistoliths of Carboniferous and Permian limestone in what he considered a matrix of Palaeozoic greywacke in northwestern Anatolia. However, Bingöl et al. (1975) were the first to draw attention to the wide distribution of the pre-Jurassic blocky series from the Biga Peninsula in northwestern Anatolia through Bilecik to Ankara. They described the Karakaya Formation as consisting of "feldspathic sandstone, quartzite, conglomerate, siltstone, which is intercalated with spilitic basalt, mudstone and radiolarian chert". A characteristic feature of the Karakaya Formation was the presence of exotic blocks of Permian and Carboniferous limestone. Kocyigit (1987) the Karakaya Complex was first proposed by kocayigit that separated the complex, for the Ankara region, into two tectonic units called "the Lower Karakaya Nappe" and "the Upper Karakaya Nappe". Okay and others (1990) they were techno stratigraphically classified and separated the units from bottom to top as; Nilüfer unit, Hodul unit, Orhanlar greywacke and Çal unit Robertson (1994) The structurally lower levels of the Karakaya Complex, represented by the Nilüfer Unit, comprise kilometres- thick, strongly deformed and metamorphosed sequences of basic volcanic and volcanogenic sedimentary rocks, together with limestones in some areas. First they want to infer the tectonic setting of formation of the Nilüfer Unit and secondly to use the Nilüfer Unit to help test alternative tectonic models of the Triassic Tethys in NW Turkey in the light of regional data and modern oceanic comparisons. Pickett and Robertson (1996) Noted the low structural position of the

Nilüfer Unit, the presence of Devonian plutons cutting the Kalabak Unit and the latest Triassic-Liassic (and younger) unconformable sedimentary cover and also adopted this division except for the Hodul Unit, which they used the Ortaoba Unit instead. Based on the classification scheme introduced by Okay et al. (1991) and Okay and Göncüoglu (2004) suggested another large-scale subdivision of the Karakaya Complex consists of highly deformed and partly metamorphosed clastic and volcanic series of Permian and Triassic age, which was somewhat similar to that of (Kocyigit,1987). Karakaya complex is generally subdivided into two parts, the lower part consists of a mafic lava-mafic pyroclastite-shale-limestone succession metamorphosed in the greenschist and blueschist facies during the Late Palaeozoic or Triassic, the upper part is made up of highly deformed Permian and Triassic clastic, volcaniclastic and volcanic rocks with exotic limestone blocks. There are currently two different models for the depositional setting and tectonic evolution of the Karakaya Complex. The rift model assumes that the Karakaya Complex was deposited in a rift, which developed into a marginal oceanic basin and closed by the latest Triassic. The subduction-accretion model regards the Karakaya Complex as subduction-accretion units of Palaeo-Tethys. Consequently, the Cal, Hodul and Orhanlar units were considered to belong to the Upper Karakaya Complex, whereas the Nilüfer Unit by itself was regarded to represent the Lower Karakaya Complex. These are the sub- division of Okay and Göncüoglu (2004), therefore, differs from that of Kocyigit (1987) in that the Nilüfer Unit (the Lower Karakaya Complex or the Upper Karakaya Nappe) is the tectonically upper unit in the Ankara region, whereas in NW Anatolia the situation is reversed (the Nilüfer Unit is the tectonically lower unit). The recent studies performed in Central and NW Anatolia Sayit and Göncüoglu (2009); Sayit et al. (2010, 2011), however, showed that the Nilüfer Unit of Okay et al.(1991) bear some similarities to those characterizing the Upper Karakaya Complex. It appeared, then, that basaltic lithologies and associated oceanic-derived sediments are also found in some of the Upper Karakaya units as well. On the basis of this fact, Sayit et al,(2010- 2011) redefined these assemblages on the basis of their age, lithology and geochemical characteristics rather than their structural setting and metamorphic grade.A.H.F. Robertson & T. Ustaömer (2011) they mentioned that in Biga peninsula, deformation of Karakaya complex complex is belongs to Late Mesozoic–Early Cenozoic collisional deformation, Cenozoic extension related to southward rollback of the South Aegean arc trench system and neotectonic strike-slip/ transpression during the tectonic escape of Anatolia along the North Anatolian Fault.

Eybek granite was emplaced into the metamorphic basement rocks of the Sakarya zone continent (Karacık and Yılmaz, 1998). The Eybek pluton is located on the southwestern edge of the Kazdağ metamorphic complex in the southern Biga Peninsula Okay and Satir, (2000); Cavazza et al.(2009), on the eastern margin of the Edremit graben bounded by ENE-WSW trending high angle normal faults. The pluton is characterized mostly by granodiorite, but granite that occurs locally along the margin of the pluton is thought to have formed by mixing of granodiorite and host metamorphic and sedimentary rocks (Murakami et al., 2005). Structural and temporal relations indicate that this pluton was emplaced shortly after peak deformation and metamorphism of the Kazdağ core complex (Dilek et al., 2009).The Eybek granodiorite has a chemical composition of typical calc-alkaline, I-type, magnetite-series. A granite body occurs at the southern margin of Eybek granodiorite. This granite has a chemical composition similar to S-type granites with high Sr isotopic ratio and ilmenite-series character. Observation of drill core indicates that the potassic-altered granodiorite rich in magnetite and K-feldspar gradually changes into the granite. This suggests that the granite formed by the mixing of granodiorite magma with host sedimentary rocks. Microdiorite and aplite intruded the granite, granodiorite and sedimentary rocks. Sedimentary rocks near the granite underwent contact metamorphism represented by andalusite and biotite. Hydrothermal breccia with a matrix of hydrothermal biotite extends southwards from the granite. Skarn represented by magnetite, garnet and epidote is associated with the granodiorite. Detailed field survey in the prospect area indicates that the Tepeoba magmatic-hydrothermal system was overturned, with its top to the south. A breccia body occurs at the upper end of the granite and extends for 280 m southwards with the maximum thickness of 80m. The breccia consists mainly of fragments of andalusite-biotite schist in a matrix of biotite, and granite breccia is recognized near the contact with the breccia and granite. Chalcopyrite and molybdenite are disseminated in the breccia. In particular, these minerals are abundant where aplite intruded and brecciated, whereas these sulfide minerals are slightly disseminated in the granite. Native gold is detected in the panned samples from the breccia (Watanabe and Yıldirim 2004).

Genç and Altunkaynak (2007) and Cavazza et al (2009), Reported that the massif is flanked by the Eybek pluton in the east and the Evciler granitoid to the west Granitic plutons were the production of the Tertiary magmatic activity in NW Anatolia postdates the continental collision between the Sakarya and Tauride-Anatolide continental fragments during the Late Cretaceous to Early Tertiary period. The Eybek granite, which exposes in Biga peninsula, is one of the typical example of plutons, and is Late Oligocene-Early Miocene (21-26 Ma) in age. Eybek granite is an epizone granite which was located into the shallow levels in the crust (~1.5 km). Eybek granite formed contact metamorphism around its boundary. They figured out that the Eybek granite shows close relationships with dioritic hypabyssal rocks and andesitic-dacitic volcanic rocks in space and time, and may be considered a "subvolcanic pluton". Eybek granit is made up of four types of rocks on the basis of their petrographic, geochemical and petrological aspects; granite, granodiorite-quartz diorite, monzonite-quartz monzonite and cataclastic granodiorite. the Eybek pluton is 34.7±2.0 Ma to 20.1± 0.7 Ma (K-Ar orthoclase and U-Pb zircon) (Murakami et al., 2005; Altunkaynak et al., 2012).

2. GENERAL GEOLOGY

2.1 Geologic and Tectonic Setting of Biga Peninsula

Biga Peninsula creates the northwestern tip of the Turkish Peninsula; tectonically assemble the westernmost part of the Sakarya Zone of the Pontides at the crossroads of Gondwana and Laurasia. Therefore it was illuminate much of complicated geologic and tectonic history of Turkey in a small area. Synchronism between Gondwana and Laurasia, expressly in Paleozoic and Mesozoic times, resulted in collision of continental fragments and amalgamation (Ozcan Yigit 2012). Ketin (1966) He distinguished the Orogenic belts are in east-trend of Turkey and classified names from north to south as pontides Laurasian zone, Anatolides, Taurides and boundary folds (Gondwana zone). These fourfold tectonic units of turkey have been reworked by other later researchers (Gorur, 1998; Okay and Tuysuz, 1999; Sengor, 1984; Sengor and Yilmaz, 1981; Sengor et al., 1980, 1984; Stampfli, 2000) and have been sub-divided into many different tectonic zones or micro terranes in later studies. Moix et al (2008) despite the fact that, age, stratigraphic relations, tectonic positions and regional correlation of these terranes remains bleary. These bequeathed geological problems come out in Biga Peninsula as well; Okay and Goncuoglu, (2004) basic of some of orogenic rocks within Sakarya zone, i.e., karakaya Complex are clear examples beccaletto (2004) and Cetmi Ophiolitic Melange is unclear.

Permo-Triassic Karakaya Complex in Sakarya Zone and rocks of the Ezine Group in Rhodope Zone, Cetmi Ophiolitic Melange and Denizgoren Ophiolite of Cretaceous age form the other prominent Pre-Cenozoic geological features in the Biga Peninsula. Cenozoic volcano-plutonic rocks, covering large-scale areas, control the geology of the Biga Peninsula (Aldanmaz et al., 2000; Altunkaynak and Genc, 2008; Borsi et al., 1972; Ercan et al., 1995; Yilmaz, 1990; Yilmaz et al., 2001).

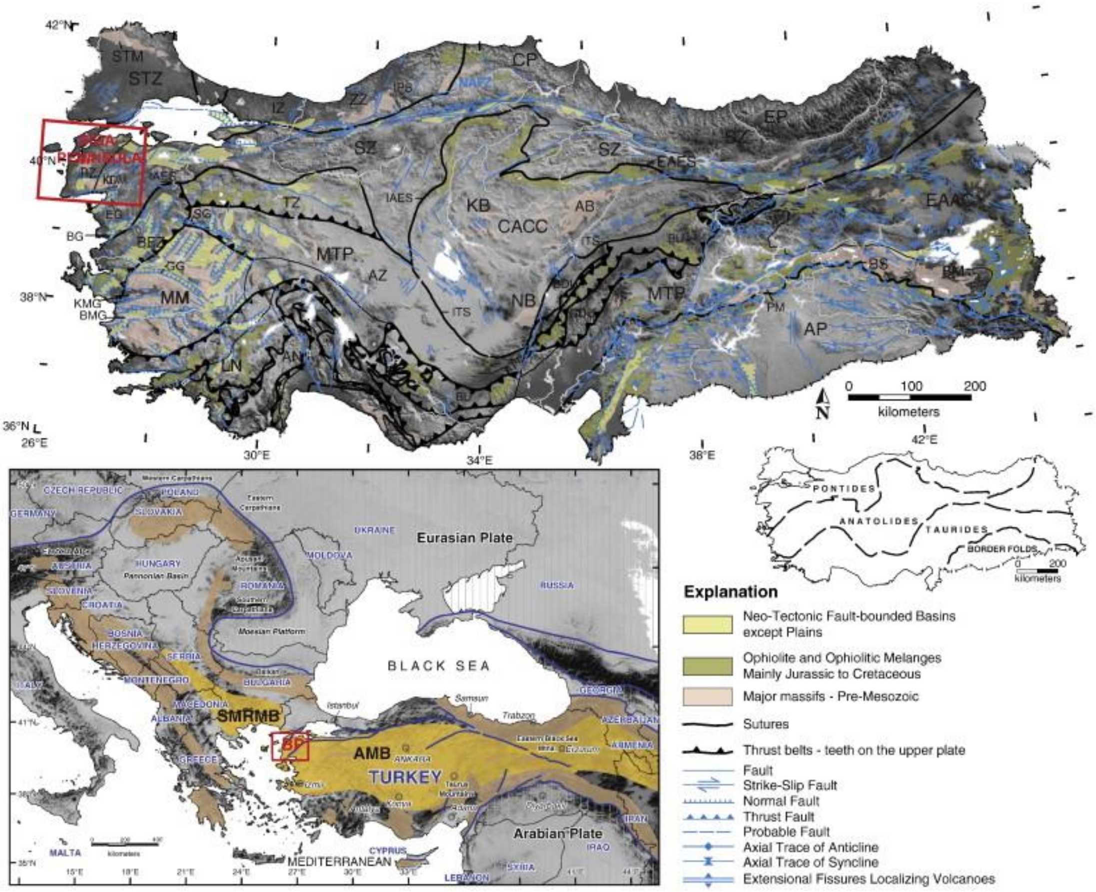

Figure 2.1 : The Biga Peninsula project area with major tectonic units of Turkey on DEM (modified from Yigit, 2009), small inset on the lower right shows major tectonic units of Ketin (1966). AB = Akdag Block, AN = Antalya Nappes, AP = Arabian Platform, AZ = Afyon Zone, BDG = Bolkardag Unit, BFZ = Bornova Flysch Zone, BG = Bergama Graben, BM = Bitlis Massif, BMG = Buyuk Menderes Graben, BS = Bitlis Suture, CACC = Central Anatolian Crystalline Complex, CP = Central Pontides, EAFZ = East Anatolian Fault, EAAC = East An- atolian Accretionary Complex, EG = Edremit Graben, EP = Eastern Pontides, GDU = Geyikdagi Unit, GG = Gediz Graben, IAES = Izmir–Ankara–Erzincan Suture, IPS = Intra- Pontide Suture, IZ = Istanbul Zone, KB = Kirsehir Block, KDM = Kazdag Massif, KM = Kirsehir Massif, KMG = Kucuk Menderes Graben, LN = Lycian Nappes, MM = Menderes Massif, MTP = Menderes-Tauride Platform, NAFZ = North Anatolian Fault Zone, NB = Nigde Block, PM = Poturge Massif, RZ = Rhodope Zone, SG = Simav Graben, STM = Strandja Massif, STZ = Strandja Zone, SZ = Sakarya Zone, TZ = Tavsanli Zone, ZZ = Zonguldak Zone. Figures use a Lambert Conformal Conic Projection for Turkey, scale accurate for the location's latitude. Large inset on the lower left shows Tethyan Metallogenic Belt.SMRMB = Serbomacedonian-Rhodope Metallogenic Belt, AMB = Anatolian Metallogenic Belt, BP = Biga Peninsula. Figure uses a Mercator projection, scale accurate for the location's latitude.

2.2 Purpose

In this chapter we are focusing on different rock types of Biga peninsula. From bottom to top are classified with titles of Metamorphic rocks, Ophiolitic rocks, Sedimentary rocks of karakaya complex, Magmatic rocks in two parts, one is plutonic, another one is volcanic rocks and explain the structural setting of Biga peninsula to gain the general geology and tectonic setting of Northwest of Turkey.

2.2.1 Metamorphic rocks

Metamorphic rocks in the Biga Peninsula can be introduced as 2 main NE-trending zones, which are the kazdag Group and karakaya Complex zone in the SE and the Ezine zone with Camlica Metamorphics in the NW (fig 2.3). These two zones were mentioned before form the basement of Sakarya and Rhodope zones. Kazdag Group makes a structural high, because of high-grade metamorphic rocks, forming a NE-trending, double-plugging anticlinorium. This structure tectonically is overlain by Permo-Triassic Karakaya Complex in the east and Cretaceous Cetmi Ophiolitic Melange in the west and north (fig. 2.2). Origin of the Kazdag Group is not displayed at surface in Biga peninsula (Bingol et al., 1975). gneiss, amphibolite and marble are the main lithologies forming the Centre of the Kazdag Mountains recognized as the Kazdag Group. Duru et al., (2004) metamorphic rocks of the kazdag Group have subdivided as recent studies, from bottom to top, Findikli Formation, Tozlu Formation, Sarikiz Marble and Sutuven Formation (fig. 2.2). Complex thermotectonic history, comes from Paleozoic continental metamorphic rocks in the Biga peninsula; Middle Carboniferous (Hercynian = Veriscan), Late Triassic (cimmeride) and Oligo-Miocene (Alpine) thermal events. Okay et al., (1996) Hercynian high-grade metamorphic basement of Kazdag gives radiometric ages of Carboniferous: 308 ± 16 Ma, Middle Pennsylvanian, Pb isotope ages in zircons from gneisses and Okay et al., (2006) 319.2 ± 1.5 to 329 ± 5 Ma, Middle to Late Mississippian, zircon ages from amphibolites. Okay and Satir, (2000a) these radiometric ages can be assigned to high-grade metamorphism and related deformation in the Kazdag Group. Muscovite and biotite in the gneisses give average ages of 19 Ma and 22 Ma Rb/Sr respectively, and it may reflect the last high-temperature metamorphic event in Latest Oligocene times causing formation of the Kazdag Metamorphic Core Complex. Cavazza et al., (2009) though, current studies using apatite fission-track ages suggest that Kazdag Massif was exhumed between 20 and 10 Ma (Early-Middle Miocene), ages clustering between 17 and 14 Ma.

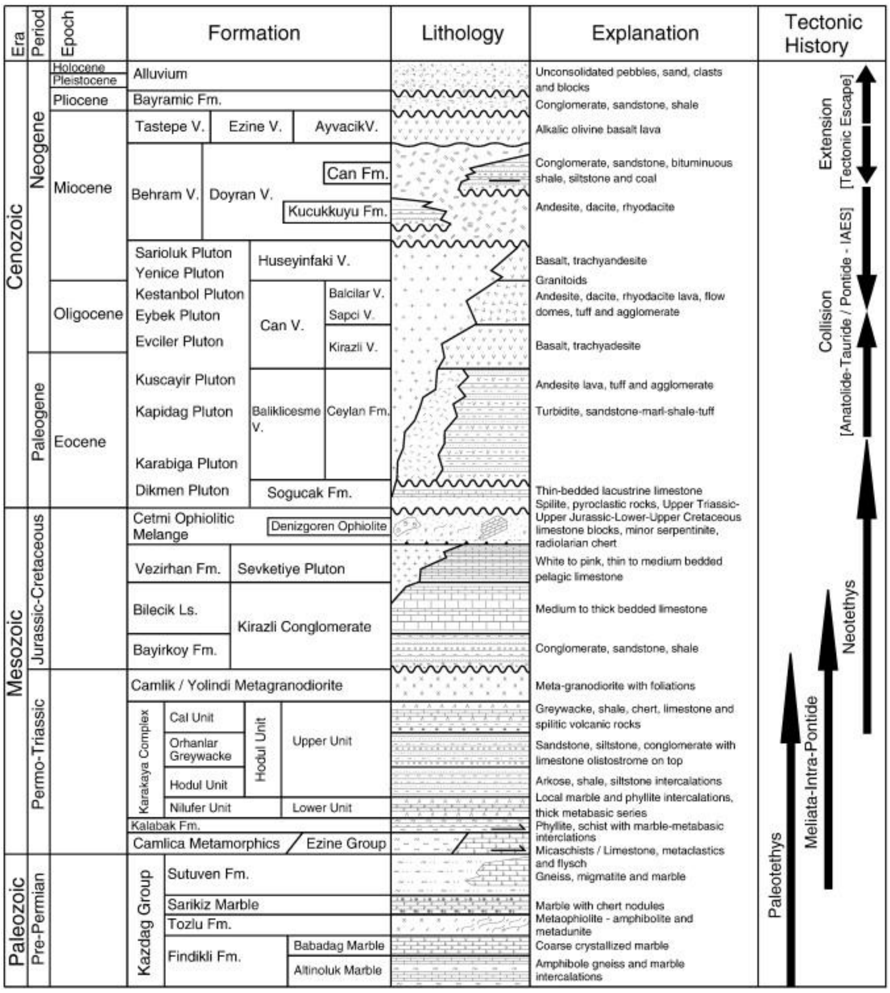

Figure 2.2 : Generalized stratigraphic section of the Biga Peninsula. Compiled from Akyurek and Soysal (1980), Duru et al. (2004), Ercan et al. (1995), Okay et al. (1990), Siyako et al. (1989), and other sources.

Great metasedimentary rock presentations in the northeast of Ezine and west of karabiga called the Camlica Metamorphics and form the basement of the Rhodope Zone (Okay et al., 1990) see at (Fig 2.3).

Fragments of eclogites in the Camlica Metamorphics indicate a metamorphism and three muscovite samples from quartz-mica schists give 69 to 65 Ma Rb/Sr age periods(Okay and Satir, 2000b). These radiometric ages indicate a regional metamorphism of Maastrichtian age. However, these metamorphic rocks were clarify as the cover of the kazdag Massif (Kalafatcioglu, 1963).

Okay and Satir, 2000b; Okay et al., (2001) this idea was come from the basis of evolution of the Camlica Metamorphics are related to Rhodope-SerboMacedonian Massif.Okay et al., (1990) most carbonates of karadag units are at the age of Permo-Triassic epicontinental sedimentary rocks and Beccaletto and Jenny, (2004) north-trending green-schist facies metamorphic rocks, outcropping northwest and east of Ezine, that called the Ezine Group see at (fig 2.3). Ezine Group rocks are suggested and subdivided by researchers into three formations, which are, from bottom to top, Geyikli, Karadag, and Camkoy Formations and these Ezine Group rocks are a product of permo-Triassic rifting in the north of Maliac/Meliata Ocean and they represent Rhodopian passive margin.

The other significant Permo-Triassic age orogenic rocks, consisting of slightly metamorphosed, strongly deformed, clastic and volcanic rocks, in the Biga Peninsula called Karakaya Complex Tekeli, (1981) and in other word Karakaya Formation (Bingol et al., 1975). Rocks of karakaya complex are shown up in the kazdag Mountains and extend northeast (fig2.3 and fig2.4), crosscutting the Biga peninsula**.** Karakaya complex rocks represent a subduction-accretion process (Yigit, 2012).

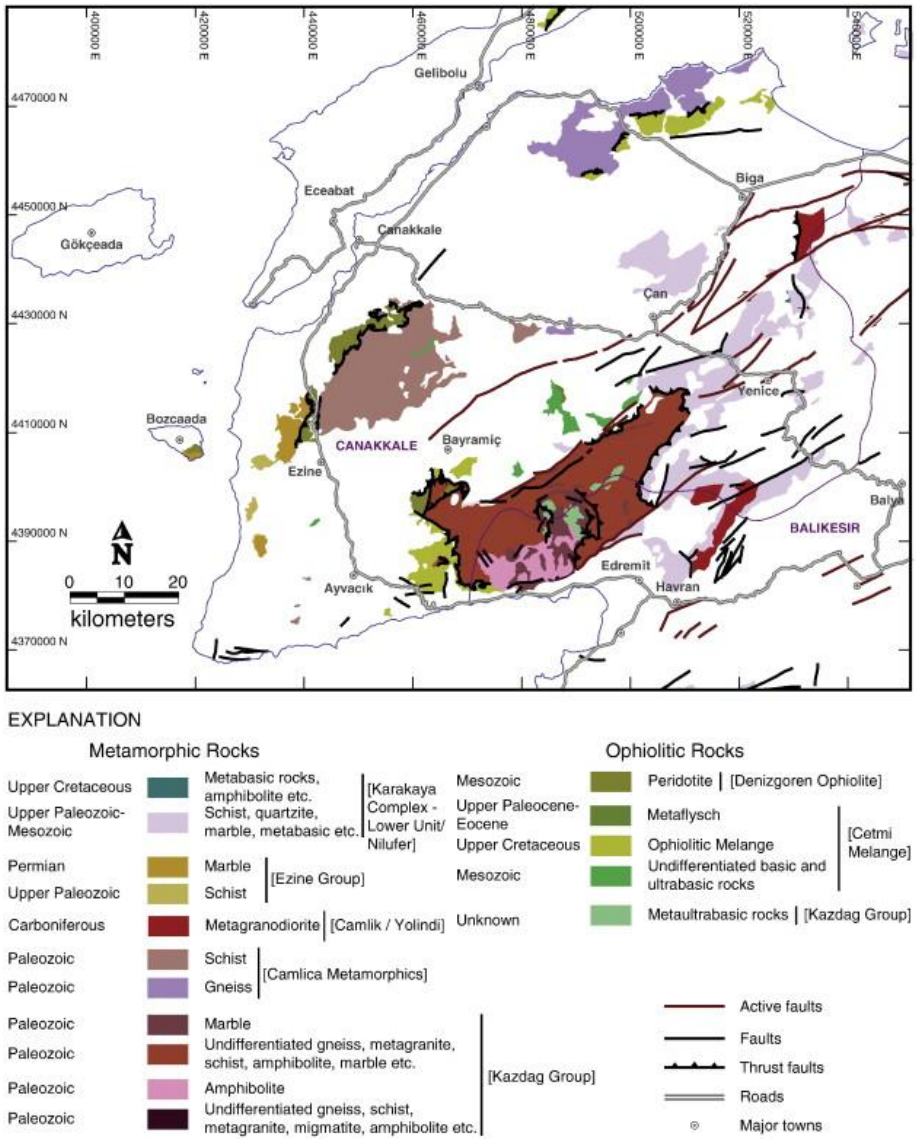

Figure 2.3: Distribution of the metamorphic and ophiolitic rocks including ophiolitic melanges in the Biga Peninsula (modified from MTA, 2001). This and all subsequent figures use Universal Transverse Mercator (UTM) projection, Zone +35 with European Datum 1950 (ED 50).

Karakaya Complex in Biga Peninsula consists of four-tectonostratigraphic unit with similar age however these units are different in depositional basin environments, which are Nilufer Unit, Hodul Unit, Orhanlar Graywacke and Cal Unit (Okay et al., 1990) see at (Fig 2.2). However, differentiation of units within the complex and their correlation within Sakarya zone in most studied for origin of karakaya complex remain incomplete (Okay and Goncuoglu, 2004). Karakaya Complex is subdivided into only Lower and Upper Units in recent studies (Okay and Altiner, 2004; Okay and Goncuoglu, 2004).

Camlik Metagranodiorite, outcropping north of the town of Havran, interrupted into quartz–feldspar schists and phyllites of the Kalabak Formation (Yigit Ozcan 2012).

2.2.2 Ophiolitic rocks

Ophiolitic rocks of Biga Peninsula are described by two major tectono-stratigraphic units; one is Cetmi Ophiolitic Melange, another one is Denizgoren Ophiolite. Nontheless some of ophiolitic rocks like metaophiolites are in the Kazdag Group and mélanges in Hodul unit of Karakaya Complex. Cetmi Ophiolitic Melange is located at the southern Biga peninsula, north of the town of kucukkuyu and in the northern Biga peninsula and west of the Kazdag Group, and northwest of the town of Biga see at (fig. 2.2 ,2.3 and 2.4). There is a tectonic contant between Cetmi Ophiolitic Melange and Camlica Metamorphics in the northern part of the Biga Peninsula, additionally it has a fault contact with underlying high-grade metamorphic rocks of the Kazdag Group and is unconformably overlain by different types of sedimentary rocks of Neogene age in the southern part of the Peninsula (Yigit Ozcan 2012). Beccaletto et al., (2005) recent biosratigraphic studies prescribe that geodynamic evolution of the mélange was completed in the Mid-Cretaceous, Okay et al., (1990) not in the paleogene. Beccaletto et al., (2005) Cetmi mélange have few familiar characteristics with other mélanges in northwestern Turkey, i.e., in the Izmir-Ankara and Intra-pontide suture; and for that reason there is no direct correlation between them. Even though, it has several similarities to mélanges in Rhodope Zone of Bulgaria and Greece. So, it is indicted that Cetmmi Ophiolitic Melange in the Biga Peninsula may represent an isolated fragment of the Rhodope Zone.

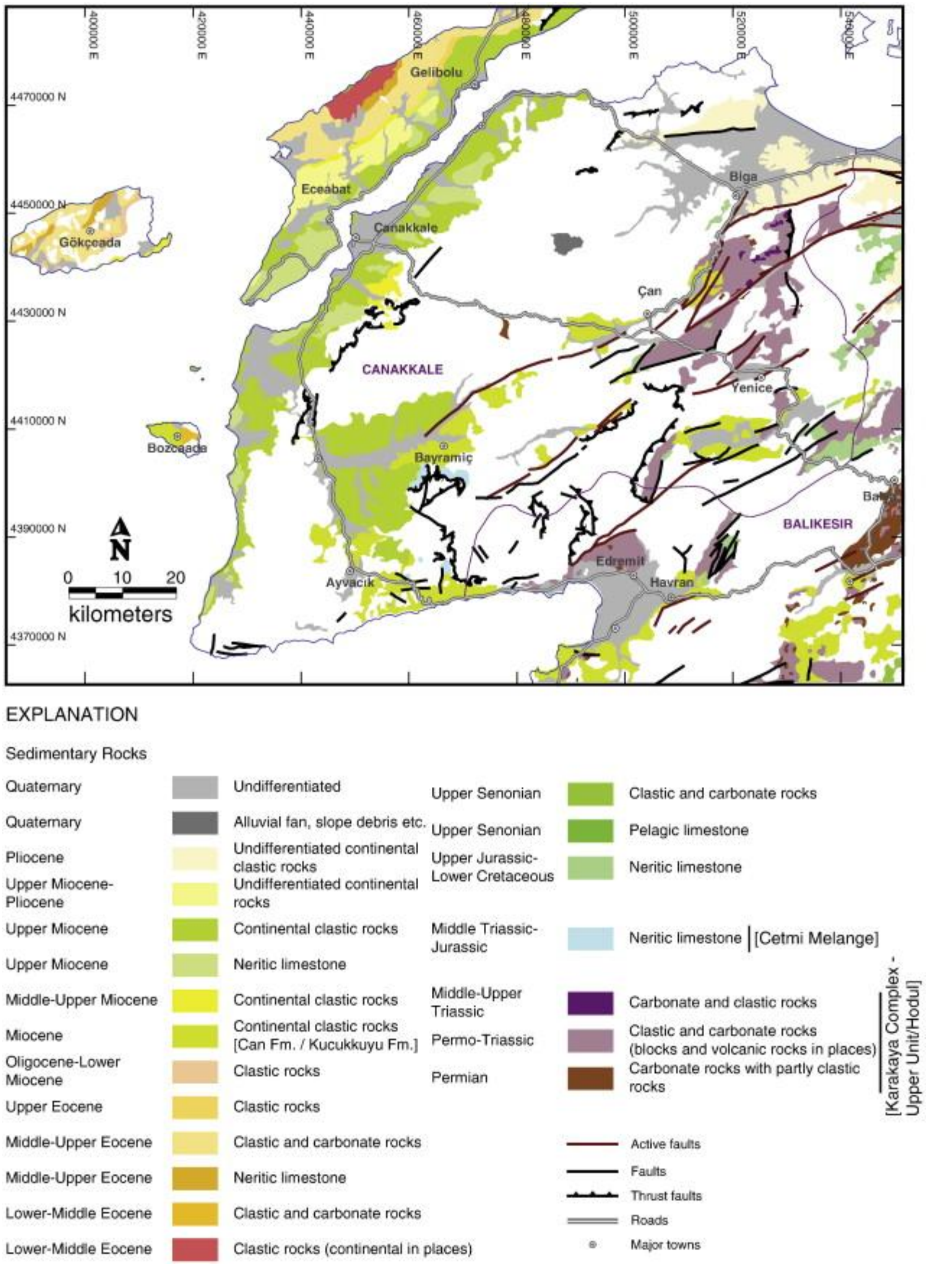

Figure 2.4 : Distribution of the sedimentary rocks in the Biga Peninsula (Modified from MTA, 2001).

Okay et al., (1990) Denizgoren Ophiolitic, forming a northeast-trending belt starting from north of the town of Ezine, consists of partly serpentinized harzburgite. Denizgoren Ophiolite tectonically overlies the Permo-Triassic sedimentary rocks of the Ezine Group in the west, along the Camkoy Thrust, and the Camlica Metamorphics in the east, along the Ovacik Thrust see at(Fig 2.3).

2.2.3 Sedimentary rocks of Karakaya Complex

The oldest non-metamorphosed sedimentary rocks in Biga peninsula are carbonate and clastic rocks of Permian and Triassic age in the Karakaya Complex. Another pre-Cenozoic sedimentary rocks are the Mid-Triassic to Jurassic neritic limestones of the Cetmi Ophiolite Mélange see at (Fig 2.4). Okay et al., (1990) most of the non-metamorphosed and non-deformed Jurassic and younger sedimentary rock series are relatively well studied in the east of the Biga Peninsula, Bursa-Bilecik area, and therefore the sedimentary rocks in the Biga Peninsula are correlated with them and the same nomenclature is used, i.e., Bayirkoy Formation, Bilecik Limestone and Vezirhan Formation see at (Fig 2.2).

Siyako et al., (1989) Cenozoic sedimentary rocks have extensive exposures in the west and northwest of the Biga Peninsula, generally northeast-trending exposures on both sides of the strait of the Dardanelles see at (Fig 2.4). Eocene carbonate and clastic rocks, trending northeast, are concentrated in the Gallipoli Peninsula and Gokceada Island. Miocene continental clastic rocks and neritic limestone have exposures along the Dardanelles strait and southwest of the Bayramic Graben see at (Fig 2.4). Cenozoic sedimentary rocks in the Biga Peninsula can be evaluated in four time-intervals, separated by disconformities: Maastrichtian–Early Eocene, Middle Eocene–Oligocene, Miocene and Pliocene–Holocene. Early-Middle Miocene times are characterized by coeval volcanism and sedimentation. Lacustrine sediments like shale, siltstone and tuffs were deposited in small basins including economic coal deposits, such as Can lignite. Furthermore, other energy raw materials such as uranium deposits were formed associated with continental clastic rocks of the Miocene Kucukkuyu Formation see at (Figs 2.2 and 2.4).

2.2.4 Magmatic rocks

Cenozoic volcano-plutonic rocks dominate the geology of the Biga Peninsula and therefore disguise older lithologies see at (Fig 2.5). Though they cover very extensive areas and host many economical metallic mineral deposits as well as industrial raw materials, volcanic successions in the Biga Peninsula are not well studied or correlated in terms of volcanic stratigraphy and thus are poorly understood. One of the main reasons is a lack of reliable radiometric age dates as well as strong and extensive hydrothermal alteration causing problems with recognition and differentiation of the protoliths in many areas. Magmatic rocks in the Biga Peninsula can be estimated in two broad categories; Pre-Cenozoic and Cenozoic(Yigit Ozcan 2012).

2.2.4.1 Plutonic rocks

The major stock size plutons are exposed in the Biga peninsula. Most of these intrusions trend either northeast, following the major tectonic grain of the peninsula, or eastnortheast, cutting the major tectonic grain (Fig2.5). The main Cenozoic intrusions in the Biga Peninsula show calc-alkaline character and are represented by, from east to west, Kestanbol, Kuscayir, Evciler, Dikmen, Yenice, Eybek and Sarioluk Plutons in the south and center of the peninsula and Karabiga and Kapidag Plutons in the north see at (Fig 2.5). Birkle and Satir, (1995); Yilmaz et al., (2001). Well-studied plutons indicate compositions ranging from granite to quartz diorite, for example Kestanbol Pluton is mainly granite and quartz monzonite and Evciler (Karakoy) Pluton is granite, quartz monzonite and quartz monzodiorite. Young granitoids in the Biga Peninsula generally are the products of Eocene to Oligo-Miocene plutonism. All dated samples from plutonic rocks suggest a younging age from north to south for plutonism in the Biga Peninsula, from Late Cretaceous to Early Miocene see at (Fig 2.5).

2.2.4.2 Volcanic rocks

Volcanic rocks of the Biga peninsula were mainly evaluated in two broad categories; pre-cenozoic, Cenozoic see at (Fig 2.5). Basic volcanic rocks, i.e., basalts and spilites, associated with the Karakaya Complex or ophiolitic melanges characterize Pre-Cenozoic volcanic rocks in the Biga Peninsula see at (Fig 2.5). Volcanic rocks related to Karakaya Complex are most probably Triassic in age. Yilmaz, (1990) Cenozoic volcanism in the Biga Peninsula started in the Eocene in extensive areas with mainly andesitic and dacitic, calc-alkaline character and continued to basaltic alkaline volcanism through Late Miocene.

Sensu lato volcanism in the Biga Peninsula initiates with Middle Eocene medium-K calc-alkaline and continues through Oligocene with high-K calc-alkaline character. Early Miocene volcanism is characterized by high-K to shoshonitic lavas. In the Middle Miocene to Late Miocene, volcanism shifted to mildly alkaline and alkaline characters respectively. Geochemistry of the volcanic rocks suggests increasing amounts of crustal contamination with decreasing subduction signature during the evolution of magmas from the Eocene through the Early Miocene. Middle to Late Miocene volcanism gives geochemical signatures indicating decreasing crustal component with an enriched asthenospheric mantle-derived melt. Cenozoic calc-alkaline volcanism hosts many important economic deposits of metallic and industrial minerals(Altunkaynak and Genc, 2008).

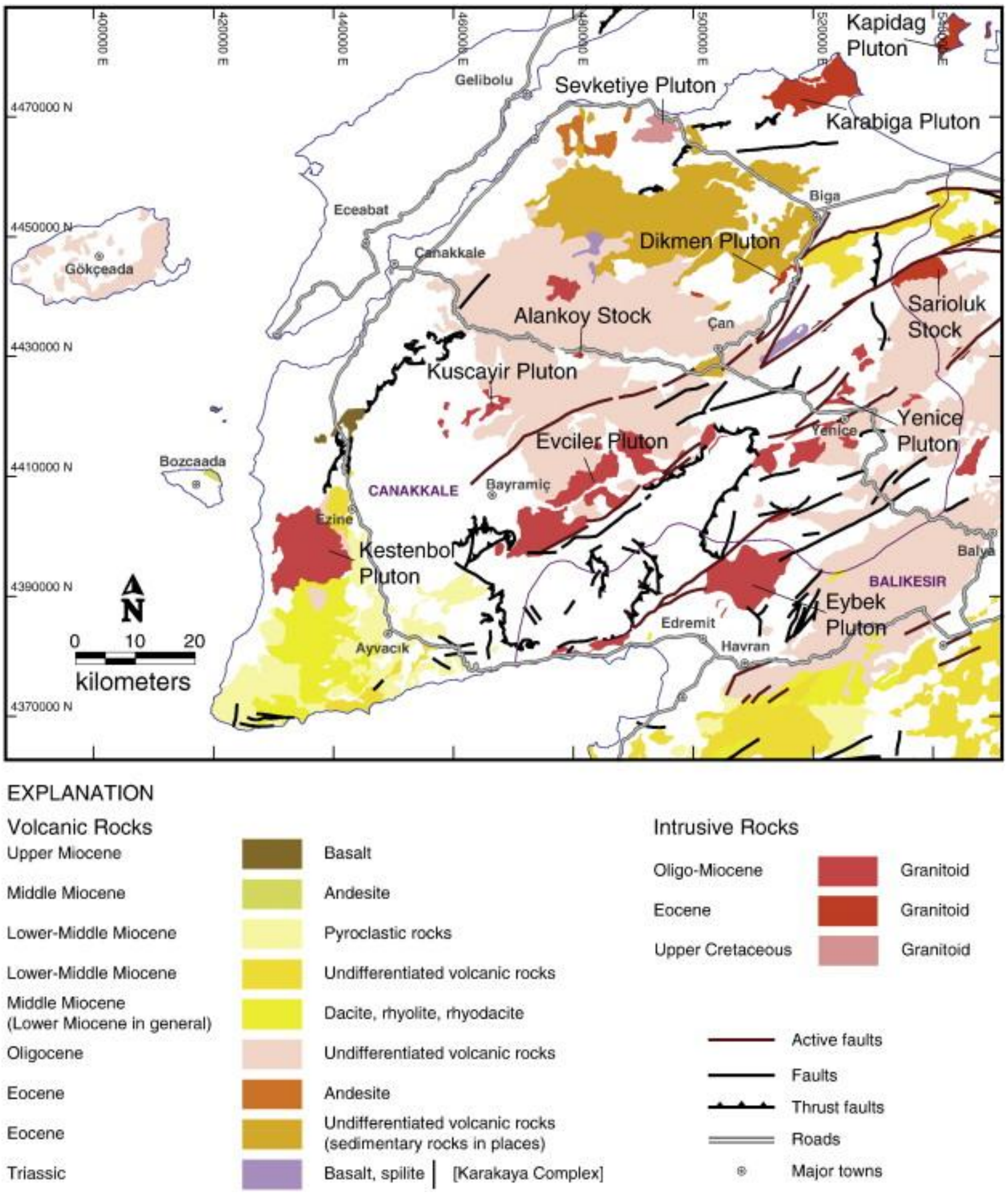

Figure 2.5 : Distribution of the plutonic and volcanic rocks in the Biga Peninsula. (Modified from MTA, 2001).

2.3 Structural Setting of Biga Peninsula

Structural geology of the Biga Peninsula is intricate; there are no available palinspastic reconstruction maps of any scale. Pre-Cenozoic structures are dominated by thrust faults associated with ophiolite obductions. The oldest thrust faults are related to metaophiolites in the Kazdag Group and melanges in Hodul unit of the Karakaya Complex. Emplacement of the Denizgoren and Cetmi Ophiolites are mainly Late Cretaceous in age, and formed NE- and N-trending thrust zones respectively see at (Fig 2.3). Cenozoic structural features are characterized by detachmentfaulting related to exhumation and core-complex development of Kazdag Massif in Oligo-Miocene, and strike-slip faulting started in Early Miocene related to development of the North Anatolian Fault Zone (NAFZ). Neotectonics of the area are subject to dextral-strike slip faulting as well as N-trending continental extension with rotations, causing challenging kinematic analysis of faults with not only strike-slip but also oblique and dip-slip components. E-trending principal deformation zone of the NAFZ bends to the SW in the Biga Peninsula and is the main control on the formation of the transtensional and transpressional fault jogs, which are favorable loci for magmatism as well as mineralization. Based on the interpretation of the geological maps, LANDSAT and ASTER images incorporated with field observations, NE-, E- and NWtrending faults form three major groups in the Biga Peninsula. The NE- and NW-trending faults are conjugate Riedel shears. The most prominent faults are NE-trending dextral-strike slip systems (~060) see at (Fig 2.5), related to the western extension of the NAFZ, which create pull-apart basins that control Oligo-Miocene sedimentation and volcanic activity. This current tectonic regime forms NE-trending basins and ranges, and forms the NW-boundary of the volcanic rocks in the Biga Peninsula see at (Figs. 2.4 and 2.5). Some of the NE-trending strikeslip faults are seismically active see at (Fig 2.5), and also control the distribution of current hot-spring activity. The same relationship may be true for paleo-hot springs related to epithermal systems in the Biga Peninsula. NW-trending faults, possibly antithetic Riedel shears of the NAFZ, are less prominent structures, and are mostly distinct in satellite image interpretations. Other conspicuous structures are E-trending normal faults and fractures (tension fractures), forming loci for magmatism, mineralization and alteration. Inferred E-trending normal faults form the southern boundary of the Biga Peninsula along the northern edge of the Gulf of Edremit.

3. REGIONAL GEOLOGY

3.1 Purpose

The pre-Jurassic basis of the field consists one of the tectono-stratigraphic units that were juxtaposed during the late Triassic: the pre-karakaya units including Torasan formation the sub-group of kalabak unit and metasedimentary and metabasite rocks which form Early-Triassic Karakaya Formation Bingöl et al , (1975) or in the other words, Karakaya Complex (Okay et al, 1990). The compositin of Eybak Granite and Granodiorite and acidic and basic rock veins have been aged about tertiary era. At the study area, Eybak Granitoid, has imposed contact metamorphism to meta-sedimentary and metabasite rocks and turned them to andalusite- Biotite schist see at (figure3.2-3.3).

3.2 Regional Geology

The study field is located in north-west of the Biga Peninsula. Approximately 10 km to the north of the town of Havran in the Balikesir province.This field is located in map of İ18-d1-d2-d3-d4 quadrangle in the geotectonical point of view, includes a part of the Sakarya Continental plate Şengör and Yılmaz, (1981) or the Sakarya Zone Okay, (1984) of the Pontides tectonical structure see at (Figure 3.1)

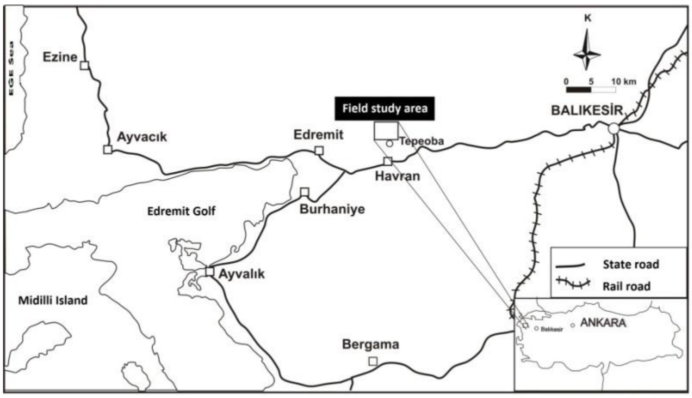

Figure 3.1 : Main location of field study area, (MTA 2006).

Sakarya zone is starting in Biga Peninsula and extending by Bursa, Bilecik, Eskisehir and Ankara is deformed in a complicated manner which normally shows a low-grade metamorphism at Pre-Jurassic but during Jurassic-Tertiary, metamorphism process didn't occur or is not visible Okay et al. (1990). This field has been separated to three units before the Jurassic era; these are the units of Pre-Karakaya, the Kazdağ group and Karakaya Complex.

Pre-Karakaya units of Biga Peninsula,at north of Edremit and Havran include low grade meta-sedimentary rocks (Kalabak Formation) and an intrusive granodiorite (the Çamlık Metagranodiorite). Pre-Triassic metasedimentary rocks have influenced by low-grade metamorphism and during Late Triassic the in the East part Çamlık Metagranodiorite has cut by the Oligo-Miocene aged Eybek Granodiorite in the west part, Bingöl et al. (1975) called metasedimentary rock "the epimetamorphic rock" and it is remarked as the epizonal overlay on the Kazdağ high-grade metamorphic rocks see at (Figure 3.3).

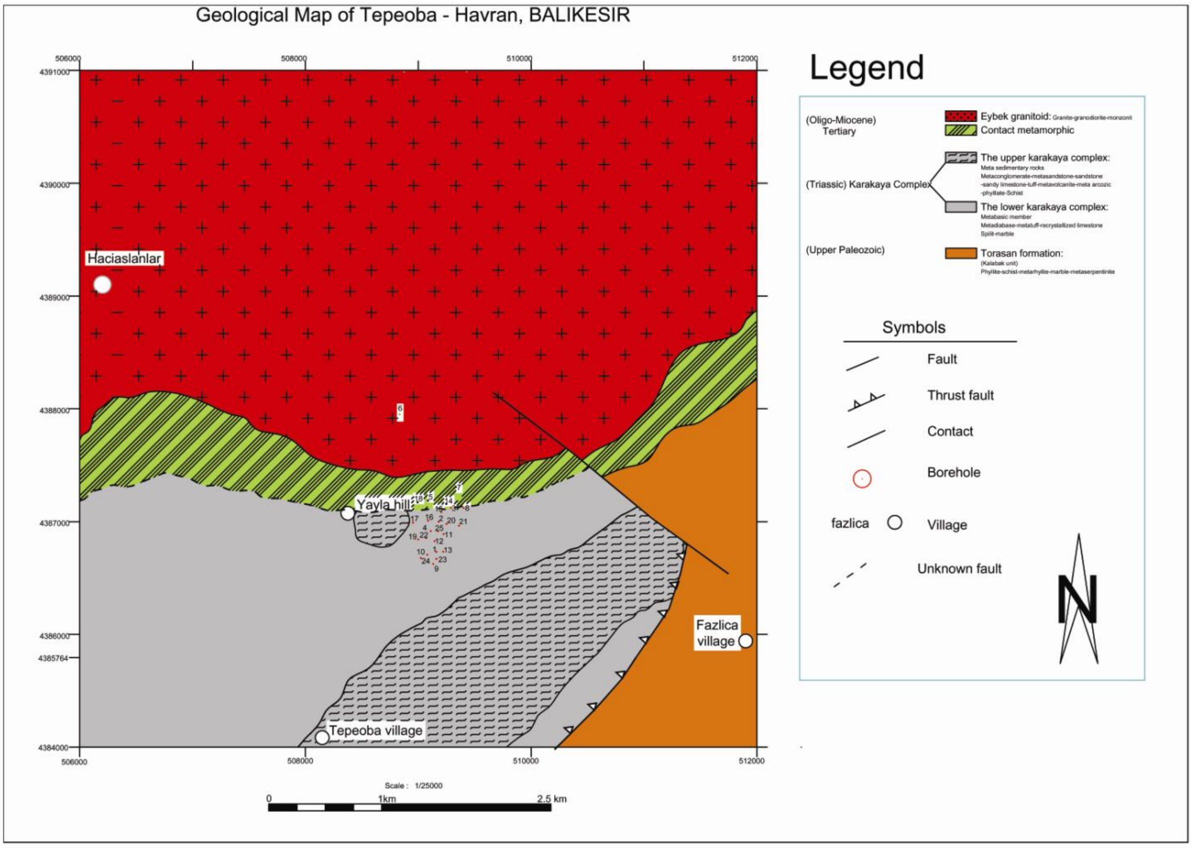

Figure 3.2 : Geological map of Havran-Tepeoba,Balikesir (modified from MTA, 2007).

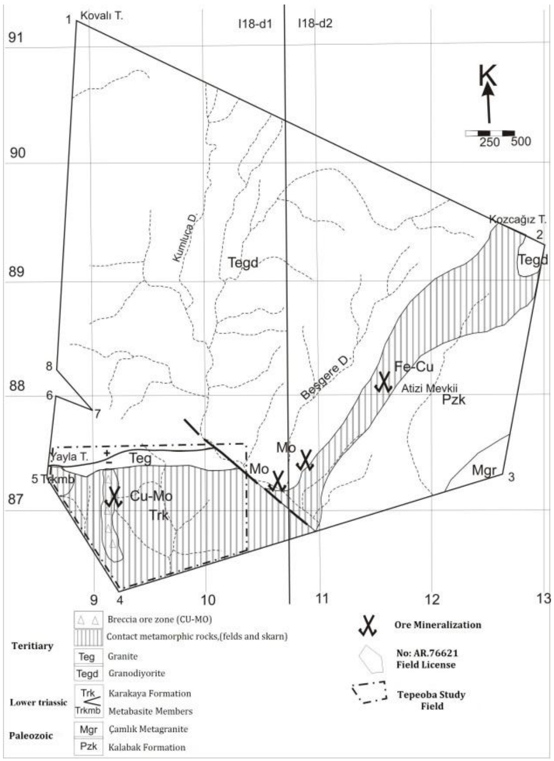

Figure 3.3 : Maps of mining area modified from MTA2006.

The consisting gneiss, amphibolite and marble metamorphic rock mass in The Kazdağ mountain, referred to the Kazdağ Group (Bingöl et al 1975). Extending up to approximately 50 km in NE-SW direction and limiting by the Late Tertiary intrusion, the Kazdağ Group, is an anticline structure. Radiometric age determinations made by the rocks of the Kazdağ Group have produced variable results. For example in gneiss cores K / Ar proportion ages vary in range of 23 to 27 Ma and Rb / Sr ages between 29 to 253 Ma. The Isochrones age is determined about 233 ± 24 million year. The tertiary ages probably have obtained from Oligo-Miocene aged Tertiary magmatism. The most significant age for geological aspects in kazdağ is Triassic age.

The youngest metamorphic part in the Sakarya Zone as known for the first time in the Biga Peninsula Brinkman, (1971; Bingöl et al., (1975) and further future studies the Karakaya Formation is Karakaya Complex. The main lithologic units start with basic volcanics, greywacke, sandstone, and lenticular limestones and contain different-sized Permo Carboniferous limestone blocks in the interior part. The age of this unit according to Bingöl et al (1973) is Early Triassic and according to Okay (1984) is Triassic.The rocks of Karakaya Group has spent low-to-moderate pressure / low temperature (D-OB/DS) conditions and low green schist facies metamorphism.

There are four divided units in the Biga Peninsula according to Okay et all (1990), which are completely similar to Karakaya Complex in age (Nilüfer, Hodul, Orhanlar and Çal).

Oligocene-Early Miocene granodiorites and their coeval calk-alkaline volcanic formation are occurred by partial melting according to Okay et al, (1990) during Pontide ocean closure in Early Tertiary and consequent increasement in the thickness of the continental crust in Late Tertiary at the Biga Peninsula.

Similar to western Anatolia, in Biga Peninsula the Late Cretaceous-Early Miocene NS tending compression transformed to Miocene aged extension and consequently, formed EW tending grabens (Edremit, Kalkım, Bayramiç, etc.), neogene volcanics, active faults and geothermal water springs. a young volcanic rocks composed of active faults and hot springs. NS extensional tectonic regime continues in the region up to now.

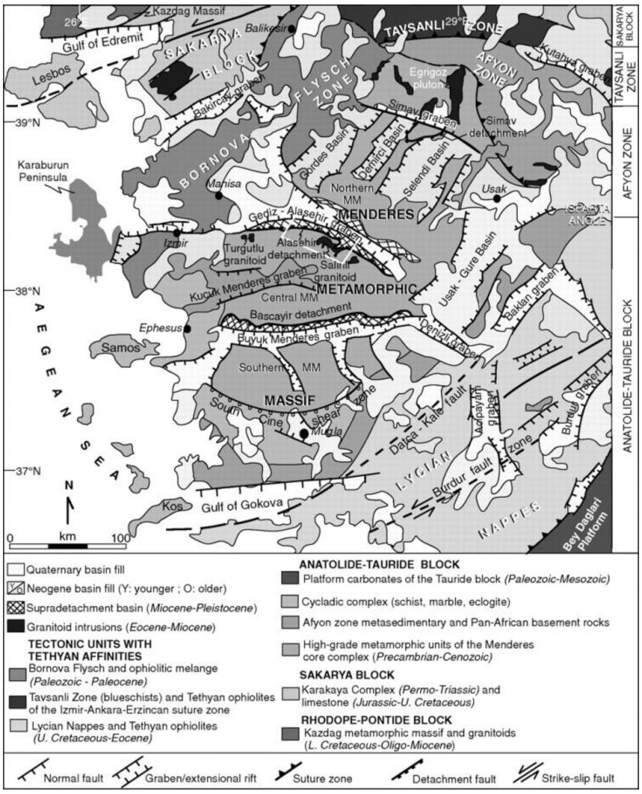

Figure 3.4 : Outline geological map of western Anatolia showing Neogene–Quaternary extensional basins in the Menderes Massif and the surrounding major crustal blocks, and some of the main tectonic boundaries and features. MM—Menderes Massif, modified from (Z.Oner and Y. Dilek 2011).

3.3 Transportation

It is possible to reach to Tepeoba field from Havran paved way. Also it is accessible to Tepeoba villages and asphalt road from Yaylaönü and Kalabak village like Çamdibi and Temaşalık village reach to.

Figure 3.5 : Map of balikesir,google earth map.

3.4 Morphology

Heights of Tepeoba region is approximately extended in NE-SW direction. Th most high hills are available at west and east part of field section. The most lower digit areas and canal drainages are at the middle section of the field (url-wikipedia).

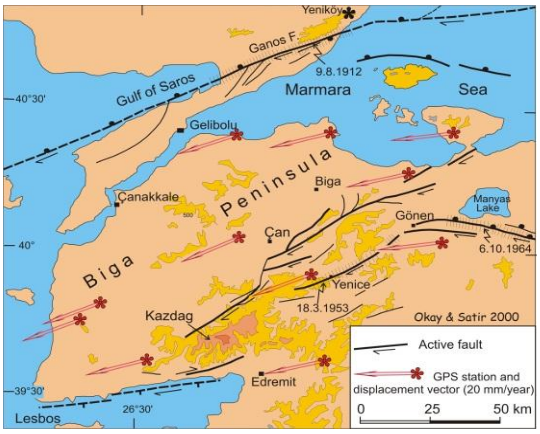

Figure 3.6 : Map of Biga Peninsula morphology by okay and satir 2000.

3.5 Climate and Vegetation

Tepeoba region's climate is related to The Mediterranean climate**,** the summer temperature of the angle of the sun's rays fall, drought depends on the air movement. The warmest month average 34-45 ° C, 8-10 ° C in the coldest month is average. The annual average temperature is 18 ° C. Snow and frost is very rare. Highest rainfall in the winter, at least, type of precipitation falls. Originate in the frontal rainfall in winter. Frontal rainfall occurs in this climate the most.

Annual rainfall varies according to altitude, Average 400-600 mm. Irregular rainfall Vegetation ,shrubs, respectively, barrenness of shrubs that can withstand the summer, Mersin, Laurel, Strawberry Tree, Olive, Oleander, Carob trees occurring in such a short stocky plant community(url-wikipedia).

3.6 Stratigraphy

The study area is approximately 10 km to the north of the town of Havran in the Balikesir province, is located in map sheets of İ18-d1-d2-d3-d4. In the geotectonical point of view, the field of study is located in the Sakarya Continental plate Şengör and Yılmaz, (1981) or the Sakarya Zone Okay, (1984) at Pontides Union.

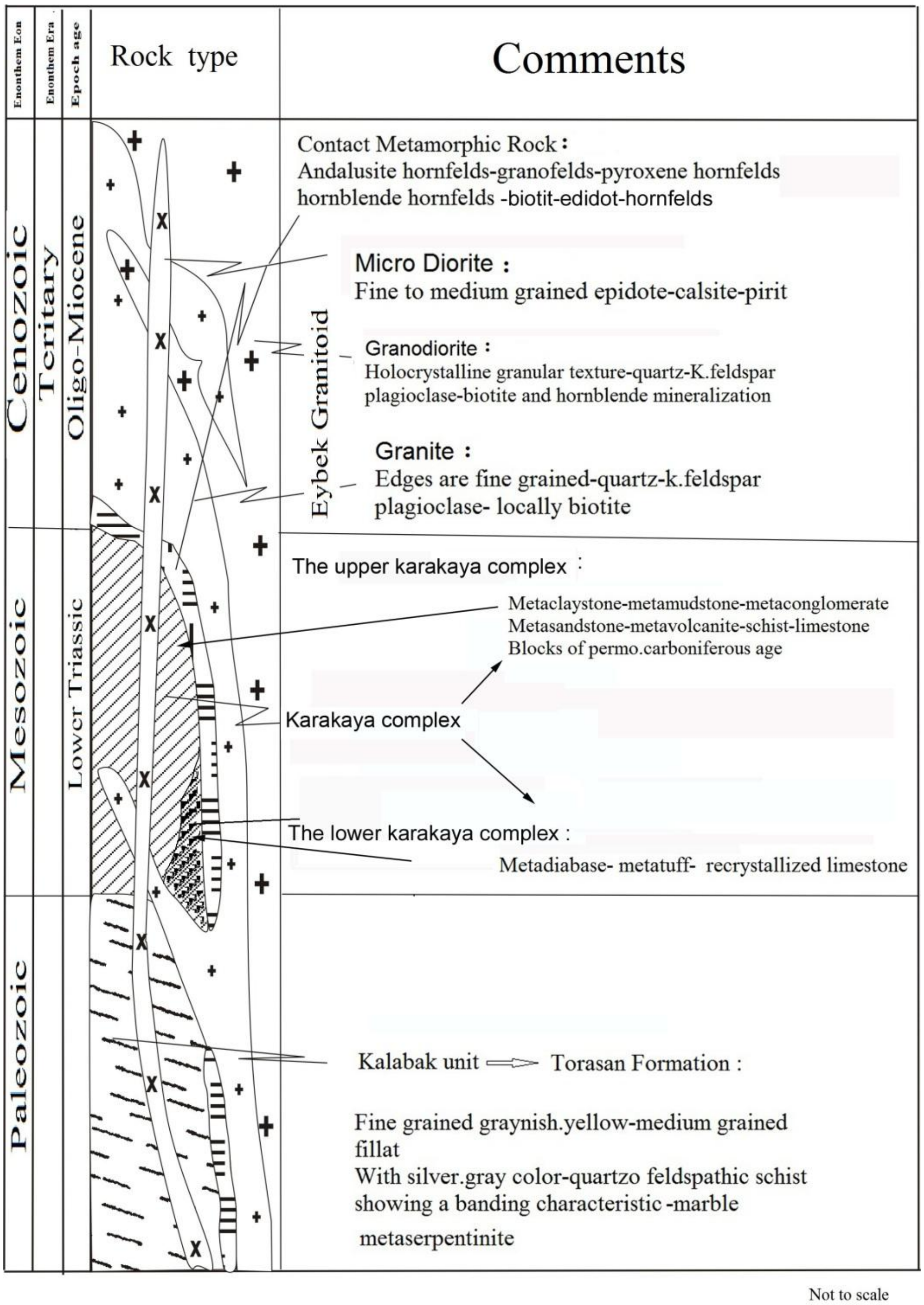

Figure 3.7 : Stratigraphic section of investigation area.

3.6.1 Torasan formation

This formation located approximately at center of field, it was extended from haciaslan hill at west and outcrop from kozcagiz hill from east and continues up to Tepeoba village, The Kalabak group rocks which are seperated from massives by detachment faults in Oligo-Miocene period, consists of schists which have different degree of metamorphism and origin (Torasan formation is continental). Torasan formation consists mostly flysch type deposits and sometimes basic and andesitic rocks. In Torasan formation the lithologies such as phillite, graphite schist, mica schist and garnet-sillimanite schist which are affected by different degree of regional metamorphism can be observed. The formation is intruded by granitic rocks in age from Early Devonian (399.6 Ma,Zircon age) to Dogger (171.1 Ma, Zircon age). The unconformities of Permo-Carboniferous, Triassic and Jurassic ages are observed on Torasan formation.

3.6.2 Karakaya Complex

This pre-Jurassic orogenic complex,that has a wide distribution in the sakarya zone,is first described from the Biga Peninsula by (Bingol et al,.1975).They described the karakaya formation as consisting of slightly metamorphosed,spilitic basalt with exotic upper permian limestone blocks, mudstone, radiolarite, quartzite, feldspathic sandstone ,conglomerate and siltstone which overlie unconformably the gneisses of the kazdag Group. The karakaya formation was ascribed an Early Triassic age based on the presence of exotic Upper Permian limestone blocks and the Middle Triassic limestone that were regarded as lying unconformable on the karakaya formation.Bingol et al.also pointed out to the wide distribution of the Karakaya Formation in the pontides and traced it from Biga Peninsula eastward to Ankara.Okay et al(1990) showed, Karakaya Complex in northwest Turkey that consists of several probably coeval, pre-Jurassic yectonostratigraphic units; In the Biga Peninsula four such major units are recognised in the Karakaya Complex: the Nilufer Unit, the Hodul Unit, the Orhanlar Greywacke and the Cal Unit.

At the study area, Karakaya forming rocks are mapped in detail. The Outcrop of Metasedimentary and metabasic rocks are surrounded by Yayla hill , Karayüksek hill ve Kumluca Valley and Tepeoba village with NE-SW extending direction.

The Folded formation has been heavily influenced by the tectonics. At the field, it primarily lost its own characteristics due to the granitoids intrusion, and often recognition of metasedimentary rocks, which is transformed to spotted andaluzite-biotite-muscovite schist, is really hard.

However, when we depart from the intrusion boundary to south gradually, spotted schists differ to claystone and then to arkosic sandstones adjoining to Tepeoba village. Formation often includes Permo-Carboniferous limestone blocks Next to Tepeoba village.

Karakaya Complex divided into two categories and describe provisionally the pre-

Jurassic epimetamorphic series under the heading of the Lower Karakaya Complex, and the overlying clastic and volcaniclastic series under the Upper Karakaya Complex.

3.6.2.1 The lower Karakaya Complex (metabasic members):

Passing through the boundary to Tepeoba village in south direction and located around yaylaonu village, as long as decreasment in metamorphism grade, lithology changes to Bazalt and Metabazalt. The last type is absolutely similar to Mehmetalan formation in the Karakaya complex group (Duru et al., 2004). Metabasite rocks of the field seem in black and greenish-black colors in macroscopic scale. In previous studies Metabasic rocks was considered as a part of SPO unit Bingöl et al., (1975), or Nilufer Unit (Okay et al., 1990). The Lower Karakaya Complex consists of a highly deformed sequence of metabasites intercalated with phyllite and marble. These three lithologies make up over 90% of the Lower Karakaya Complex. They are accompanied by minor amounts of metachert, metagabbro and serpentinite. The marble occurs both as syndepositional beds and as olistoliths. Due to intense boudinage, it is frequently difficult to distinguish boudins from olistoliths. In this study, metabasite rocks are not categorized as a separated formation, and mapped as metabasite member of the Karakaya complex.

Metabasic rocks have outcrops only around Yayla hill. Some cores, which were obtained from Meta-Sedimentary rocks, have been cut in angular form in range of 2-60 meters thickness. These are: TPS-1, TPS-9, TPS-10, TPS-16, TPS-19, TPS-21 and TPS-23. The majority of interlying metabasic rocks with Contact metamorphic rocks in the intrusion boundary consist of amphibolite-amphibolite schist, which is similar to metabazite bearing Kalabak Paleozoic schists (Sazak Meta-tuf).

3.6.2.2 The upper Karakaya Complex (metasedimentary rocks):

Samples of metasedimentary rocks in the field, are defined as cataclastic-andaluzite hornfels, mylonite, mylonitic hornfels, pyroxene hornfels (Küçükefe et al., 2005), metaconglomerate, sandstone, metasandstone. The same rocks, in another study about this field have been named andalusite schist, andalusite-muscovite schist, muscovite-andalusite schist, muscovite-andalusite-biotite schist (Watanabe et al., 2003). Silicified, biotitization, altrated rock, contact metamorphosed shale, pelitic hornfels and Phyllite have been recognized In applied borehole samples. According to Duru et al (2004), the metasedimentary rocks of the Hodul Formation (a piece of Karakaya Group) spreads both in horizontal and vertical directions. İn (Appendix–A).

3.6.3 Eybek granotoid

This name refers to Eybek Mountain, which is located in the northern part of the area. Eybek Granotoid covers north angle of the study area with approximately EW direction. According to Krushensky (1971), İntrusive mass consisting of the mixture of granodiorite-quartz monzonite has become light-colored, coarse grained, and with these properties is recognizable from porphyritic rocks. According to Ercan and Türkecan (1984) granodiorite has been miscible and mixed by orthoclase, plagioclase, quartz, hornblende, biotite and opaque minerals. According to Pluton, Ayan (1979) the rock mass can be named "hornblende-granodiorite". In the studied area, the peripheral zones of upper oligo-lower Miocene Eybek Granotoid, the outside granite zone and the interior granodiorite zone are mixed. The boundary of granite-ganodiorite from a place to place is transformed and sometimes tectonized. Acidic Granophyre grains are limited by granular basic veins (Küçükefe et al.,2005). According to relationship of the granitoid with its surrounding rocks, it would be said much younger than early Triassic. However, based on radiometric age determinations, pluton age is about 35-22 Ma (Oligo-Miocene) (Bürküt, 1966; Krushensky, 1976; Ayan, 1979; Bingöl et al., 1982; Watanabe et al., 2003). The results of borehole samples shows us four units extended in 4 different direction in field area.

Granit: The granodiorite and metasedimentary masses have outcrops extending to N-NE direction at the field.

The rock mass that has felsic minerals with mafic inclusion and is located next to granodiorite in the north should be called granite. The course-graded type is noted microgranite or aplitic granite (Kucukefe et al,2005).

Surveying practices between drilling and well logging operations revealed that that name is suitable. However, belonging to the analysis of microscopic samples, borehole logs illustrate being Locogranite of the mentioned rock. A granite which is formed by quartz, alkali feldspar (orthoclase) and plagioclase was recognized in applied samples from drilling cores.

It seems pink in color and with blocky index form. In some sample cores, mineral concentration is visible in a registerable amount (such as %0.3 equivalent for Cu). These zones are from MTA2006:

TPS-3: In range of 48.15-71.95, 85.00-87.00, 111.00-117.40 meters,

TPS-8: In range of 127.70-147.85, 186.00-198.00 meters,

TPS-11: In range of 211.50-215.50, 229.00-241.00 meters,

TPS-14: In range of 85.70-135.00 meters,

TPS-15: In range of 126.00-156.70 meters,

TPS-16: In range of 196.50-203.00 meters,

TPS-21: In range of 175.00-184.00, 212.00-214.00 meters and

TPS-25: In range of 230.00-257.20 meters.

Chalcopyrite, pyrite, molybdenite and magnetite mineralization is observed in the form of veins and veinlets at these zones. In some drillings (TPS-4, 5, 6, 7, 9, 10, 17, 18, 19) chalcopyrite, pyrite and molybdenite mineralization is observed with trace amounts.

In Some of the drill holes (TPS-5,TPS-15),it is very difficult to distinguish the exact boundary of granite and surrounding rocks. The fine granular Metasedimentary rocks have confined some pieces of underlying rocks in enclave form. A number of granite vein samples are such transition between rock and host rock ocurres in (TPS-2) and other ones are cut in 5-10 meter pieces (TPS-4). The boundary of granite and granodiorite is obvious through the Tepeoba to Kalkim road though, it is not this much obvious in the north part of granitoid body. Applied samples prove the fact: Amount of mica minerals (in biotite type) shows a gradual increasment passing through the boundary in TPS-4, TPS-6, TPS-7,TPS-8 samples. At the all of sample cores, contact metamorphism zone, crushed zone and granitoid zone have formed an interlying structure.

Analysis results on the granite, meta-sedimentary and metabasic rock samples illustrate that mica has been turned to andaluzite, biotite, muscovite, tremolite and aktinolite.

Quartz veins often (with 1-5cm thickness) intersect the granitoid mass in 1-2m intervals; Low-grade sericitification(turning to muscovite) process is usual next to these veins. The veins due to pegmatitization are bearing separated biotite, muscovite

and feldspars. Some parts transformed to Chalcopyrite, Molybdenite, limonitization and malachitization type oxidation is visible.
K-Ar proportion analysis on geological and core samples proved that the body age is about **34.7 ±1.0** Ma (Watanabe et al, 2003).
Another unit is granodiorite: The body extends in EW direction at the study area. It has contacts with Kalabak Paleozoic schists, Early-Triassic Karakaya Formation and granite in the eastern part of the area. This mass has been named “Granodiorite” by Küçükefe et al. (2005). This name is accepted in this study and furthur surveying has not been used. However, the microscopic analyses of core samples and logging exercises shows it’s better to call the body “granite”. It has more mafic minerals than granite even though, the rock properties are the same. Its norm minerals includes quartz, plagioclase, hornblende, biotite, sphen, apatite, carbonate and opaque minerals (obtained by petrographic determination).
it has obvious boundries with host rock and there isn’t any granite vein in the body(TPS-20). Any way, the granodiorite boundaries in both(TPS-20 and TPS-4) are such as crushed zones.
Granodiorite core samples entirely or seldom contains chalcopyrite. Mineralization is observed in several drill cores. For example:
TPS-5 Between 171.6-205.35 meters; chalcopyrite, molybdenite and pyrite mineralization in potasic zone, TPS-18 Between 179-181 meters; two molybdenite-rich quartz veins (potasic-phyllic zone) with 50 and 25 cm thickness. Granodiorite have cut meta-sedimentary rocks and imposed contact metamorphism with hornblende-hornfels facies to them in the study field (Krushensky, 1971). The age of 21.4 ± 0.6 Ma is derived from K-Ar method for this rock(Watanabe et al., 2003).
İn the study area two types of vein are obtained, one **is acidic rock veins** (Küçükefe et al.2005) called aplitic, well-grained, white to pinkish-white, 5cm-5m thick, 20-25m long which intered to contact metamorphic rocks, “Acidic rock veins” (figure2). This structure is thickly obvious in the north part of the field but is rare in the south and it blends to fine-grained microgranite in the boundary. One of obtained cores from this rock is named “granophyre”. For example, it is defined as porphyric microgranodiorite. Core samples are locally disseminated and pyrite, chalcopyrite and molybdenite mineralization is observed. The relative age of acidic veins which cause boundary fractures of intrusive mass during intrusion and crystallization, and intrusive rocks is the same(Oligo-Miocene).

Another one is **basic rock veins (**Küçükefe et al. 2005) have expressed that this part is the youngest unit of the study field. Basic veins cut Early-Triassic metasedimentary and metabasic rocks (Karakaya Formation) and the Oligo-Miocene aged Eybek Granitoid. Extending direction is normally N-E but locally is E-W. Its continuities was often interrupted because of new tectonics. The color has been changed to dark green and its mafic minerals changed to epidote, pyrite and calcite.

Core samples include micro quartz-diorite, quartz diorite and lava flow-form basic rocks. The texture is often granular and often microgranular. Pyrite veins are epidote-calcitic.

Enclaves are visible in Granite-granophyre body that is located in yayla hill-kumluca valley road. The result of core analysis says the same. Asidic rock stocks have got observed in the granodiorie rock in the Yayla hill cross road in the Tepeoba village - Kalkim road.

There is not anything definite about the age determination of the rock. Because of that, Oligo-Miocene age (belonging to the last stage of basic Eybek Granotoid lamprophyre is considered to be correct.

Last unit of eybek granite is **contact metamorphic rocks:** Eybek Granotoid caused contact metamorphism of metasedimentary and metabasite rocks of the Karakaya Formation in the Tepeoba area. As an effect of intrusion, in meta-sedimentary rocks, andalusite, biotite, muscovite, corundum and often silimanite; and in metabasic rocks tremolite, actinolite, plagioclase and somewhere garnet minerals got generated.

Tertiary aged Eybek Granotoid has cut Paleozoic Kalabak schists and imposed contact metamorphism on the mass in the east part of the study area.

Contact metamorphic zone extends from interface of Kumluca and Beşgere valley parallel to intrusion boundary to Kozcağız cemetery in the approximately NE direction. According to previous studies in the field, the width of the contact metamorphic zone reaches up to 2 km in some places, particularly in marble and spilitic rocks in Kalabak schists (Cetinkaya et al., 1983).

Magnetite mineralization is developed in skarn zones of marbly part of the kalabak schists in Atizi location. Low-grade copper concentration is accompanied by magnetite mineralization. Turning into garnet due to intrusion is locally observed in marble. Pistasite, actinolite, diopside, vezuvianite, hidrogrosularite and other skarn minerals have been observed along garnet minerals (Krushensky, 1971).

Contact metamorphic rocks are named "phyllite", "contact metamorphic rock" and "pelitic hornfels" as a result of microscopic examination in drilling cores. Similarity of contact metamorphism minerals and magmatic-hydrothermal minerals (biotite, tourmaline, quartz, muscovite) made it difficult to correlate alteration properties and borehole analysis results on the field. Andalusite, biotite, muscovite and corundum minerals in "hornblende-hornfels" facies and sillimanite mineral occurrence in "pyroxene-hornfels" facies suggests that contact metamorphism probably has been occured. (Küçükefe et al. 2005). (see all formations of study area on Appendix-A).

3.7 Magmatism

Igneous rocks characteristics are entirely described above. Formation of these diverse rocks in a magma chamber depends on magmatic differentiation and or contamination or magma "migning / mixing" "thermo-gravitational" model. In fact, this acidic rocks, occupy the upper part of the magma chamber, and rocks which are less acidic and relatively dense fill the inner parts of the magma chamber. Naturally, the acidic and basic vein rocks reflect the features of the feeding sector (Boztuğ and Otlu, 2001). However, difference in age of magmas or "gravity differentiation" of the same rock would possibly cause to have various magma compositions.

As mentioned, even rare presence of sillimanite in contact metamorphic zone brings to mind the possibility of "pyroxene hornfels" facies grade of contact metamorphism occurence in host rocks. However, the highest grade of metamorphic facies developing around granitoidic composition of magmas are hornblende-hornfels facies (Winkler, 1977). In this case, contact metamorphism of gabbroic magma (more basic and older than granitoid) might form a granite and granodiorite-rich composition during the evolution of magma in the crust (magma differentiation-assimilation-contamination and mining / mixing). Perhaps, the young, often completely granular, rarely intrrupted by acidic vein rocks, epidote, calcite, pyrite-rich microdiorite dikes are a product of this basic magma. Igneous rocks has been totally described in "Stratigraphy" chapter .

3.8 Metamorphism

During Hercynian and Alpine orogeny, Kalabak Paleozoic schists have been affected by the Alpine orogeny due to Early-Triassic Karakaya Formation, in general, spent green schist metamorphism facies. It is not clearly discussed whether regional metamorphism is the forming factor of observed minerals (such as andalusite, tourmaline, biotite, muscovite, corundum and sillimanite) or the factor is partial contact metamorphic. Toward north direction right to intrusion sequence, the metasedimentary rocks in some places transform to gneiss, metabasite also amphibolite and amphibolite schist. Increasement in metamorphic grade toward the north can be explained as a reason of this transformation (regarding to the highest degree of contact metamorphism in the area (pyroxene-hornfels).

3.9 Structural Geology

Until Late-Miocene, probably granite and granodiorite compound (Eybek Granotoid) rocks were formed by N-S the influence of compressional regime on its remaining region. Microdiorite dikes spread might be controlled by N-S E-W extension which has also formed compressional regime.

E-W compressional and N-S tensional stress regimes have been subjected to Biga Peninsula and in a larger scale to Anatolia plate during neotectonic period.
NS extending, 1 km long, with about 70 degrees westward tilt, two reverse faults, in the eastern area of the Kumluca valley and strike-slip fault which brought together the metamorphic contact and granitoid masses with approximately 500 m length, probably are developed as a result of compressional regime. Four dip-slip normal faults which have cut the field in E-W direction are resultants of the N-S extensional fault.

4. GEOCHEMICAL PROSPECTING

4.1 Geochemical analyses for major elements

Major element compositions of pre-mineralization, mineralized, and post mineralization rocks have been determined for many individual porphyry copper deposits and districts. For rock geochemistry I used TAS diagram method to figure out the classification of volcanic samples and the result are based on the total alkali (Na_2O + K_2O wt. %) vs. SiO_2 classification TAS diagram in (Figure 4.1) Wilson, (1989), samples from copper molybdenum deposit are mostly granite, and also show the range between monzonite and quartz monzonite and siyenite are include in diagram. SiO_2 content in volcanic rocks efficiently separates petrographical suites: it is below 50 wt% in the mafic suite, between 50 and 60% in the tonalite suite and approximately between 62 to 72% in the granite suite.

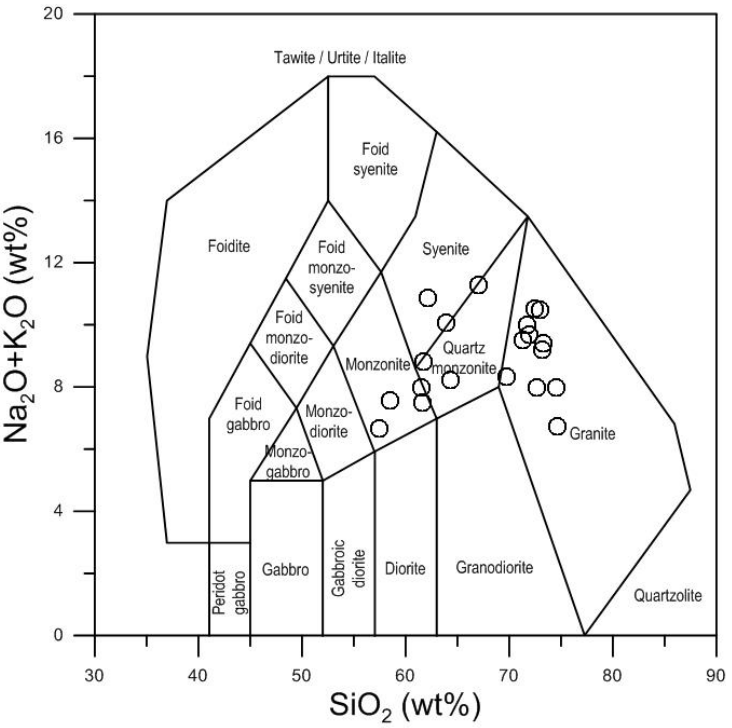

Figure 4.1 : Based on the total alkali (Na2O + K2O wt. %) vs. SiO2 classification TAS diagram (e.g., Wilson, 1989), samples from copper molybdenum deposit are mostly granite, and also show the range between monzonite and quartz monzonite and siyenite are include in diagram.

4.1.1 Results of Major Elements

Most of the samples show large variation in their elemental concentration. For example, SiO_2 which plays an important role in the determination of various rock types ranges from 60 wt% to 73.25 wt% with an average of 64.50 wt% for the mafic volcanics. Fe_2O_3 contents in these volcanic ranges from 3.5 wt% to 10.7 wt% with an average of 7.1 wt%. Al_2O_3 varies from 14 wt% to 19.73 wt% with an average of 16.8 wt%. A few variations are also observed in CaO contents. It ranges from 1.5 wt% to 7.79 wt% with an average of 4.6 wt%. K_2O varies from 2.5 wt% to 7.73 wt% with an average of 5.1 wt%.TiO_2 show fewer variations from 0.3 wt% to 0.7 wt% with an average of 0.5 wt%. P_2O_5 ranges between 0.05 wt% and 0.34 wt% with an average of 0.19 wt%.

Discussion:

This study reports geochemical compositions of samples with specific locations for copper-molybdenum deposit. And figure out that majority of sample of volcanic rocks are belongs to granit and others are detected between monzonite and quartz monzonite and siyenite in diagram.

4.1.2 Basic Harker diagram for major elements

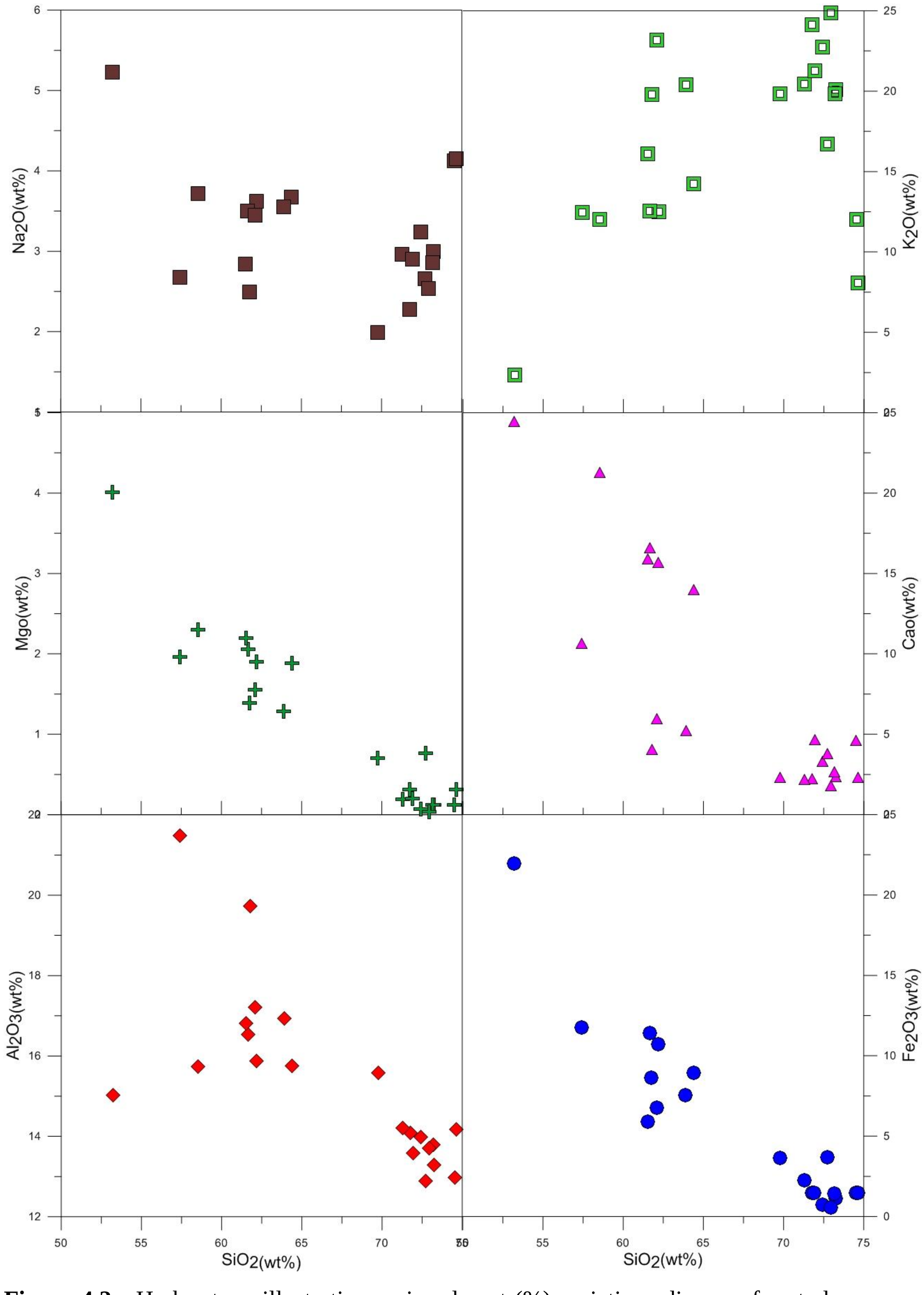

Figure 4.2 : Harker type illustrating major elemet (%) variations diagram for study area.

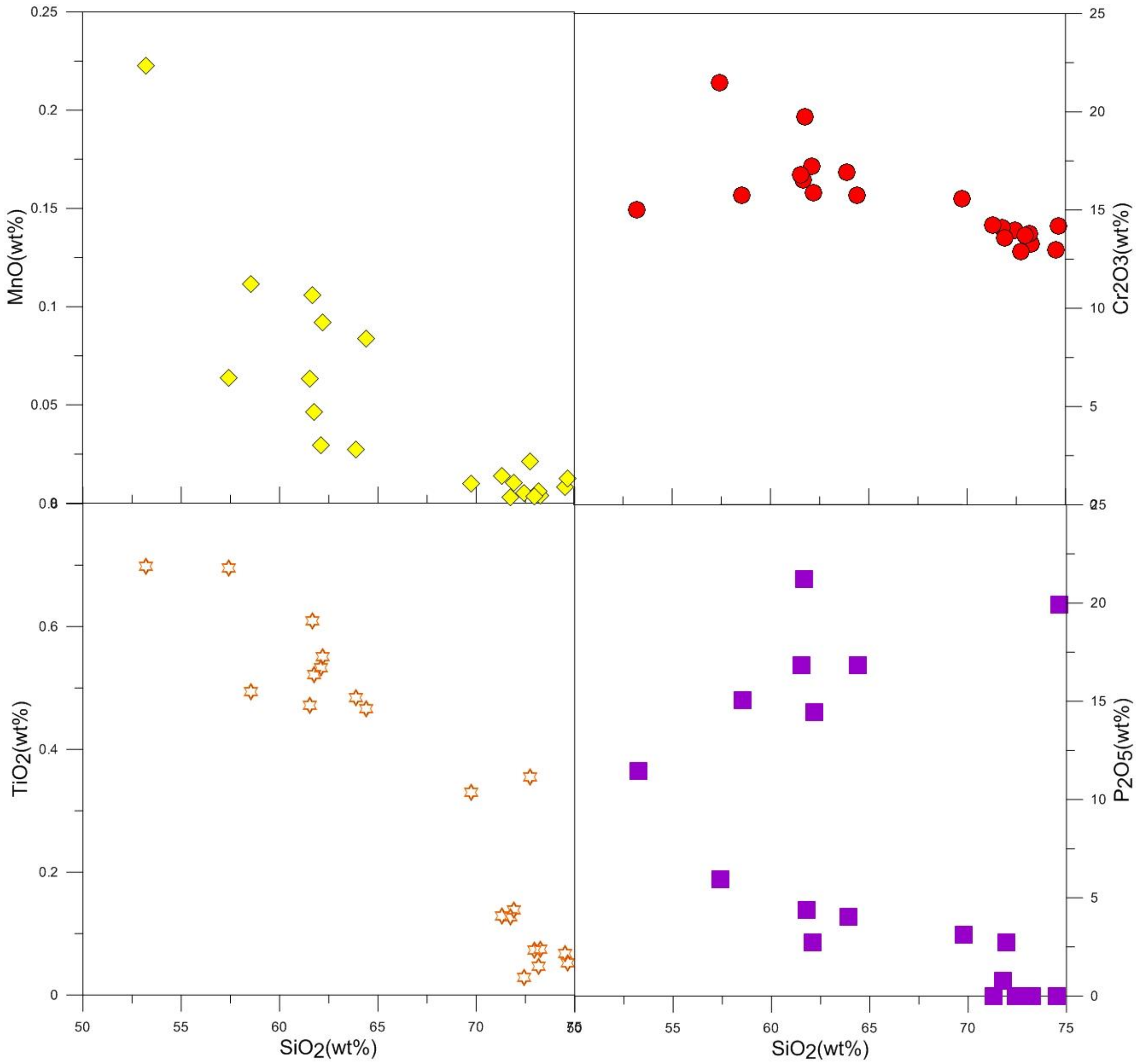

Figure 4.3 : Continuing of Harker type illustrating major elemet (%) variations diagram for study area.

The oldest method is the variation diagram or Harker diagram which dates from 1909, and plots oxides of elements against SiO_2. SiO_2 is generally chosen because it is the most abundant oxide in igneous rocks and exhibits a wide variation in composition.

Basic Harker diagrams show that K_2O increases with increasing SiO_2 and Cr_2O_3 remains constant with increasing SiO_2. Oxides Al_2O_3, Fe_2O_3, CaO, MgO, P_2O_5, MnO, Na_2O and TiO_2 decrease with increasing SiO_2, consistent with fractional crystallization of plagioclase, alkali feldspar, amphiboles, biotite, muscovite, quartz, magnetite, and titanite phases, respectively. Figure 4.2 and 4.3 shows two Harker diagrams that display patterns consistent with fractional crystallization common in granites.

4.2 Optical Mineralogy and Petrography Study for Each Formation

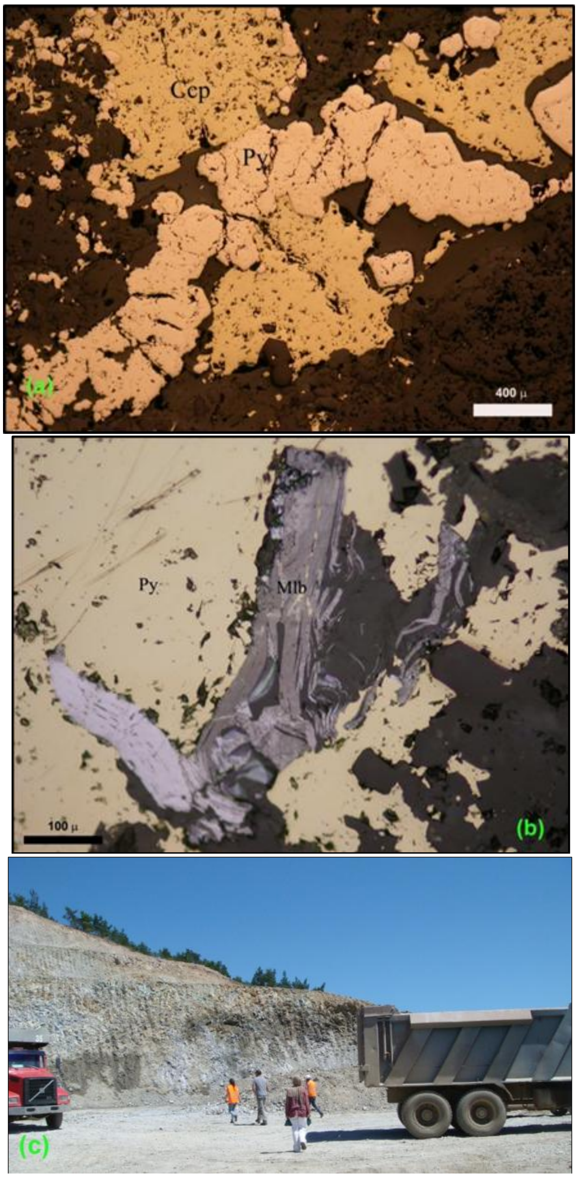

Figure 4.4 : a) Polished section of ore microscopy photograph that was observed calcopirite and pirit mineralization. b) Polish section of ore microscopy photograph was observed molybdenite and pirit mineralization . C) field study of mining area (people are for scale)

4.2.1 Torasan Formation

The Kalabak group rocks which are seperated from massives by detachment faults in Oligo-Miocene period, consists of schists which have different degree of metamorphism and origin (Torasan formation is continental). Torasan formation consists mostly flysch type deposits and sometimes basic and andesitic rocks. In Torasan formation the lithologies such as phillite, graphite schist, mica schist and garnet-sillimanite schist which are affected by different degree of regional metamorphism can be observed. The formation is intruded by granitic rocks in age from Early Devonian (399.6 Ma,Zircon age) to Dogger (171.1 Ma, Zircon age). The unconformities of Permo-Carboniferous, Triassic and Jurassic ages are observed on Torasan formation.

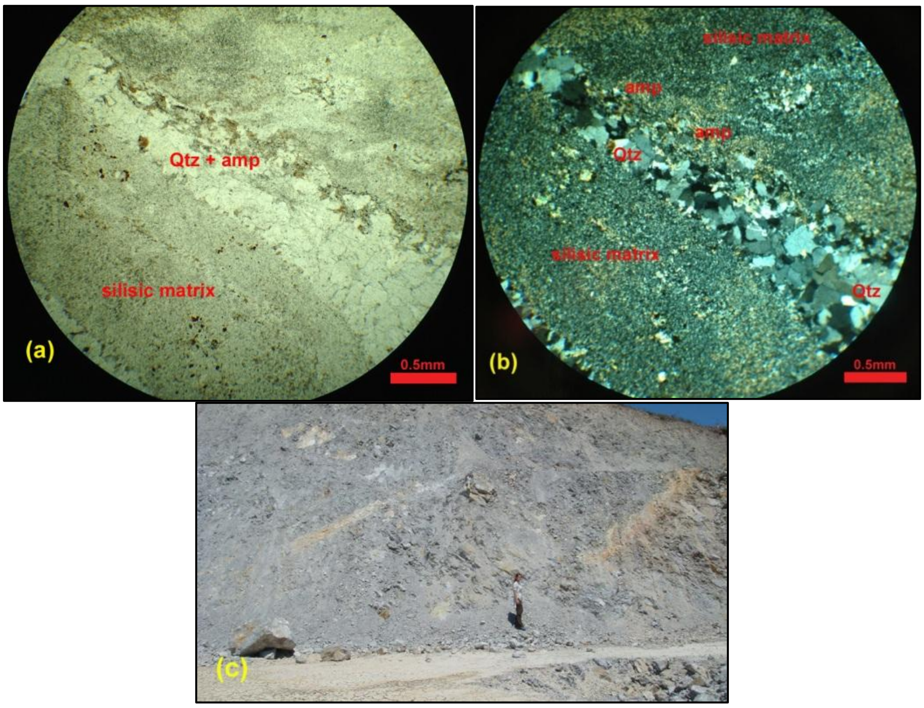

Figure 4.5 : (a) Thin section photograph of Torasan formation, sample is biotit-phyillate that consist, quartz-amphibolite- with fine grained silisic matrix texture in plane polarised light. (b) Granite that consist, quartz-amphibolite- with fine grained silisic matrix texture in cross polarised light. (c) Field photo of Torasan Formation (people in background is for scale). (sample No:50).

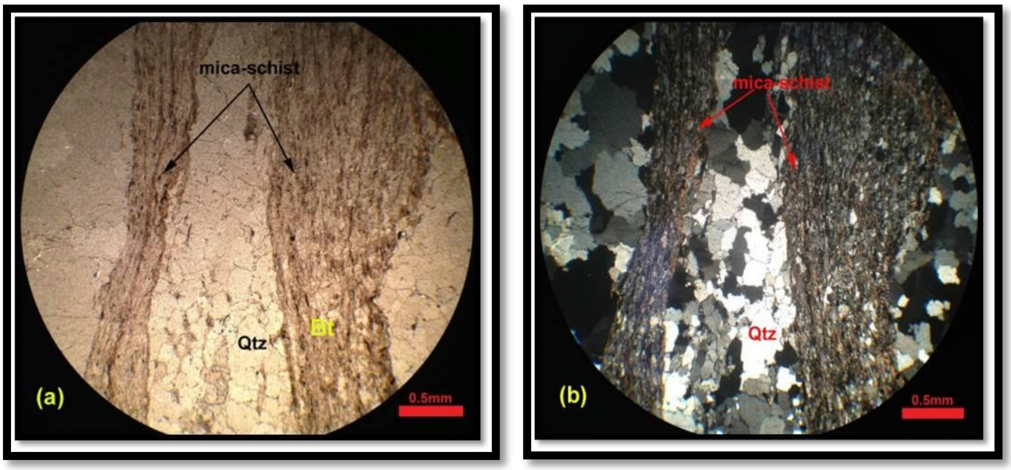

Figure 4.6 : (a) Thin section sample from Torasan formation ,describe as higher temperatures of metamorphism, new mica flakes grow larger. If they line up parallel to each other, they form a schistosity - the rock will split along these directions- this sample has quartz-micaschist –biotit-muscovite in plane polarized light. (b) Thin section sample from Torasan formation, describe as higher temperatures of metamorphism, new mica flakes grow larger. If they line up parallel to each other, they form a schistosity - the rock will split along these directions- this sample has quartz-micaschist–biotit-muscovite in cross polarized light.(sample no: 53 in table).

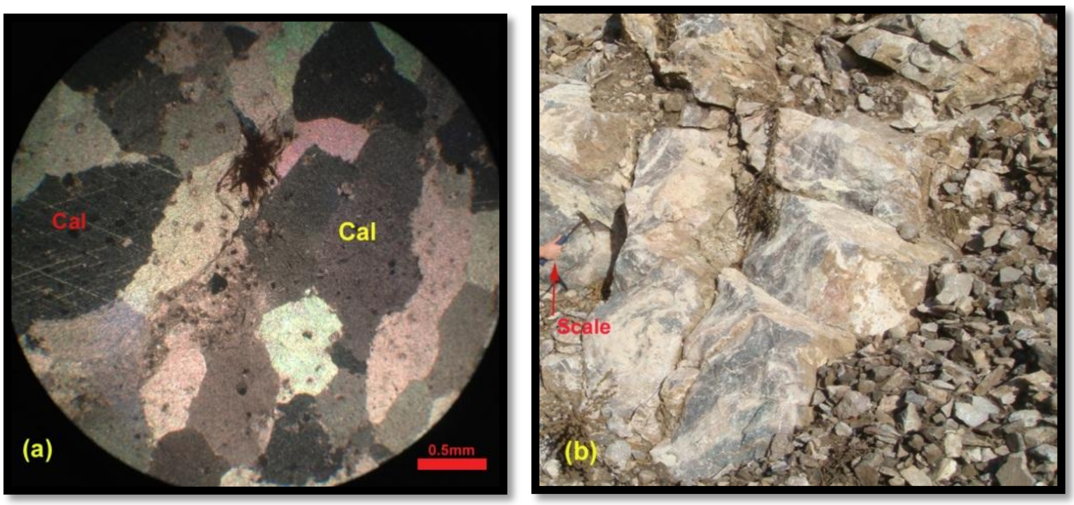

Figure 4.7 : (a) Metamorphosed limestone is called marble from Torasan formation. Calcium carbonate re-forms itself into larger, interlocking crystals of calcite in cross polarised light. (b) Field photo of Torasan Formation. (sample no: 76).

Table 4.1 : The result of XRF major element of ore samples for Torasan formation.

Sample (wt%)	SiO2	Al2O3	Fe2O3	MgO	CaO	Na2O	K2O	TiO2	P2O5	MnO	Cr2O3	LOI	TOTAL
53	59.68	16.23	6.95	4.58	1.69	3.34	2.46	0.71	0.25	0.13	0.02	3.76	99.82
50	63.9	16.93	3.03	1.28	1.64	3.55	6.53	0.48	0.06	0.03	-	2.06	99.49
76	1.21	0.66	3.37	1.99	50.89	0	0.01	0.04	0	0.08	0	41.68	99.92

4.2.2 Karakaya complex

This pre-Jurassic orogenic complex, that has a wide distribution in the sakarya zone, is first described from the Biga Peninsula by Bingol et al. They described the karakaya formation as consisting of slightly metamorphosed, spilitic basalt with exotic upper permian limestone blocks , mudstone, radiolarite, quartzite, feldspathic sandstone, conglomerate and siltstone which overlie unconformably the gneisses of the kazdag Group. The karakaya formation was ascribed an Early Triassic age based on the presence of exotic Upper Permian limestone blocks and the Middle Triassic limestone that were regarded as lying unconformable on the karakaya formation,(Bingol et al2007). At the study area, Karakaya forming rocks are mapped in detail. The Outcrop of Metasedimentary and metabasic rocks are surrounded by Yayla hill , Karayüksek hill ve Kumluca Valley and Tepeoba village with NE-SW extending direction.

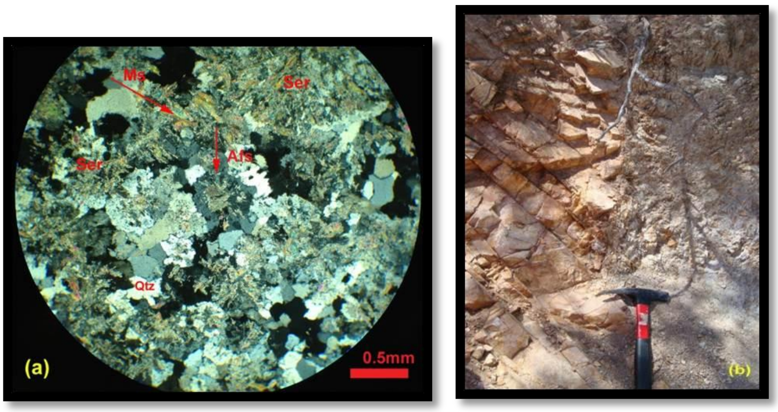

Figure 4.8 : (a) Thin section of Karakaya complex area, showing quartz-Sericite schist with hight amount quartz- alkali, this sample is granite between crossed polarisers. The rock is made up of interlocking rectangular feldspars and irregular clear quartz, all in shades of dark grey through to white. The crystals showing yellow colours are mica (muscovite) in cross polarising filters. (b) Photo of field that is belong to karakaya complex(object is for scale). (Sample no:6).

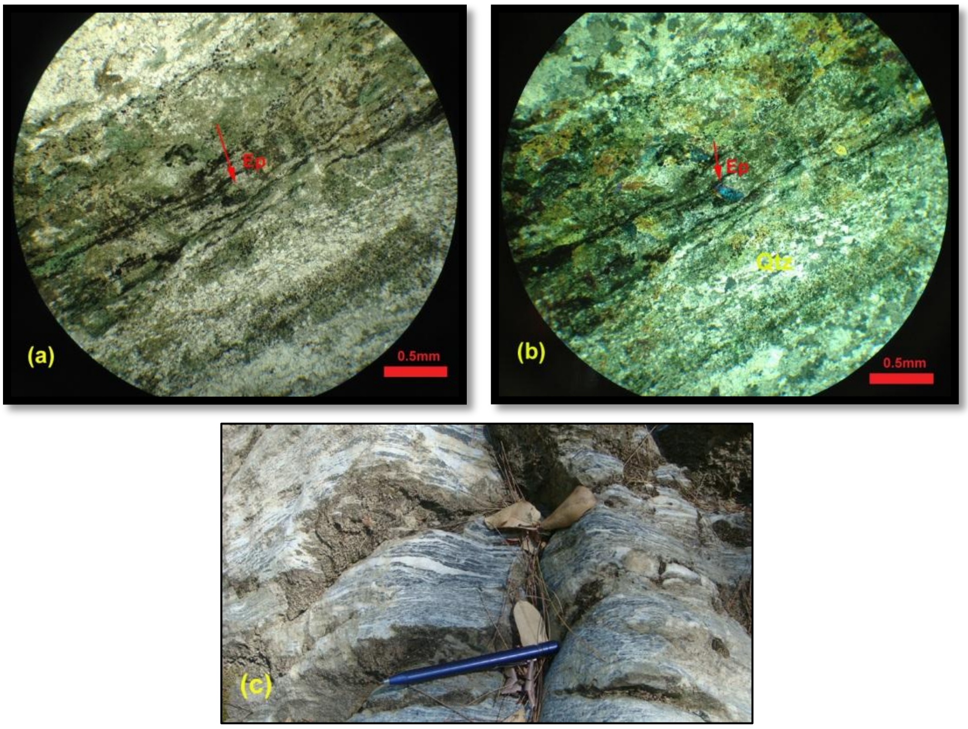

Figure 4.9 : (a) Thin section sample from Karakaya complex is containing calcite, quartz, epidote, carbonateschist in plane polarized light. (b) Thin section sample from Karakaya complex is contain calcite, quartz, epidote, carbonateschist in cross polarized light. (c) Field photo of Karakaya complex (pen is for scale).(sample no :55).

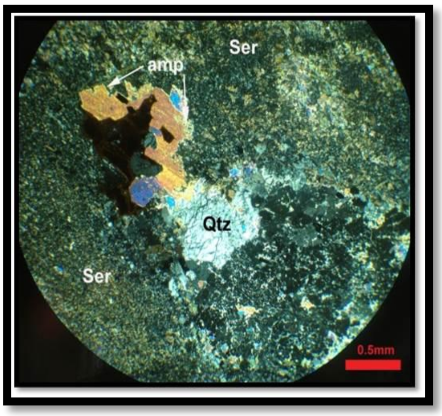

Figure 4.10 : Thin section photograph of karakaya complex is , it has quartz-sericite-amphibolite-background sericite texture in cross polarized light.(sample no 48-2 in table).

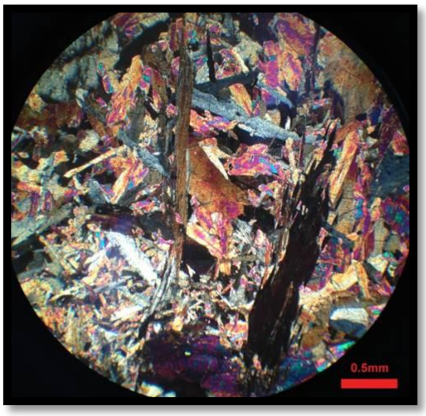

Figure 4.11 : Thin section photofraph of karakaya Complex is Amphibolite, it contains 90% of Amphibol. There has been a certain amount of contact metamorphism by adjacent granitic masses for the appearance of this texture. Sample no :51.

Table 4.2 : The result of XRF major element of ore samples for Karakaya complex.

Sample (wt%)	SiO2	Al2O3	Fe2O3	MgO	CaO	Na2O	K2O	TiO2	P2O5	MnO	Cr2O3	LOI	TOTAL
6	73.88	14.68	1.72	0.46	0.18	0.41	4.41	0.1	0.01	0.01	-	3.94	99.81
55	14.28	5.58	6.19	5.26	40.26	0.38	1.27	1.27	0.16	0.07	0.02	25.02	99.76
51	43.11	11.16	13.61	12.81	10.69	2.15	1.61	2.87	0.47	0.19	0.09	0.18	99.57
48-2	49.38	24.79	5.38	2.21	5.2	3.33	4.09	0.87	0.12	0.08	0.01	3.52	98.99

4.2.3 Eybek Granotoid

This name refers to Eybek Mountain, which is located in the northern part of the area. Eybek Granotoid covers north angle of the study area with approximately EW direction. According to Krushensky (1971), İntrusive mass consisting of the mixture of granodiorite-quartz monzonite has become light-colored, coarse grained, and with these properties is recognizable from porphyritic rocks. According to Ercan and Türkecan (1984) granodiorite has been miscible and mixed by orthoclase, plagioclase, quartz, hornblende, biotite and opaque minerals. According to Pluton, Ayan (1979) the rock mass can be named "hornblende-granodiorite". In the studied area, the peripheral zones of upper oligo-lower Miocene Eybek Granotoid, the outside granite zone and the interior granodiorite zone are mixed. The boundary of granite-ganodiorite from a place to place is transformed and sometimes tectonized. Acidic Granophyre grains are limited by granular basic veins(Küçükefe et al.,2005). According to relationship of the granitoid with its surrounding rocks, it would be said much younger than early Triassic. However, based on radiometric age determinations, pluton age is about 35-22 Ma (Oligo-Miocene) (Bürküt, 1966; Krushensky, 1976; Ayan, 1979; Bingöl et al., 1982; Watanabe et al., 2003).

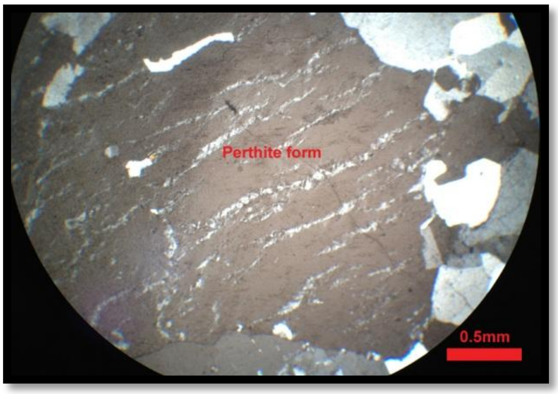

Figure 4.12 : Thin section photograph is showing Biotit-granite from Eybek granodiorite with Perthite texture from a metaluminous biotite granite. The lighter irregular stripes and patches of bright yellowish-white albite between dimmer gray stripes and patches of microcline. The color difference is mostly caused by the different optical orientations of the two different minerals in cross polarized light.(sample no:20 in table).

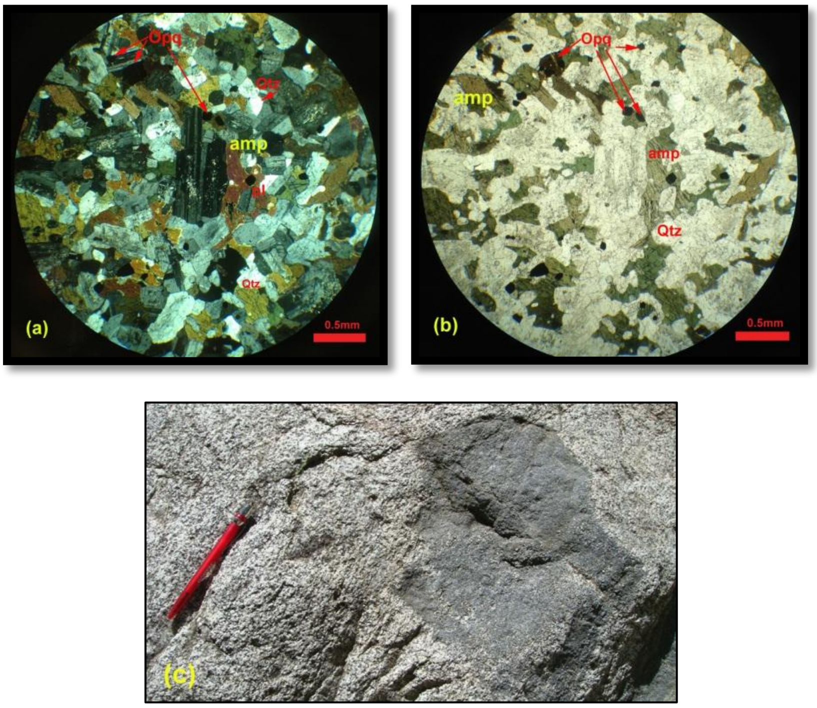

Figure 4.13 : (a)Thin section photograph is showing granodiorite from Eybek granitoid.it is very similar to granite. It has less of the potassium variety of feldspar, more of the sodium feldspar (plagioclase). The dark minerals in this rock include green hornblende and brown mica (biotite).Plagioclase amount is 40%, alkali feldspar amount is 30%, amphibolite amount is 20%,biotit amount is 15%,sphene 2%.sample has opaque minerals in cross plane polarized light. (b) thin section is

showing granodiorite in plane polarized light. (c) Field photo of Eybek granotoid(pen is for scale).(sample no:25 in table).

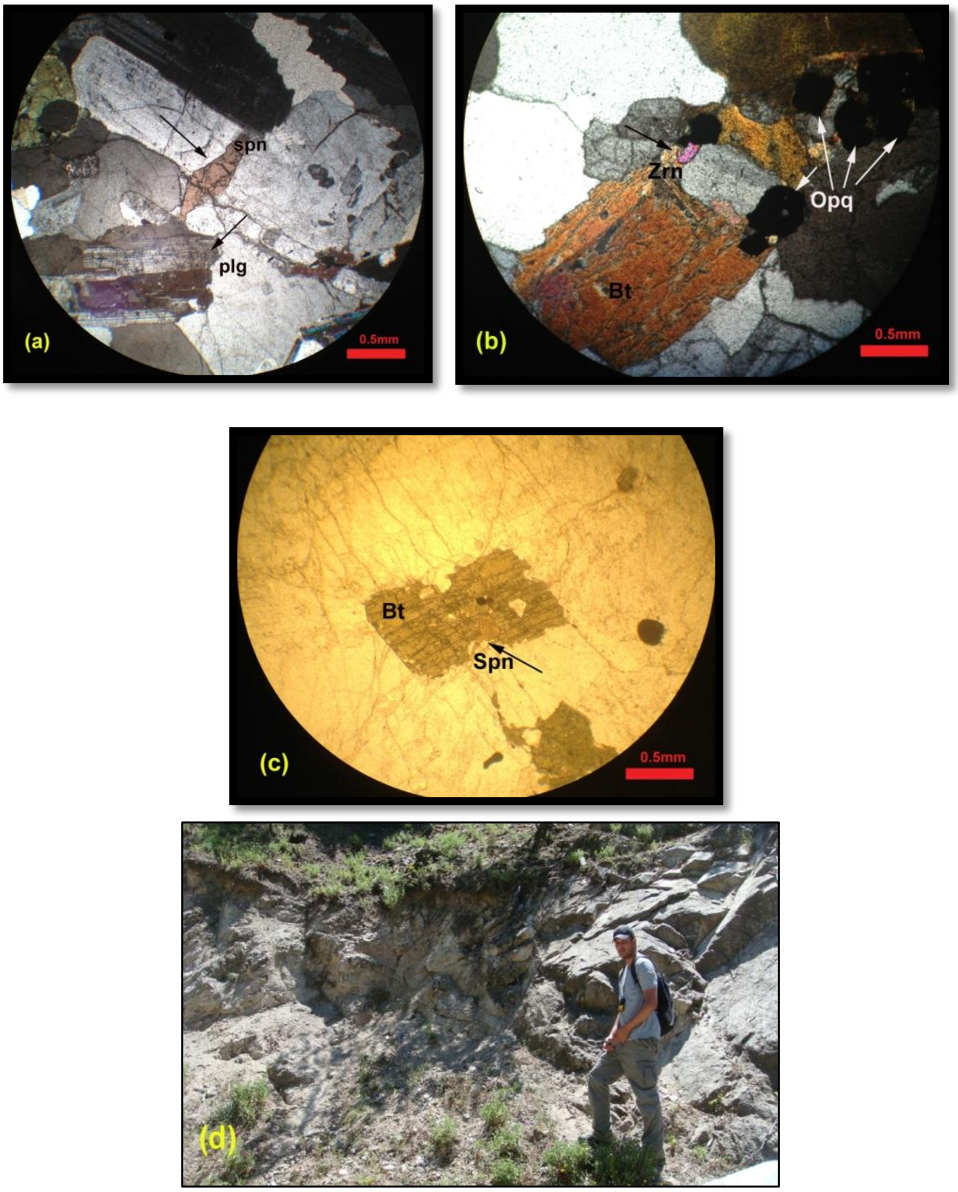

Figure 4.14 : (a) Thin section photograph of Eybek granotoid is showing granodiorite with sphene and high amount of plagioclase in cross polarized light. (b) Thin section photograph of Eybek granotoid is showing zircon and biotit with opaque minerals in cross polarized light. (c) Thin section photograph in Eybek Granotoid is showing a primary (chloritized) biotite crystal rimmed by finer grained secondary biotites.it contains opaque minerals-alkali feldspar-quartz in plane polarized light .(d) Field photo of Eybek granotoid(people is for scale). Spn=sphene, plg=plagioclase, Zircon=zrn, biotit=bt, opaque = opq.(Sample no :33 and 44 in table).

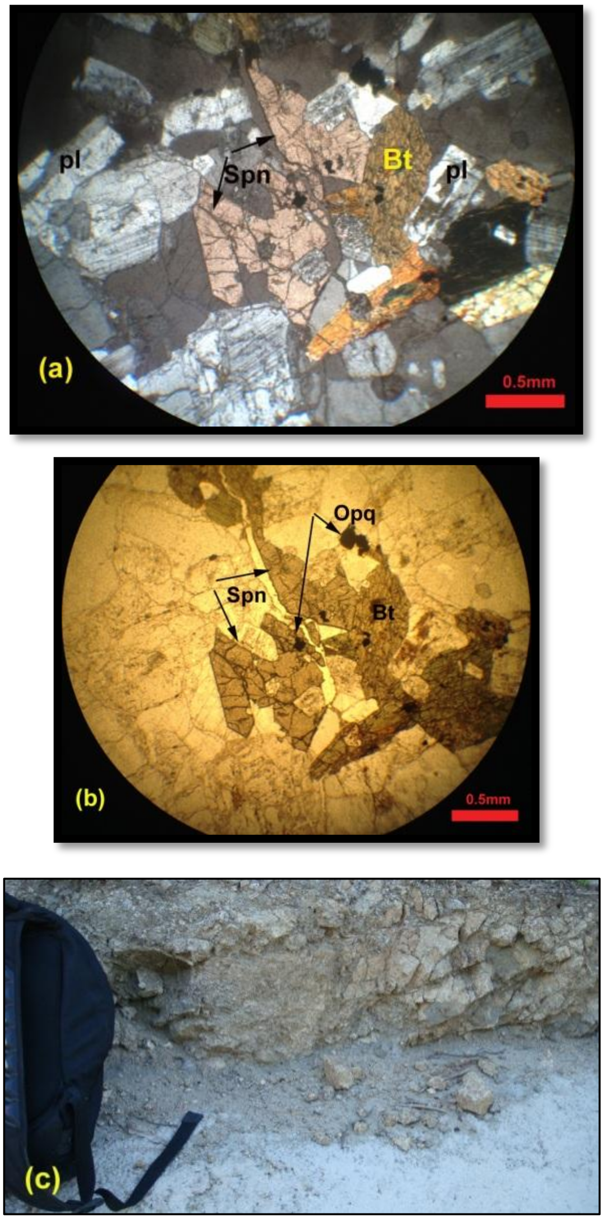

Figure 4.15 : (a) Thin section photograph is granite of Eybek granotoid, it have amphibolite- Plagioclase and alkali feldspar are at the same amount- quartz-high amount of sphene- biotit- This sample has more biotit and amphibolite than other granite samples-contain opaque minerals in cross polarized light.(b) Thin section photogragh is granit in plane polarized light. (c) Field photo of Eybek granit(bag is for scale).sample no 15.

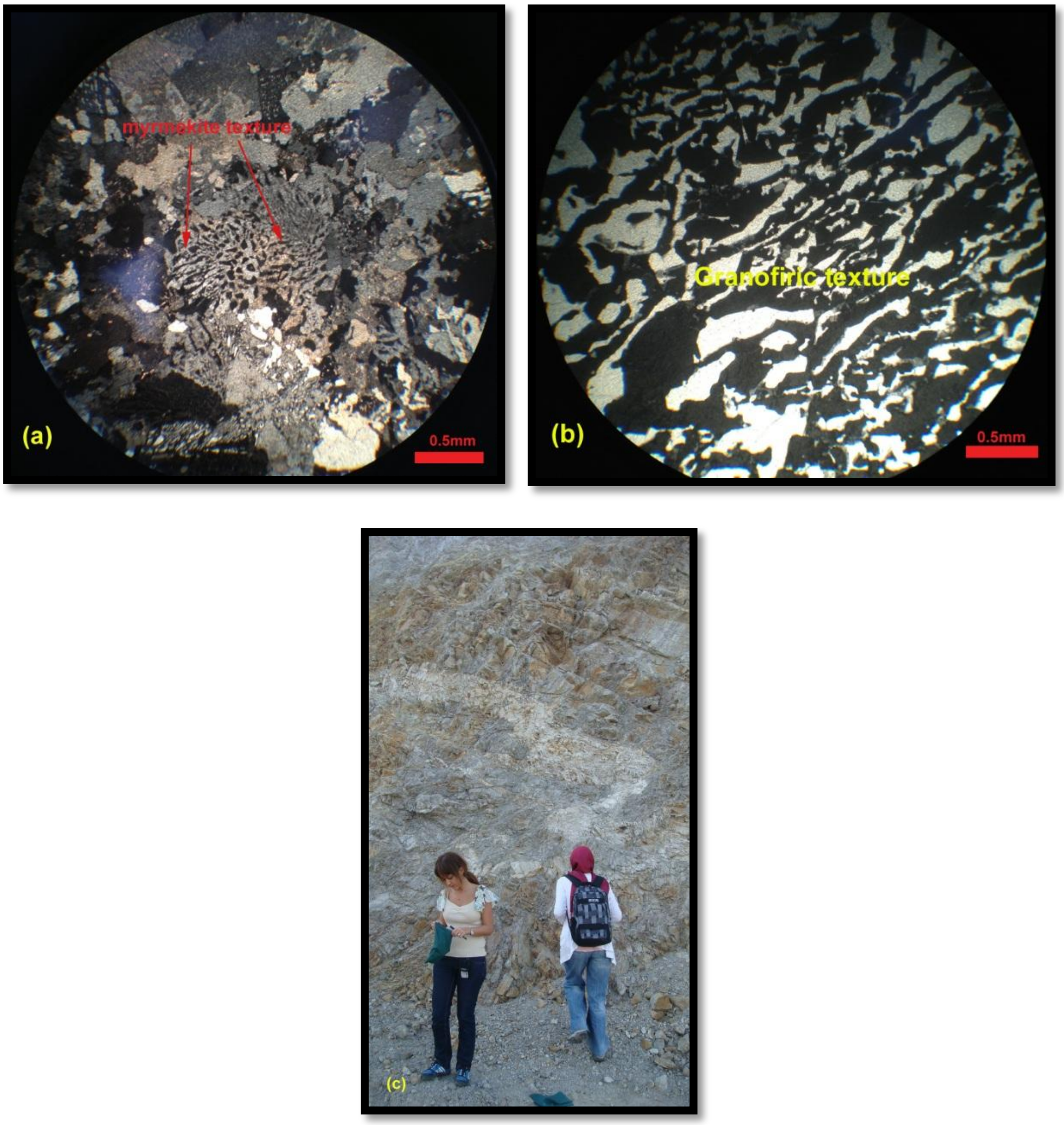

Figure 4.16 : (a) Myrmekite patch that appears to be replacing microcline. Twins in the myrmekite clearly show that the quartz "worms" are in a plagioclase matrix. Myrmekite is a subsolidus reaction texture that generally results from fluid flow. Here, K-feldpar was removed and quartz and plagioclase deposited in its place with fine-grained granite in cross polarised light. (b) Granophyr from Eybek granotoid. It is commonly coarse-grained and consists of about 3 parts granophyric intergrowth of quartz and feldspar to 1 part plagioclase, with minor amounts of biotite and opaque oxide minerals,it contains fine-grained granite displaying granophyric texture in cross polarised light. (c) Field photo of Eybek granotoid (people in background is for scale). (sample no:59)

Table 4.3 : The result of XRF major element of ore samples for Eybek granotoid.

Sample (wt%)	SiO_2	Al_2O_3	Fe_2O_3	MgO	CaO	Na_2O	K_2O	TiO_2	P_2O_5	MnO	Cr_2O_3	LOI	TOTAL
15	58.54	15.74	5.06	2.3	6.78	3.72	3.84	0.49	0.24	0.11	-	2.83	99.66
20	72.43	13.98	0.3	0.07	1.03	3.24	7.28	0.03	0	0.01	-	1.47	99.82
25	49.6	17.1	9.06	5.16	7.3	3.38	3.05	1.49	0.6	0.19	0.01	2.75	99.68
33	62.2	15.88	4.29	1.9	4.98	3.62	4	0.55	0.23	0.09	-	1.9	99.64
59	59.92	20.55	4.25	1.31	2.09	2.1	5.38	0.64	0.09	0.05	0.01	3.33	99.72
44	61.65	16.54	4.57	2.06	5.28	3.5	4.01	0.61	0.34	0.11	-	0.98	99.64

Conclusion of thin sections :

Thin section images document a complex history including magma mixing, multiple episodes of brittle deformation, and alteration.

5. SUBSURFACE MODELLING OF PORPHYRY COPPER DEPOSIT

5.1 Introduction

Three dimensional (3D) interpretations of subsurface characteristics have been realized in the mining sector for a long time. Before the use of “state-of-the-art” computer software, portrayal of the three-dimensional features was done using two-dimensional (2D) specialized maps, cross-sections, and fence diagrams. Currently, it is possible to construct 3D subsurface models easily using 3D Geoscientific Information Systems (3D GSIS), which have efficient data-management capabilities (Rahman 2007). In the last two decades, the number of 3D subsurface modeling studies has increased due to the use of computer software (e.g. Renard & Courrioux 1994; de Kemp 2000; Xue *et al.* 2004; Feltrin *et al.* 2009; Ming *et al.* 2010; Akıska *et al.* 2010a).

The main aim of 3D modeling of ore deposits is to determine the complex geological, structural, and mineralogical conditions in these areas and to detect the location of these deposits in the subsurface environment. With the help of recent 3D subsurface modeling studies, some information can be gained not only about detecting ore locations but also about the formation conditions of the deposits (e.g. Feltrin *et al.* 2009). Optimizing the subsurface data collected from various sources (boreholes, geophysical methods, well logs, etc, could minimize the costs of many operations. Because of the complex spatial relationship existing in the subsurface environment, regularly spaced boreholes and good-quality data are necessary to solve this complexity (Hack *et al.* 2006). However, this situation is not always possible due to economic constraints and the difficulties of field conditions. In Turkey, some institutions such as MTA (General Directorate of Mineral Research and Exploration of Turkey), TPAO (Turkish Petroleum Corporation), DSI (General Directorate of State Hydraulic Works), and others have thousands of meters of borehole log data. This data was interpreted with the old technology, and much of it is not used today. In fact, some of this data was taken casually and could not be associated with the subsurface characteristics (especially due to the technological deficiencies at that time) and/or could not be interpreted due to inadequacies in the number of boreholes in the study areas. With the development of technology, this unused data needs to be gathered and reviewed. New ore zones can then be detected, and unnecessary costs can be prevented by means of the reviewed data.

5.2 Methods and Approach

As pointed out previously, subsurface modeling studies are quite important in mining sectors, and detailed modeling studies can be achieved as a result of developments in computer technology. Particularly, assigning adit directions accurately in an underground mining area can reduce the various operating costs associated with minin In this study several software programs that are used for surface and subsurface modeling and accomplished with commercial RockWorks15® software, which enables the use and capability of the interpretation in conjunction with all of the data in much less time. This program includes two main windows: *Borehole Manager* and *Geologic Utilities*. *Borehole Manager* contains the borehole procedures such as entry, management, and analysis of borehole data. *Geologic Utilities* has mapping, gridding, and contouring properties (Rahman 2007). In this project, *Borehole Manager* is used for subsurface modeling.

In the Havran-Tepeoba area, 25 borehole drilling was done by MTA institution (General Directorate of Mineral Research and Exploration of Turkey) in 2006, and all geological and geochemical data was gathered together for Cu-Mo mining in study location. In my research I used borehole data's to subsurface the licensee area, so the rockworks software suite was used for the subsurface modeling. All of the borehole data was entered into the Rockworks data format, which is specific to the Rockworks program.

The Rockworks software can be used to create a 3D model of the Cu-Mo-Au mineralization as well as the lithology and I-data. The lithology and I-data capabilities are rather straight forward and the software gives a good representation of the subsurface geometries. So I entered all geochemical and lithology of every borehole with their depth to get semi-quantitative model of the Cu-Mo-Au mineralization in related study area. The figures that will see above are snapshots of the model. In actuality, these are 3-D figures that can be rotated and viewed from any angle when using the Rockworks software. This software is not meant to be used in designing mines. Rather it is meant to be used to get a feeling for the geology as one is drilling and to plan successive drill holes. It is essentially an advanced electronic cross section, down hole modeling program and get reservoir of deposits.

The goals of this study are to determine the potential Cu-Mo-Au ore zones in the subsurface environment of the Havran-Tepeoba Cu-Mo deposit by means of the surface and borehole geologic data and to provide focus to mining operations about the specific areas, in spite of negations such as insufficient borehole units, structural factors, and intensive vegetation. In addition, it is hoped that this study will make a contribution to more detailed modeling studies.

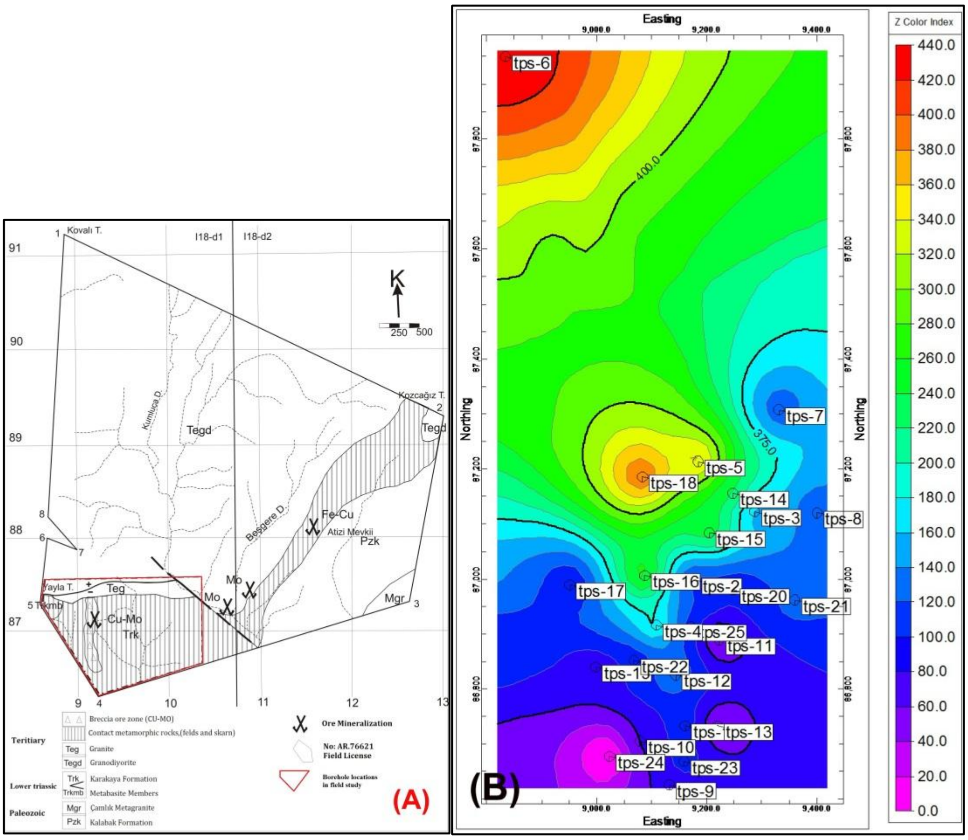

Figure 5.1 : (A) Surface map of study area and red part is related to borehole locations. (B) Surface map of borehole location drowned exported from Rockworks15.

5.3 Outputs of Copper, Molybdenum and Gold in different amounts:

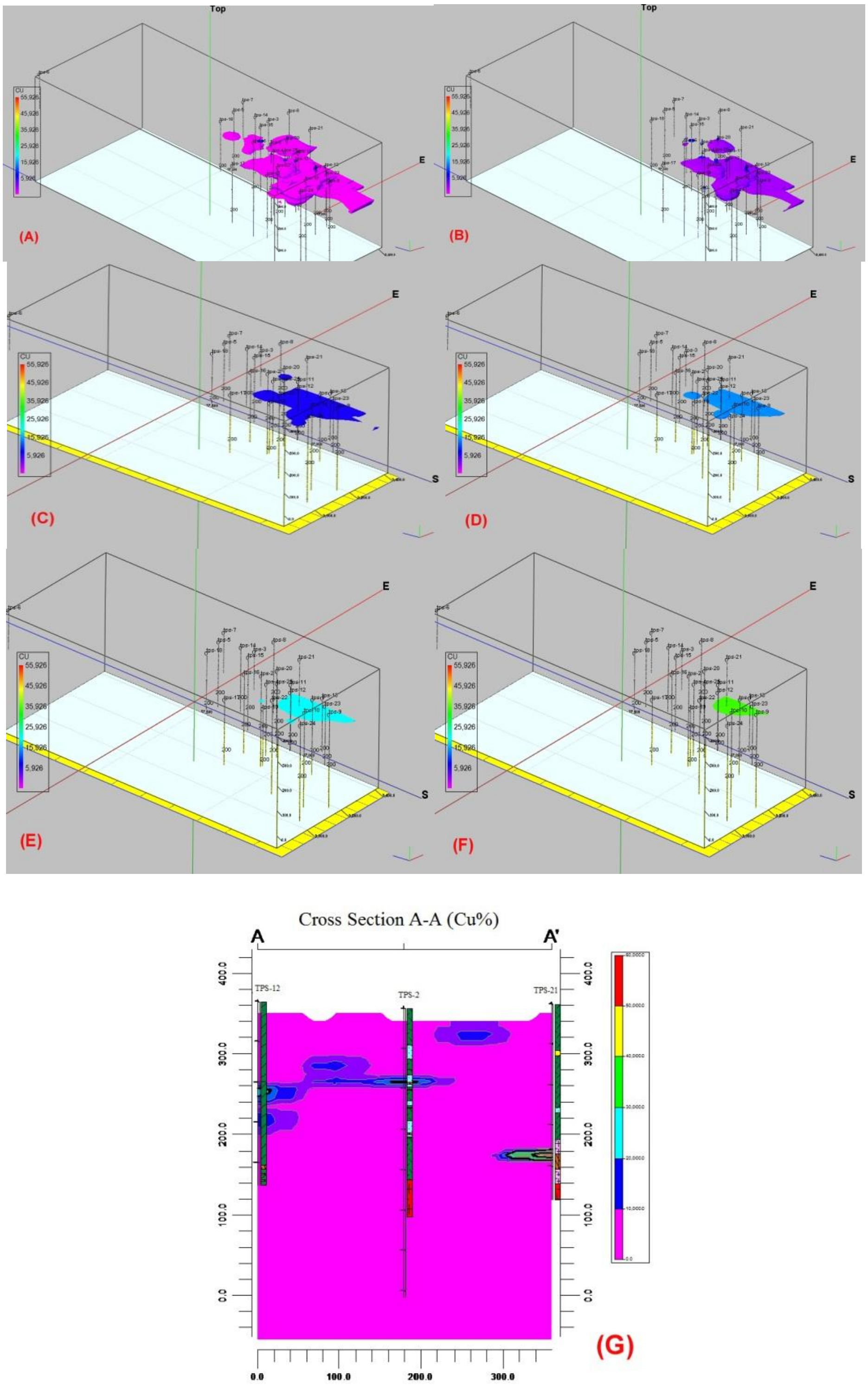

Figure 5.2 : (A) Shows copper amount in 3000 ppm. (B) shows copper amount in 6000ppm. (C) shows copper amount in 10000ppm.(D) shows copper amount in 15000ppm.(E) shows copper amount in 20000ppm.(F) shows copper amount in 35000ppm.(G) shows cross section of copper in different elevation of three borehole 12-2-21 .

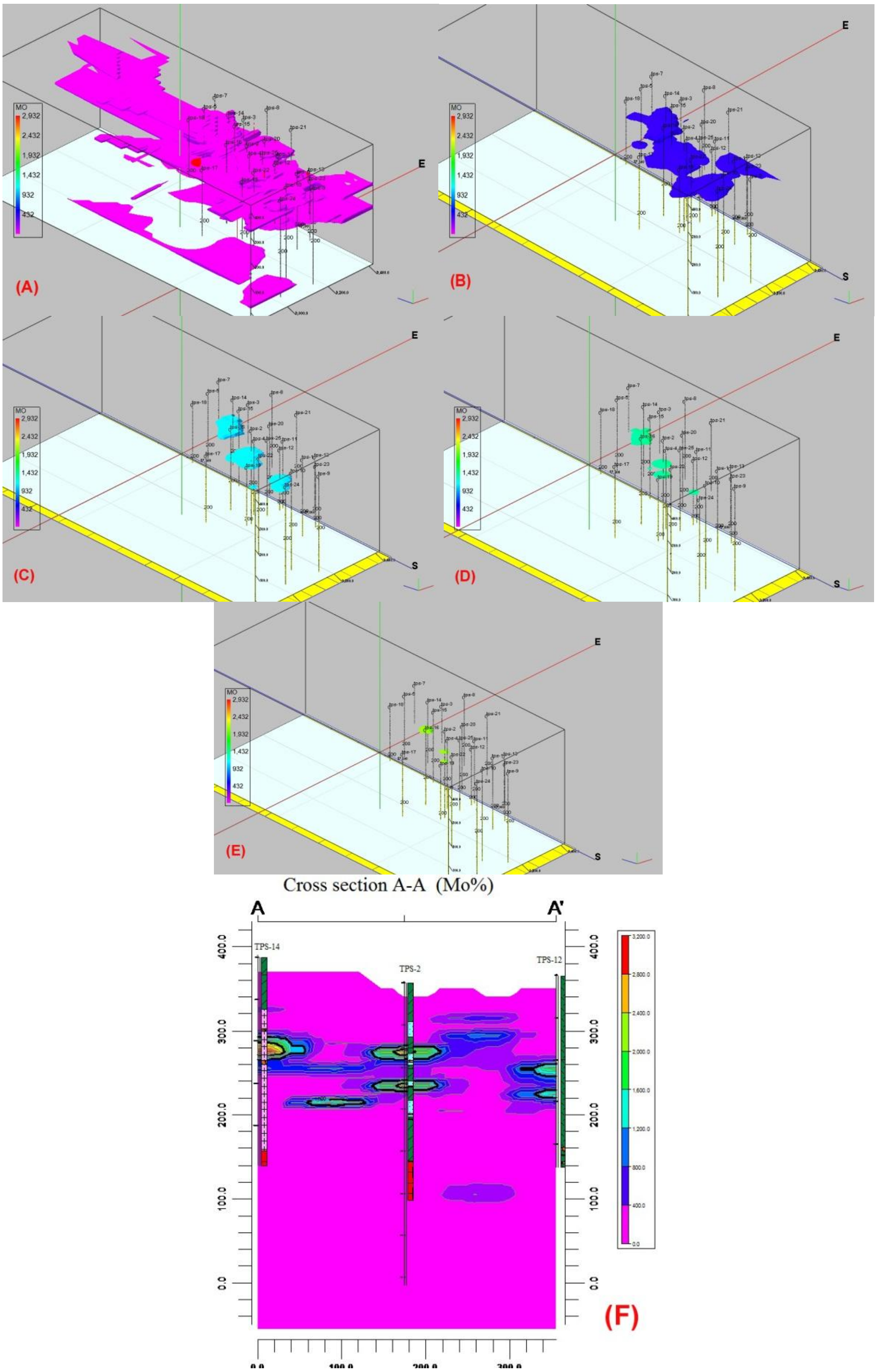

Figure 5.3 : (A) shows molybdenum amount in 100 ppm.(B) shows molybdenum amount in 500 ppm. (C) shows molybdenum amount in 1000 ppm.(D) shows molybdenum amount in 1500 ppm.(E) show molybdenum in 2000 ppm. (F) shows cross section of molybdenum in different elevation of three borehole 14-2-12 .

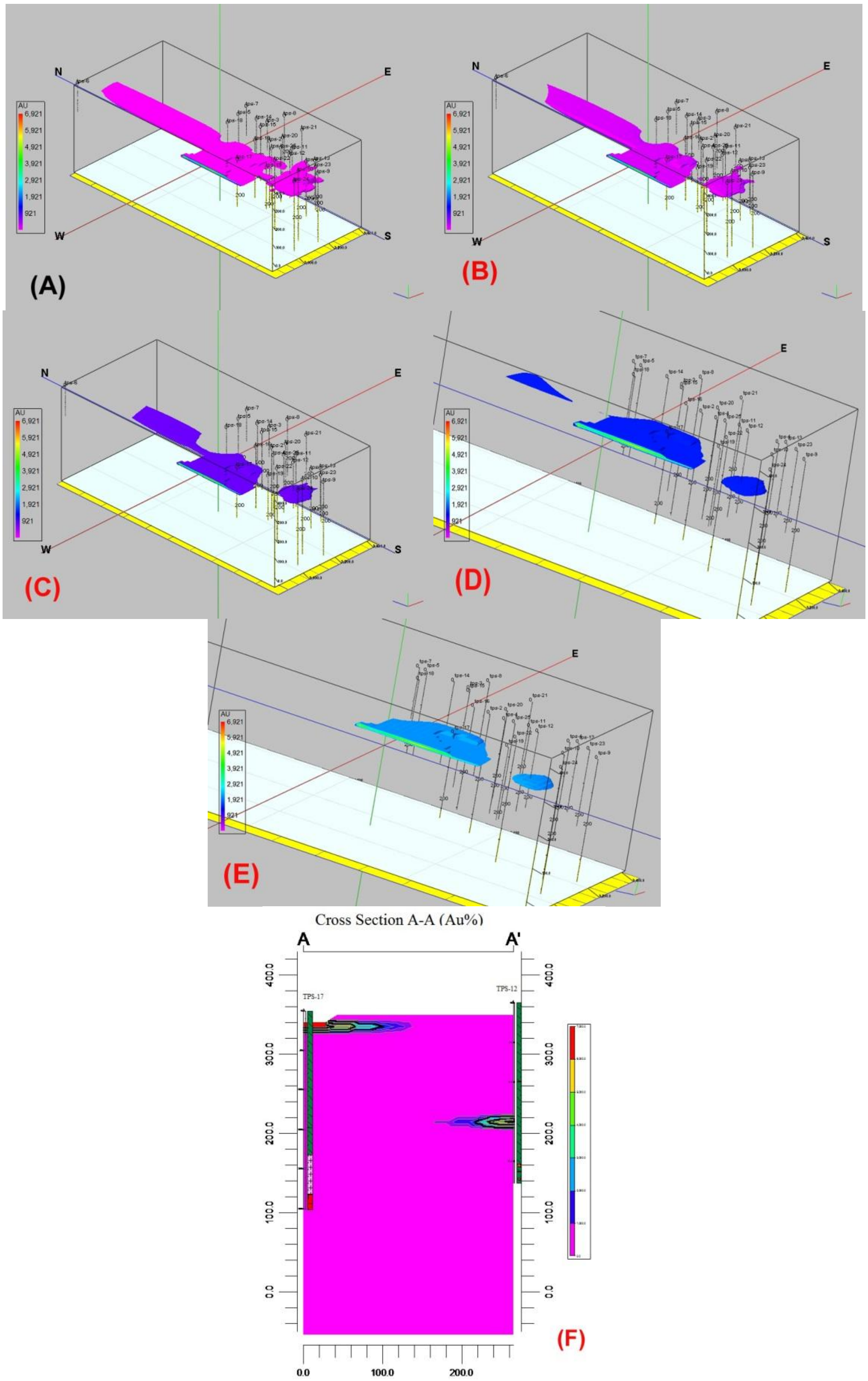

Figure 5.4 : (A) show gold amout in 200 ppb. (B) shows gold amout in 500 ppb. (C) shows gold amount in 1000 ppb. (D) shows gold amount in 1500 ppb. (E) shows gold amount in 2000 ppb. (F) shows cross section of gold in different elevation of two borehole 12-17 .

5.4 Report High Amount of Copper-Molybdenum and Gold Amount from Top to Depth in Different Boreholes :

In some sample cores, mineral concentration are visible in a registerable amounts. Chalcopyrite, pyrite, molybdenite and magnetite mineralization is observed in the form of veins and veinlets at these zones.

Reported the high potential borehole detail :

1: borehole 2 contains high amount of copper and partly molybdenum between elevations of 1 to 5 and 18.15 to 19.15 and 70.8 to 74.8 and 98 to 102 and 109 to 111 meter inside hornfelds. Between 82.6 to 89 observed high amounts of copper and molybdenum inside granophyre layers.

2: In borhole 4, there is countable amount of Molybdenum in elevation of 127 to 197 in granophyre dykes and these dykes were cut the hornfelds and breccia layers.

3: In borehole 5, there are molybdenite, pyrite and chalcopyrite mineralization Between 171.6-205.35 meters; in potasic zone.

4: Borehole 12 observed Copper between 19 to 20 meter in lithology of andalusite-biotit-hornfelds . In another elevations copper and partly molybdenum and gold was detected between 47 to 48 meter and 88 to 98 and 103 to 160 meters.

5: Borehole 14 has Molybdenum between 85.7 to 112 meter and contains Copper and Molybdenum between 117 to 118 meter and 128 to 134 meters in locogranite layers with fully amount of enclave and micro veins and calcite veins inside layers.

6: In borehole 16 , 4000 ppb Gold has been detected in elevation of 92 to 94 meter inside metabasic and hornfels skarn.

7: In borehole 17 has been observed 14000 ppb Gold between elevation of 12 to 14 meter in hornfels layer.

8: In borhole 18 , two molybdenite-rich quartz veins(potasic-phyllic zone) with 50 and 25 cm thickness, Between 179-181 meters;has been detected.

9: borehole 21 sample has been obtained high amounts of copper and molybdenum in elevation between 175-182 meter between locogranite, quartz veins and metabasic enclaves .

5.5 Reported Trasition Zones Between Selected Boreholes:

There were three transition zones, detected in different borehole elevation which are (TPS-4 observed at elevation of 40meter – TPS8 observed at elevation of 220 meter and TPS 22 observed at elevation of 170 meter). These three transition zone was imaged to show the changes of lithology in different elevation in plan maps.

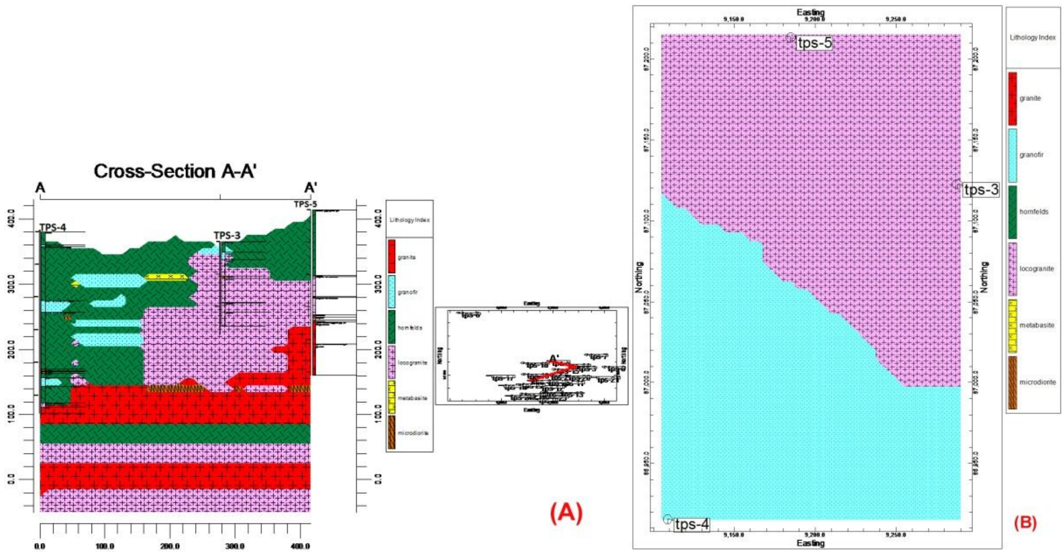

Figure 5.5 : (A) Cross section between three boreholes TPS3-4-5, shows lithology of them. (B) Figure is showing the transition zones in elevation of 40 meter.

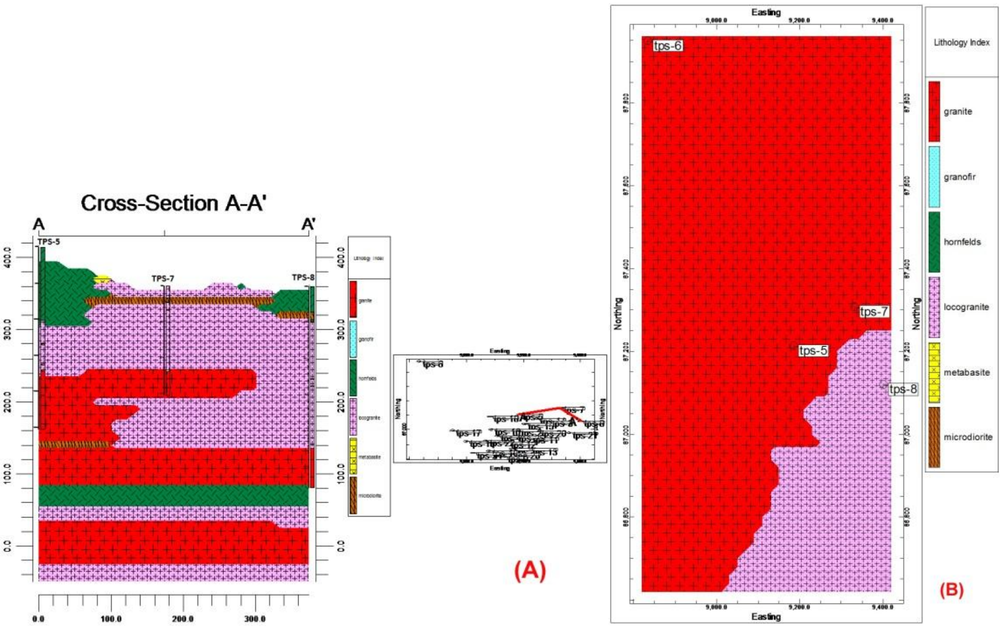

Figure5.6 : (a) Cross section between three boreholes TPS5-7-8, shows lithology of them. (b) Figure is showing the transition zones in plan map of the same boreholes in elevation of 220 meters.

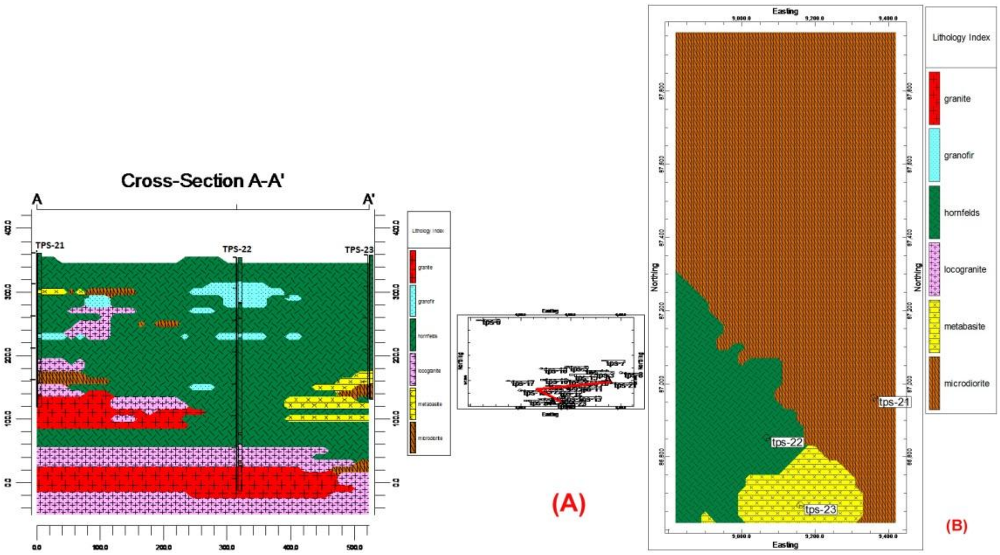

Figure 5.7 : (a) Cross section between three boreholes TPS5-7-8, shows lithology of them. (b) Figure is showing transition zones in plan map of the same boreholes in elevation of 170 meters.

6. CONCLUSIONS AND RECOMMENDATIONS

The Biga Penninsula contains a very rich zone in terms of metallic ores. There are many known sulphur mineralizations (bornite, pirit, calcopyrite...etc.) which are describing in the study area. Some of these mineralizations being produced for metals like Cu-Mo-Au. In addition, these mineralizations are important for some precious elements like gold. Nowadays, these precious metals have not been any investigated in Biga Penninsula and even in Turkey.

With the help of computer technology, 3D subsurface modeling has been used quite frequently in the field of mineral exploration in recent years. The large amount of data obtained at regular spaces plays an important role in recognizing the subsurface structures. Also, reviewing previously collected inadequate data is very important in order to both clarify previously missed potential amount and concentrate on the work underway in specific areas. The uses of active mining works are very important to compare the results with own works to better understand misty point of potential amount.

In the Tepeoba-Havran, near Balikesir area in Turkey, 25 borehole drilling were done by MTA institution, (General Directorate of Mineral Research and Exploration of Turkey) in 2006, and all geological and geochemical data was gathered together for Cu-Mo mining in study location. Some boreholes have high amount of copper-molybdenum and gold in different depths and lithology's, here are description and results of nine important boreholes (2-4-5-12-14-15-16-17-18-21) catch from geochemical analyzes of major elements:

1: borehole 2 contains high amount of copper and partly molybdenum between elevations of 1 to 5 and 18.15 to 19.15 and 70.8 to 74.8 and 98 to 102 and 109 to 111 meter inside hornfelds. Between 82.6 to 89 observed high amounts of copper and molybdenum inside granophyre layers.

2: In borhole 4,there is countable amount of Molybdenum in elevation of 127 to 197 in granophyre dykes and these dykes were cut the hornfelds and breccia layers.

3: In borehole 5,there are molybdenite, pyrite and chalcopyrite mineralization Between 171.6-205.35 meters; in potasic zone.

4: Borehole 12 observed Copper between 19 to 20 meter in lithology of andalusite-biotit-hornfelds . In another elevations copper and partly molybdenum and gold was detected between 47 to 48 meter and 88 to 98 and 103 to 160 meters.

5: Borehole 14 has Molybdenum between 85.7 to 112 meter and contains Copper and Molybdenum between 117 to 118 meter and 128 to 134 meters in locogranite layers with fully amount of enclave and micro veins and calcite veins inside layers.

6: In borehole 16 , 4000 ppb Gold has been detected in elevation of 92 to 94 meter inside metabasic and hornfels skarn.

7: In borehole 17 has been observed 14000 ppb Gold between elevation of 12 to 14 meter in hornfels layer.

8: In borhole 18 , two molybdenite-rich quartz veins (potasic-phyllic zone) with 50 and 25 cm thickness, Between 179-181 meters;has been detected.

9: borehole 21 sample has been obtained high amounts of copper and molybdenum in elevation between 175-182 meter between locogranite, quartz veins and metabasic enclaves .

The main subjects are of this thesis showing high potential of copper-molybdenum and gold by subsurface mining area to detect the potential of ore deposit in depth. The images of These boreholes that describing above are in separate Appendix display the high potensial copper, molydenum and gold amount in different depth in study area:

1) Figure 5.2 is displaying 6 Solid Models and 3D Diagrams of Interval Data in different amount, those amounts are start in 3000 ppm and Ends up to 35000 ppm for copper with cross section of some copper content in borholes.

2) Figure 5.3 is displaying 5 Solid Models and 3D Diagrams of Interval Data in different amount, those amounts are start in 100 ppm and Ends up to 2000 ppm for Molybdenum with cross section of some molybdenum content in borholes.

3) Figure 5.4 is displaying 5 Solid Models and 3D Diagrams of Interval Data in different amount, those amounts are start in 200 ppb and Ends up to 2000 ppb for gold with cross section of some Gold content in borholes.

Images are going to make purify hypothesis about copper-molybdenum and gold amout for next future of mining area.

Results of mineralogical study about each formation represent the main lithologic units start with basic volcanics, greywacke, sandstone, and lenticular limestones and contain different-sized Permo Carboniferous limestone blocks in the interior part. The oldest tectonic unit that consist : calc schist, phyllite and existance of marble between this units, represents Torasan formation is subgroup of kalabak unit. At the top of this unit, marble lenses,spilite and metatuffites took place in metabasic member represents lower karakaya complex. Metasedimentar rocks represents the upper karakaya complex that consising Arkosic metasandstone, phyllites and schist, meta conglomerates, sandstone. Both metasedimentary and metabasite rocks are form Early-Triassic Karakaya complex. The compositin of Eybak Granite and Granodiorite and acidic and basic rock veins have been aged about tertiary era. At the study area, Eybak Granitoid, has imposed contact metamorphism to meta-sedimentary and metabasite rocks and turned them to andalusite-biotite schist. A mineralogical study about each formation is helps to understand better the geology and the structural of those formations on investigation area.

Aslo several analyses done on granite rock were prepared besides subsurface modeling like XRF for detecting major elements. Major element compositions of pre-mineralization, mineralized, and post mineralization rocks have been determined for many individual porphyry copper deposits and districts.

Results of two diagram about major elements :

1) The results of TAS diagram shows us copper molybdenum deposit are mostly granite, and also shows the range between monzonite and quartz monzonite and siyenite.

2) The result of Harker diagram that all major elements against Sio_2 display patterns Basic Harker diagrams show that K_2O increases with increasing SiO_2 and Cr_2O_3 remains constant with increasing SiO_2. Oxides Al_2O_3, Fe_2O_3, CaO, MgO, P_2O_5, MnO, Na_2O and TiO_2 decrease with increasing SiO_2, consistent with fractional

crystallization of plagioclase, alkali feldspar, amphiboles, biotite, muscovite, quartz, magnetite, and titanite phases, respectively and display patterns consistent with fractional crystallization common in granites.

REFERENCES

Akiska, S. Sayili, I, S. and Demirela, G. (2010). The subsurface 3D modelling of the Handeresi (Kalkim-Canakkale) area, NW of Turkey, Pb-Zn-Cu ore zones. *EGU2010 General Assembly, Vienna, Abstracts* 1636.

APelke, P. (2009). Ni 43-101 technical report on the groete creek property guyana, california registered geologist, no. 4150 1350 grand summit drive, 94 reno, nevada 89523.

Aslaner, M., (1965). Etude Geologique et Petrographique de la Region d'Edremit-Havran (Turquie), Maden Tetkik ve Arama Enstitüsü Yayini, 119, 98. S

Augé, T., Petrunov, R., and Bailly, L., (2005). On the origin of the PGE mineralization in the Elatsite porphyry Cu-Au deposit, Bulgaria—Comparison with the Baula-Nuasahi complex, India, and other alkaline PGE-rich porphyries: The Canadian Mineralogist, v. 43, p. 1355–1372.

Altunkaynak, S., Genc, S.C., (2007). Eybek graniti (Biga yar›madas›, KB Anadolu) üzerine: Yeni jeokimya verileri ›fl›¤›nda yeni bir de¤erlendirme, Yerbilimleri, 28(2), 75-98.

Altunkaynak, S,, Genç, S.C., (2008). Petrogenesis and time-progressive evolution of the Cenozoic continental volcanism in the Biga Peninsula, NW Anatoli (Turkey), Lithos 102 (2008) 316–340.

Ayan, M. (1979). The origin of the some granites occurringin the Menderes massif and their relations with the uranium mineralization : Comm. de la Fac desScien. de L'Univ. d'Ankara, Cı, 22, 91-128.

Aldanmaz, E., Pearce, J.A., Thirwall, M.F., Mitchell, J.G., (2000). Petrogenetic evolution oflate Cenozoic, post-collision volcanism in western Anatolia, Turkey. J. Volcanol.Geotherm. Res. 102, 67–95.

Burger, R, B. and others. (2008). Preliminary Model of Porphyry Copper Deposits, U.S. Geological Survey, Reston, Virginia.

Black, K,N. (2012). Geochemical and Geochronological Relationships between Granitoid Plutons of the Biga Peninsula, NW Turkey, The University of Texas at Austin.

Babcock, R.C., Jr., Ballantyne, G.H., and Phillips, C.H., (1995).Summary of the geology of the Bingham district, Utah, *in* Pierce, F.W., and Bolm, J.G., eds., Porphyry copper deposits of the American Cordillera: Arizona Geological Society Digest 20, p. 316–335.

Bryant, D.G., and Metz, H.E., (1966). Geology and ore deposits of the Warren mining district, *in* Titley, S.R., and Hicks, C.L., eds., Geology of the porphyry copper deposits, Southwestern North America: Tucson, The University of Arizona Press, p. 189–203.

Beccaletto, L. (2004). Geology, Correlations, and Geodynamic Evolution of the Biga Peninsula (NW Turkey).*M´emoires de G´eologie de l'Universit´e de Lausanne* **43**,146 pp.

Beccaletto, L., Bartolini, A.C., Martini, R., Hochuli, P.A., Kozur, H., (2005). Biostratigraphic data from the Cetmi Melange, northwest Turkey: paleogeographic and tectonic implications. Palaeogeogr. Palaeoclimatol. Palaeocl. 221, 215–244.

Birkle, P., Satir, M., (1995). Dating, geochemistry and geodynamic significance of the Tertiary magmatism of the Biga Peninsula, NW Turkey. In: Erler, A., Ercan, T.,

Bingol, E., Orcen, S. (Eds.),(1979). Geology of the Black Sea Region, General Directorate of Mineral Research and Exploration & Chamber of Geological Engineers, Ankara, pp. 171–180.

Bingöl, E., Akyürek, B. and Korkmazer, B. (1975). Biga yarımadasının jeolojisi ve Karakaya Formasyonunun bazı özellikleri. Proceedings of 50th Anniv. of Turkish Republic, MTA Publ., 70-77.

Bürküt, Y,. (1966). Kuzeybatı Anadolu'da yer alan plütonların mukayese! i jenetik etüdü: Doktora tez i, İTÜ Maden Fak., İstanbul, 272 s.

Boztuğ, D. ve Otlu, N., (2001). Mağmatik Petrojenez:Jeoloji Mühendisleri Odası Yayını:61, s.19-60.

Çetinkaya, N., Karul, B., Yenigün, K., ve Önal, R., (1983). Türk-Alman Projesi, Biga Yarımadası Metalik Madenler (Pb-Zn-Cu) Arama Projesi Raporu: MTA Der. Rap. No. 7813.

Doygun,Z. (2010). Geological, mineralogical and petrographical study of evciler and tepeobe area and evaluation about ore deposition. Pamukkale Üniversitesi Fen Bikimleri Enstitüsü Yüksek Lisans Tezi Jeoloji Anabilim Dali.

Duru, M., Pehlivan, S¸., Şentürk, Y., Yavaş¸, F. and Kar, H. (2004). New result on the lithostratigraphy of the Kazdağ˘ Massif in northwest Turkey. Turkish Journ. Earth Sci., 13, 177–186.

Durul, M. Pehlivan, S. Kar, H. Kandemir, O. Tok, T. Kanar, F. Cakir, K. Akcay, A,E. (2007). Basement rock unit of sakarya zone and setting of karakaya complex. c511f7c5caa34d7_ek.

Einaudi, M.T., Meinert, L.D., and Newberry, R.J., (1981), Skarn deposits: Society of Economic Geologists, 75th Anniversary Volume, p. 317–391.

Ercan, T.,Türkecan, A., Günay, E., Çevikbaş, A., Ateş, M., Can, B.,ve Erkan, M. (1984). Dikili-Çandarlı-Bergama (İzmir), Ayvalık-Edremit-Korucu (Balıkesir) yöresinin jeolojisi ve mağmatik kayaçların petrolojisi: MTA Der. Rap. No: 7600.

Feltrin,E,G,. *et,al.* (2009). Modelling the giant, Zn–Pb–Ag Century deposit,Queensland, Australia , Computers & Geosciences 35 (2009) 108–133.

Gümüs, A., (1964). Contribution a l'etude Geologique du Sectur Septentrional de Kalabak Köy-Eymir Köy (Region d'Edremit) Turquie. Maden Tetkik ve Arama Enstitüsü Yayini, 117, 109 s.

Görür, N., Tüysüz, O. and Şengör, A.M.C.(1998). Tectonic evolution of the Central Anatolian Basins. Int. Geol. Rev., 40, 831-850.

Genc, S,C and Altunkaynak, S. (2007). On the Eybek granite (Biga peninsula, NW Anatolia): A new evaluation in the light of new geochemical data.Journal of the Earth Sciences Application and Research Centre of Hacettepe University.Yerbilimleri, 28 (2), 75-98.

Hack *et al*. (2006).The Community Climate System Model Version 3 (CCSM3). 2122 JOURNAL OF CLIMATE VOLUME 19.

Ketin, I. *(*1966). Anadolu'nun tektonik birlikleri. *İstanbul Teknik Üniversitesi, Maden Fakültesi, Sayı 66 (1966) Sayfa 20-34.*

Kirkham, (1972). Porphyry deposits, in Blackadar, R.G., ed., Report of Activities Part B, November 1971 to March 1972: Geological Survey of Canada, Paper 72-1b, p. 62-64.

Kucukefe, S. Sari, R. Kilic, M. Avsar, M. Tekin, Z. (2006). Tepeoba (havran-balıkesir) cu-mo-au sahasının maden jeolojisi raporu.

Küçükefe, Ş., Sarı, R., Kılıç, M. ve Avşar, M. (2005). Tepeoba (Havran-Balıkesir) Cu-Mo-Au sahasının jeoloji ve jeokimya Raporu: MTA Rap. Der. No. 10848.

Krushensky, R.D. (1971).Biga Yarımadası, Edremit doğusunun jeolojisi: MTA Der. Rap. No. 5646.

Kaaden, G.V.D., (1957). Çanakkale Biga Edremit Yarimadasi Bölgesindeki Jeolojik Etüd Çalismalari, MTA Rapor.(YAyainlanmamistir), Ankara.

Kaaden, G.V.D., (1959). Anadolu'da kuzeybati kisminda yer alan metamorfik olaylarla magmatik faaliyetler arasindaki yas münasebetleri. M.T.A. Derg. No.52.

Meinert, L.D., Dipple, G.M., and Nicolescu, S., (2005). World skarn deposits: Society of Economic Geologists, Economic Geology 100th Anniversary Volume, p. 299–336.

Murakami, H., Watanabe, Y., and Stein, H., (2005). Re-Os ages for molybdenite from the Tepeoba breccia-centered Cu-Mo- Au deposit, western Turkey: Brecciation- triggered mineralization. Mineral Deposit Research, 1, 805-808.

Moix, P., Beccaletto, L., Kozur, H.W., Hochard, C., Rosselet, F. & Stampfli, G. (2008). A new classification of the Turkish terranes and sutures and its implication for the paleotectonic history of this region. - Tectonophys., **451**: 7-39.

Okay,et,aI. (1990). Geology and tectonic evolution of the Biga peninsula. TPJD.p.83-121. Rahman,K,M. Settlement prediction on the basis of a 3D subsurface model. Reeuwijk area, the Netherlands.

Okay, A,I. Siyako, M. Burkan, K,A. (1991). Geology and tectonic evolution of the Biga peninsula, northwest TURKEY.vol.44, pp.191-256,1991.

Okay, A.İ. (1984). Kuzeybatı Anadolu'da yeralan metamorfik kuşaklar: Ketin Simpozyumu, TJK Yay.

Okay, A.I. and Göncüoğlu, M.C. (2004). The Karakaya Complex: A Review of Data and Concepts. Turkish Journal of Earth Sciences (Turkish J. Earth Sci.), Vol. 13, 2004, pp. 77-95.

Pickett E.A. and Robertson A.H.F. (2004). Significance of the Volcanogenic Nilüfer Unit and Related Components of the Triassic Karakaya Complex for Tethyan Subduction/Accretion Processes in NW Turkey, Turkish Journal of Earth Sciences (Turkish J. Earth Sci.), Vol. 13, 2004, pp. 97-143.

Robertson A.H.F and Ustaömer,T. (2012). Ion Probe U-Pb Dating of the Central Sakarya Basement: A peri-Gondwana Terrane Intruded by Late Lower Carboniferous Subduction/Collision-related Granitic Rocks.Turkish Journal of Earth Sciences (Turkish J. Earth Sci.), Vol. 21, 2012, pp. 961–1007.

Rahman,K,M. (2007).Settlement prediction on the basis of a 3D subsurface model. Reeuwijk area, the Netherlands.

Renard, P. & Courrioux, G. (1994). Three-dimensional geometric modeling of a faulted domain: the Soultz Horst example (Alsace, France). *Computer & Geosciences* 20, 1379-1390.

Phillipson, A., (1958). HAndbuch der Regional Geologie: Heidelberg Carl Winters Universtaatbuchhandlung,185s.

Siyako, M., Bürkan, K.A. & Okay, A.I. (1989). Biga ve Gelibolu yarımadalarının Tersiyer jeolojisi ve hidrokarbon olanakları [Tertiary geology and hydrocarbon potential of the Biga and Gelibolu peninsulas]. *Türkiye Petrol Jeologlari Derneği Bülteni* **1**, 183−199 [in Turkish with English abstract].

Sayit, K. and Göncüoglu M.C. (2012). Geodynamic evolution of the Karakaya Mélange Complex, Turkey: A review of geological and petrological constraints , GEOD-1151; No. of Pages 10.

Smith, C,M. (2007). Geology and petrology of the Catface porphyry Cu-Mo deposit, Vancouver Island, and linkages to the Paleogene Cascade Arc, University of British Columbia.

Sinclair,W,D. (2007). Porphyry deposits, *in* Goodfellow, W.D., ed., Mineral Deposits of Canada: A Synthesis of Major Deposit-Types, District Metallogeny, the Evolution of Geological Provinces, and Exploration Methods: Geological Association of Canada, Mineral Deposits Division, Special Publication No. 5, p. 223-243.

Şengör, A.M.C., ve Yılmaz. Y. (1981).Tethyan Evolution of Türkey: A Plate Tectonic Approach: Tectonophysics, c.75, s.181-241.

Tchihatchef, P., (1967). Reisen in Keinasien und Armenien 1847-1863: Patermans Geol.Min.68, 69s.

Turhani,N. Okuyucu,C. Goncuoglu, M,C. (2004). Autochthonous Upper Permian (Midian) Carbonates in the Western Sakarya Composite Terrane, Geyve Area, Turkey: Preliminary Data, Turkish Journal of Earth Sciences (Turkish J. Earth Sci.), Vol. 13, , pp. 215-229.

Uyanik,T. (2010). Mining industry in turkey, igeme- export promotion center of turkey.

Watanabe M., Kikawada,T. & Okuda, T. (2003). Increase of internal ion concentration triggers trehalose synthesis associated with cryptobiosis in larvae of Polypedilum vanderplanki. J. Exp. Biol. 206: 2281–2286.

Watanabe,Y and Yildirim, S. (2004). Japan-Turkey Project Study on Hydrothermal Deposits and Metallogeny of Western Turkey between the Institute for Geo-Resources and Environment, AIST and Mineral Research and Exploration Department, General Directorate of Mineral Research and Exploration of Turkey from 2001 to 2004.

Whitney, D, L. and Evans, B, W. (2010). Abbreviations for names of rock-forming minerals. American Mineralogist, Volume 95, pages 185–187.

Winkler, G. ve Helmut, F. (1977). Metamorfik kayaçların oluşumu: İTÜ Yayını, No. 118. s. 52-65.

Yigit, O. (2012). A prospective sector in the Tethyan Metallogenic Belt: Geology and geochronology of mineral deposits in the Biga Peninsula, NW Turkey.

Yilmaz, Y., Genç, S.C., Karacik, Z., & Altunkaynak, S., (2001). Two contrasting magmatic associations of NW Anatolia and their tectonic significance, Journal of Geodynamics 31, 243-271.

Yilmaz, Y., (1990). Comparison of young volcanic associations of western and eastern Anatolia formed under a compressional regime: a review. Jour. of Volc. and Geoth. Res. Vol. 44, pp.1-19.

Url-1 http://en.wikipedia.org/wiki/Mediterranean_climate date of receipt :20.10.2012

Url-2 http://www.columbuscopper.com/s/turkey.asp date of receipt: 21.04.2013

Url-3 http://www.mapsofworld.com/minerals/world-copper-producers.html date receipt : 21.04.2013

Url-4 http://www.earth.ox.ac.uk/~oesis/micro/ date of receipt: 11.04.2013

Url-5 http://www.gly.bris.ac.uk/www/teach/opmin/mins.html date of receipt: 12.04.2013

APPENDICES

APPENDIX-A

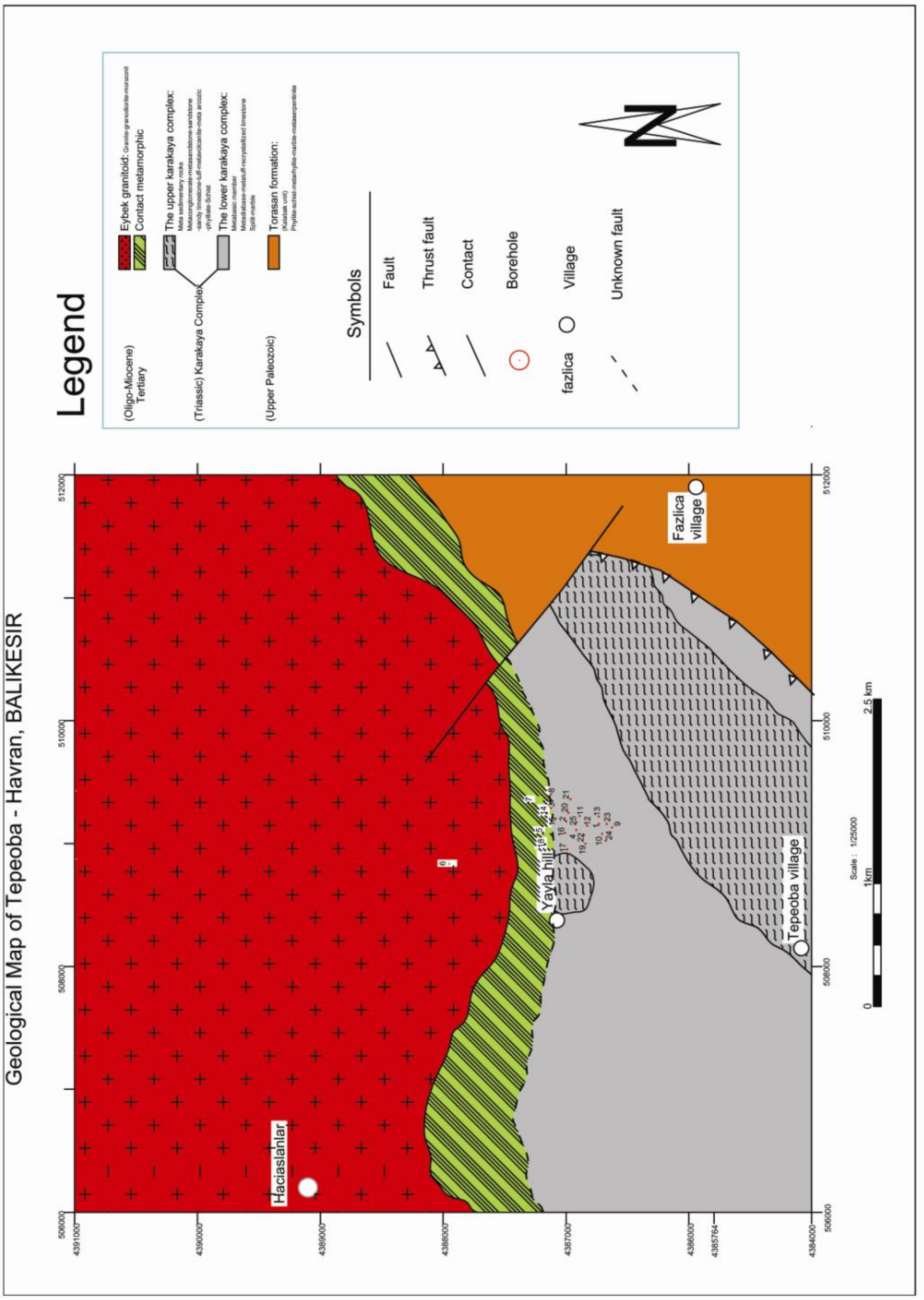

Appendix –A : Geological map of Tepeoba-Havran, (modified from MTA, 2007).

APPENDIX-B

Table B.1 The results of XRF for major element of selected ore samples.

Sample (wt%)	SiO2	Al2O3	Fe2O3	MgO	CaO	Na2O	K2O	TiO2	P2O5	MnO	Cr2O3	LOI	TOTAL
6	73.88	14.68	1.72	0.46	0.18	0.41	4.41	0.1	0.01	0.01	-	3.94	99.81
15	58.54	15.74	5.06	2.3	6.78	3.72	3.84	0.49	0.24	0.11	-	2.83	99.66
20	72.43	13.98	0.3	0.07	1.03	3.24	7.28	0.03	0	0.01	-	1.47	99.82
25	49.6	17.1	9.06	5.16	7.3	3.38	3.05	1.49	0.6	0.19	0.01	2.75	99.68
33	62.2	15.88	4.29	1.9	4.98	3.62	4	0.55	0.23	0.09	-	1.9	99.64
35	53.22	15.03	10.77	4.01	7.79	5.22	0.75	0.7	0.18	0.22	-	1.84	99.74
44	61.65	16.54	4.57	2.06	5.28	3.5	4.01	0.61	0.34	0.11	-	0.98	99.64
48-2	49.38	24.79	5.38	2.21	5.2	3.33	4.09	0.87	0.12	0.08	0.01	3.52	98.99
50	63.9	16.93	3.03	1.28	1.64	3.55	6.53	0.48	0.06	0.03	-	2.06	99.49
53	59.68	16.23	6.95	4.58	1.69	3.34	2.46	0.71	0.25	0.13	0.02	3.76	99.82
59	59.92	20.55	4.25	1.31	2.09	2.1	5.38	0.64	0.09	0.05	0.01	3.33	99.72
76	1.21	0.66	3.37	1.99	50.89	0	0.01	0.04	0	0.08	0	41.68	99.92
51	43.11	11.16	13.61	12.81	10.69	2.15	1.61	2.87	0.47	0.19	0.09	0.81	99.57

Table B.2. The results of XRF major elements for Harker and TAS diagram.

Sample No	SiO_2	Al_2O_3	Fe_2O_3	MgO	CaO	Na_2O	K_2O	TiO_2	P_2O_5	MnO	Cr_2O_3	LOI	TOTAL
1	69.76	15.58	1.46	0.70	0.71	1.99	6.35	0.33	0.05	0.01	0.01	2.83	99.78
4	61.77	19.73	3.45	1.39	1.27	2.50	6.33	0.52	0.07	0.05	0.01	2.67	99.74
15	58.54	15.74	5.06	2.30	6.78	3.72	3.84	0.49	0.24	0.11	-	2.83	99.66
20	72.43	13.98	0.30	0.07	1.03	3.24	7.28	0.03	0	0.01	-	1.47	99.82
33	62.20	15.88	4.29	1.90	4.98	3.62	4.00	0.55	0.23	0.09	-	1.90	99.64
35	53.22	15.03	10.77	4.01	7.79	5.22	0.75	0.70	0.18	0.22	-	1.84	99.74
38	73.25	13.29	0.45	0.12	0.73	3.00	6.43	0.07	0	0.00	-	2.49	99.83
40	64.38	15.76	3.58	1.88	4.44	3.67	4.55	0.47	0.27	0.08	-	0.55	99.63
43	72.72	12.88	1.47	0.76	1.18	2.65	5.34	0.35	0	0.02	-	2.32	99.71
44	61.65	16.54	4.57	2.06	5.28	3.50	4.01	0.61	0.34	0.11	-	0.98	99.64
45	74.53	12.98	0.58	0.12	1.44	4.13	3.84	0.07	0	0.01	-	2.19	99.90
46	73.18	13.78	0.57	0.12	0.82	2.86	6.34	0.05	0	0.01	-	2.05	99.77
47	57.42	21.48	4.72	1.96	3.37	2.67	3.98	0.69	0.09	0.06	0.01	2.71	99.17
48-1	62.10	17.21	2.71	1.56	1.88	3.45	7.41	0.53	0.04	0.03	-	2.09	99.01
50	63.90	16.93	3.03	1.28	1.64	3.55	6.53	0.48	0.06	0.03	-	2.06	99.49
56	71.76	14.08	0.59	0.31	0.68	2.28	7.73	0.13	0.01	0.00	0.00	2.22	99.78
58	71.28	14.22	0.90	0.19	0.66	2.96	6.54	0.13	0.00	0.01	0.00	2.94	99.83
64	72.94	13.71	0.22	0.03	0.55	2.53	7.96	0.07	0.00	0.00	0.00	1.75	99.76
73	74.65	14.18	0.58	0.31	0.71	4.15	2.58	0.05	0.32	0.01	0.00	2.36	99.90
74	61.52	16.80	2.37	2.19	5.05	2.84	5.15	0.47	0.27	0.06	0.00	2.91	99.65
75	71.93	13.58	0.59	0.20	1.46	2.90	6.80	0.14	0.04	0.01	0.00	2.16	99.81

APPENDIX-C

Table C.1 Data of borehole 1 for Cu-Mo-Au from MTA 2006.

From (m)	To (m)	Cu (ppm)	Mo (ppm)	Au (ppm)	From (m)	To (m)	Cu (ppm)	Mo (ppm)	Au (ppm)	From (m)	To (m)	Cu (ppm)	Mo (ppm)	Au (ppm)
0	1.35	4180	310	200	73	75	458	82	K40	151.95	154.95	108	14	K40
1.35	3.05	3900	260	230	75	77	514	34	K40	154.95	157.95	115	13	K40
3.05	4	4590	100	70	77	79	697	17	K40	157.95	161.5	89	16	K40
4	5.1	5100	550	380	79	81	325	30	K40	161.5	164.6	130	10	K40
5.1	7.4	4700	68	70	81	83	2100	6	K40	164.6	169.25	104	14	K40
7.4	8.1	2500	1425	2000	83	84.9	180	9	K40	169.25	172.25	228	13	K40
8.1	10.1	3000	3200	2000	84.9	85.15	1200	50	K40	172.25	175.25	89	11	K40
10.1	11.15	1200	460	180	85.15	87.15	647	44	K40	175.25	178.25	268	17	K40
11.15	11.8	13200	1000	380	87.15	89.35	270	9	K40	178.25	179.95	93	14/K5	K40
11.8	13.6	6500	240	220	89.35	91.06	388	800	K40	179.95	182.95	253	8	K40
13.6	15.15	7000	190	40	91.06	93.6	4200	2000	K40	182.95	185	249	22	K40
15.15	17.15	11300	600	70	93.6	94.25	27500	6500	1000	185	187.5	500	11	K40
17.15	19.15	2400	580	1100	94.25	95.95	25000	490	890	187.5	189.7	84	K5	K40
19.15	21.15	12300	180	120	95.95	97.55	4000	245	50	189.7	192.7	180	K5	K40
21.15	23.15	2700	340	150	97.55	98.55	1250	123	K40	192.7	195.7	120	K5	K40
23.15	24.8	15000	1000	550	98.55	100	3300	88	250	195.7	196.7	220	K5	K40
24.8	26.8	3600	276	K40	100	102	790	27	K40	196.7	203.3	90	K5	K40
26.8	28.8	13800	470	160	102	103.5	1400	44	K40	203.3	206.35	113	K5	K40
28.8	30.8	17600	486	360	103.5	104	2400	175	K40	206.35	209.35	68	K5	K40
30.8	31.9	26500	500	700	104	105.5	540	49	K40	209.35	212.35	87	6	K40
31.9	32.9	4380	197	K40	105.5	107.25	340	36	K40	212.35	215.5	69	K5	K40
32.9	34.9	4050	54	40	107.25	108.25	430	95	K40	215.5	220	167	6	K40
34.9	36.9	8200	550	140	108.25	111.25	777	56	K40	220	223.3	280	K5	K40
36.9	38.9	4200	273	50	111.25	113.25	204	25	K40	223.3	226.6	94	K5	K40
38.9	40.9	6850	1100	80	113.25	115.25	544	62	K40	226.6	229.6	340	5	40
40.9	42.9	5700	610	100	115.25	117.25	600	24	K40	229.6	232.6	485	5	40
42.9	44.9	1900	184	60	117.25	120	473	82		232.6	235.6	345	K5	K40
44.9	46.9	4450	52	90	120	122	2000	95	K40	235.6	238.6	220	7	K40
46.9	48.9	640	136	K40	122	123.75	412	26	K40	238.6	240.3	600	K5	K40
48.9	50.9	1130	140	K40	123.75	125.75	3500	189	K40	240.3	243.5	64	K5	K40
50.9	52.9	680	130	K40	125.75	128	339	25	K40	243.5	248.5	52	6	K40
52.9	54.9	326	35	K40	128	128.95	176	12	K40	248.5	249.5	70	7	K40

Table C.1(Continue) Data of borehole 1 for Cu-Mo-Au from MTA 2006.

54.9	56.2	960	440	K40	128.95	130.95	3500	50	K40	249.5	258	75	10	K40
56.2	56.8	4900	150	70	130.95	132.95	174	60	K40	258	259.25	187	5	K40
56.8	58.6	580	22	50	132.95	134.95	175	330	K40	259.25	262.4	208	K5	K40
58.6	60.6	4200	90	60	134.95	136.95	116	30	K40	262.4	267.35	555	K5	200
60.6	61.8	565	27	K40	136.95	138.95	720	45	K40	267.35	270.65	167	K5	K40
61.8	63	830	84	50	138.95	140.95	336	16	K40	270.65	274.05	162	8	K40
63	65	255	55	K40	140.95	142.95	375	44	K40	274.05	278.55	90	5	K40
65	67	133	6	K40	142.95	144.95	747	55	K40	278.55	282.6	246	31	K40
67	69	212	54	K40	144.95	146.95	430	30	K40	282.6	287.05	1300	26	K40
69	71	300	23	K40	146.95	148.95	175	40	K40	287.05	294.2	162	8	K40
71	73	315	115	K40	148.95	151.95	170	25	K40					

Table C.2 Data of borehole 2 from MTA 2006

From (m)	To (m)	Cu (ppm)	Mo (ppm)	Au (ppm)	From (m)	To (m)	Cu (ppm)	Mo (ppm)	Au (ppm)	From (m)	To (m)	Cu (ppm)	Mo (ppm)	Au (ppm)
0	1.5	7000	79	60	80.8	82.6	350	140	40	145	147	2240	83	40
1.5	3.95	3400	36	40	82.6	84.6	19100	6500	340	147	149	1370	65	40
3.95	5	3000	42	80	84.6	85.4	40000	1750	450	149	151	1650	57	40
5	7	1250	75	40	85.4	87.4	5660	135	60	151	153	975	38	40
7	8.6	2160	27	40	87.4	89.45	5885	260	70	153	154.3	550	48	40
8.6	10.65	3970	310	40	89.45	91.45	1700	38	40	154.3	156.7	198	15	40
10.65	12.05	215	28	40	91.45	92	800	35	40	156.7	158.7	980	38	40
12.05	14.05	940	26	40	92	94.05	940	25	40	158.7	160.6	264	55	40
14.05	16.25	2200	220	40	94.05	96.05	1260	220	40	160.6	161.45	65	5	40
16.25	18.15	4500	86	50	96.05	97.2	2050	200	40	161.45	163.25	124	7	40
18.15	19.15	11200	120	120	97.2	97.5	50	180	40	163.25	165.75	193	62	40
19.15	21.15	1180	270	40	97.5	98.35	1150	210	40	165.75	167.75	118	55	40
21.15	23.45	390	39	40	98.35	98.85	95	20	40	167.75	169.75	92	9	40
23.45	25.45	583	9	40	98.85	99.5	1215	185	40	169.75	171.75	175	5	40
25.45	27.45	1200	19	40	99.5	100.2	2334	225	40	171.75	173.75	277	6	40
27.45	29.55	550	56	40	100.2	101	5970	880	70	173.75	175.75	232	13	40
29.55	32	337	60	40	101	101.5	7900	44	130	175.75	177.75	229	10	40
32	34.65	337	100	40	101.5	102.8	2300	1200	40	177.75	179.75	214	6	40
34.65	36.7	278	250	40	102.8	105.2	1240	200	40	179.75	181.75	190	8	40
36.7	38.85	310	50	40	105.2	107.35	1820	280	40	181.75	183.75	82	5	40

Table C.2(Continue) Data of borehole 2 for Cu-Mo-Au from MTA 2006.

38.85	40.85	915	55	40	107.35	109.7	7600	168	90	183.75	185.75	778	49	40
40.85	42.85	500	170	40	109.7	111.7	11400	358	90	185.75	187.75	127	20	40
42.85	45.1	538	140	40	111.7	113.35	9700	176	90	187.75	190.15	515	16	40
45.1	47	620	150	40	113.35	115.35	2050	207	40	190.15	192.15	122	11	40
47	48.95	2250	110	40	115.35	117	2020	3970	40	192.15	194.8	115	10	40
48.95	51.2	2330	50	40	117	119	930	930	40	194.8	196.8	100	20	40
51.2	53.35	890	40	40	119	120.65	1490	250	40	196.8	198.8	127	5	40
53.35	55.5	2200	53	40	120.65	122.75	2080	350	40	198.8	200.8	280	5	40
55.5	57.75	1080	85	40	122.75	123.5	178	35	40	200.8	202.8	145	5	40
57.75	59.55	1120	34	40	123.5	125.5	2980	200	40	202.8	204.8	276	20	40
59.55	61.55	7500	16	40	125.5	127.5	2400	290	50	204.8	206.8	81	5	40
61.55	62.8	1800	250	40	127.5	129.5	2980	274	60	206.8	208.8	98	5	40
62.8	64.8	470	247	40	129.5	131.5	900	190	40	208.8	209.9	59	7	40
64.8	66.8	577	160	40	131.5	133.65	1800	180	40	209.9	211.45	31	5	40
66.8	68.8	648	230	40	133.65	136.6	1550	150	40	211.45	213	18	5	40
68.8	70.8	2350	950	40	136.6	138	385	98	40	213	215.5	39	5	40
70.8	72.8	6550	450	120	138	138.85	759	135	40	215.5	217.5	5	5	40
72.8	74.8	7000	1300	50	138.85	140.85	1200	160	40	217.5	219.5	51	19	40
74.8	76.8	970	4450	50	140.85	142.86	1500	75	40	219.5	221.5	15	5	40
76.8	78.8	2000	145	40	142.86	143.4	1150	59	40	221.5	224.5	11	5	40
78.8	80.8	360	60	40	143.4	145	1500	580	40	224.5	227.5	22	5	40
										227.5	231	40	5	40
										231	234	89	5	40

Table C.3 Data of borehole 3 from MTA 2006.

From (m)	To (m)	Cu (ppm)	Mo (ppm)	Au (ppm)	From (m)	To (m)	Cu (ppm)	Mo (ppm)	Au (ppm)
0	3	241	10	40	75.95	77.75	1260	48	40
3	5.4	326	7	40	77.75	79	1720	67	40
5.4	7.2	299	7	40	79	81	1350	48	40
7.2	9.2	834	18	40	81	83	1155	52	40
9.2	11.7	450	10	40	83	85	1775	63	40
11.7	13.7	190	5	40	85	87	1680	95	40
13.7	15.7	189	5	40	87	89	1420	30	40
15.7	17	179	5	40	89	90.05	1310	26	40
17	19	340	5	40	90.05	92	80	5	40
19	21	650	5	40	92	93.3	485	10	40
21	22.5	275	12	40	93.3	94.5	70	5	40

Table C.3 (Continue) Data of borehole 3 for Cu-Mo-Au from MTA 2006.

22.5	25.05	405	48	40	94.5	95	790	10	40
25.05	27.95	410	12	40	95	97	640	40	40
27.95	29.95	885	8	40	97	99	170	55	40
29.95	32	765	5	40	99	101	230	21	40
32	34	840	10	40	101	101.75	450	18	40
34	36	775	5	40	101.75	103.75	1490	48	40
36	38	954	7	40	103.75	105.75	1350	13	40
38	40.15	1170	32	40	105.75	107.75	420	5	40
40.15	42.15	1640	21	40	107.75	108.25	680	15	40
42.15	44.15	1710	18	40	108.25	109	1615	5	40
44.15	46.15	1775	52	40	109	111	500	81	40
46.15	48.15	900	32	40	111	113	940	780	40
48.15	50.15	1775	87	40	113	115	320	250	40
50.15	51.15	1330	37	40	115	117.4	310	220	40
51.15	53.1	710	59	40	117.4	120.45	680	40	40
53.1	54.85	116	5	40	120.45	122.9	1450	84	50
54.85	56.6	127	5	40	122.9	124	1530	72	40
56.6	58.8	2045	180	50	124	126.55	1200	46	40
58.8	60.6	1880	195	40	126.55	128.55	1090	32	40
60.6	62.6	2140	770	40	128.55	130	1180	15	40
62.6	64.6	290	620	40	130	132	825	42	40
64.6	65.2	52	47	40	132	134.3	710	12	40
65.2	67.2	865	23	40	134.3	136.75	215	44	40
67.2	69.95	970	80	40	136.75	138.4	160	13	40
69.95	71.95	1800	110	40	138.4	139.6	155	38	40
71.95	73.95	1350	40	40	139.6	142.25	170	10	40
73.95	75.95	1450	43	40	142.25	143.35	245	9	40

Table C.4 Data of borehole 4 from MTA 2006.

From (m)	To (m)	Cu (ppm)	Mo (ppm)	Au (ppm)	From (m)	To (m)	Cu (ppm)	Mo (ppm)	Au (ppm)	From (m)	To (m)	Cu (ppm)	Mo (ppm)	Au (ppm)
0	3.05	785	13	40	90.9	93.2	835	60	40	177.25	179	12000	85	40
3.05	5.05	370	26	40	93.2	95.2	700	37	40	179	181	2130	110	40
5.05	6.75	245	11	40	95.2	97.2	810	52	40	181	183	940	110	40
6.75	8.1	260	18	40	97.2	99.2	1000	108	40	183	186	1330	180	40
8.1	10.1	300	22	40	99.2	101.2	570	150	40	186	186.9	8700	2100	40
10.1	12.1	238	15	40	101.2	103.4	1100	27	40	186.9	188.9	6700	180	40
12.1	14.1	398	20	40	103.4	105.7	1600	29	40	188.9	190.9	2070	135	40
14.1	16.75	1000	15	40	105.7	107.95	1450	24	40	190.9	193.15	1410	90	40
16.75	18.75	510	23	40	107.95	109.5	1160	21	40	193.15	195.15	1115	260	40

Table C.4(Continue) Data of borehole 4 for Cu-Mo-Au from MTA 2006.

18.75	20.3	570	40	40	109.5	111.3	175	10	40	195.15	197.2	7700	590	40
20.3	22.3	535	11	40	111.3	113.3	240	16	40	197.2	198.5	2900	75	40
22.3	24.3	400	16	40	113.3	115.3	230	188	40	198.5	201	1420	80	40
24.3	26.3	254	7	40	115.3	117.3	1050	135	40	201	206.35	158	23	40
26.3	28.3	216	11	40	117.3	119.3	2550	13	40	206.35	210.1	370	8	40
28.3	30.3	610	27	40	119.3	121.3	1700	20	40	210.1	213.25	25	5	40
30.3	32.3	206	6	40	121.3	123.3	750	100	40	213.25	214	540	6	40
32.3	34.3	428	6	40	123.3	125.05	1800	590	40	214	216.2	43	5	40
34.3	36.3	432	12	40	125.05	127.05	950	410	40	216.2	218.2	180	22	40
36.3	38.3	542	11	40	127.05	129.55	2040	660	40	218.2	220.2	125	55	40
38.3	40.3	211	11	40	129.55	130.8	1190	770	40	220.2	223.15	110	128	40
40.3	42.3	223	7	40	130.8	132.8	1790	260	40	223.15	226.7	600	20	40
42.3	44.3	2070	8	40	132.8	135.2	740	200	40	226.7	230.75	570	52	40
44.3	46.3	310	12	40	135.2	137.2	1350	470	40	230.75	238.85	525	21	40
46.3	48.3	365	15	40	137.2	139.2	3070	340	40	238.85	239	590	87	40
48.3	50.3	203	50	40	139.2	141.2	1530	480	40	239	241	400	20	40
50.3	53.65	558	41	40	141.2	143.2	1870	495	40	241	243	205	8	40
53.65	56.85	128	32	40	143.2	145.2	810	370	40	243	245	128	7	40
56.85	58.15	700	33	40	145.2	147.2	500	285	40	245	247	155	67	40
58.15	60.15	970	150	40	147.2	149.2	980	480	40	247	251	90	32	40
60.15	62.15	428	145	40	149.2	151.2	3150	1360	40	251	253	88	32	40
62.15	64.15	400	138	40	151.2	153.2	3390	1950	40	253	255	98	27	40
64.15	66.15	1000	240	40	153.2	155.2	1230	610	40	255	257.85	120	22	40
66.15	69.1	850	330	40	155.2	157.2	1080	580	40	257.85	259.85	87	118	40
69.1	71.1	530	165	40	157.2	159.2	465	170	40	259.85	262	69	5	40
71.1	73.1	470	90	40	159.2	161.6	800	310	40	262	264	15	5	40
73.1	75.1	530	170	40	161.6	163.65	1230	480	40	264	266	15	5	40
75.1	78.25	460	90	40	163.65	165.85	1550	545	40	266	268.5	28	39	40
78.25	81.3	830	210	40	165.85	167.65	2250	1700	40	268.5	270.25	45	5	40
81.3	84.35	540	100	40	167.65	169.65	1290	1580	40	270.25	272.25	35	6	40
84.35	85.9	2080	110	40	169.65	171.65	1710	735	40	272.25	274.25	16	8	40
85.9	87.9	585	100	40	171.65	173.65	860	920	40	274.25	276.2	35	7	40
87.9	89.9	1200	220	40	173.65	175.65	885	235	40	276.2	277.7	41	5	40
89.9	90.9	430	107	40	175.65	177.25	1940	630	40					

Table C.5 Data of borehole 5 from MTA 2006.

From (m)	To (m)	Cu (ppm)	Mo (ppm)	Au (ppm)	From (m)	To (m)	Cu (ppm)	Mo (ppm)	Au (ppm)	From (m)	To (m)	Cu (ppm)	Mo (ppm)	Au (ppm)
0	2.55	410	7	40	84.75	86.9	210	10	40	167	168.7	13	5	40
2.55	4.55	400	5	40	86.9	88.5	160	28	40	168.7	170	11	5	40
4.55	6.2	310	5	40	88.5	90.5	120	10	40	170	171.6	40	17	40
6.2	8.15	209	5	40	90.5	92.5	190	18	40	171.6	173.6	67	92	40
8.15	10.15	810	15	40	92.5	94.9	146	33	40	173.6	175.35	33	87	40
10.15	12.7	228	5	40	94.9	96.9	80	11	40	175.35	177.35	110	230	40
12.7	14.7	181	5	40	96.9	100.85	83	5	40	177.35	179.35	800	550	40
14.7	16.7	286	5	40	100.85	102.5	20	200	40	179.35	181.35	310	265	40
16.7	18.7	275	5	40	102.5	104.2	2080	72	40	181.35	183.35	175	175	40
18.7	20.7	196	5	40	104.2	105.95	5600	156	80	183.35	185.35	80	270	40
20.7	22.7	235	5	40	105.95	107.05	97	21	40	185.35	187.35	121	730	40
22.7	24.7	264	5	40	107.05	109	210	42	40	187.35	189.35	460	540	40
24.7	26.7	883	5	40	109	111.3	50	5	40	189.35	191.35	36	370	40
26.7	28.7	351	5	40	111.3	113.3	50	8	40	191.35	193.35	1400	280	40
28.7	30.7	600	17	40	113.3	115.5	20	5	40	193.35	195.35	51	880	40
30.7	32.7	313	6	40	115.5	117.5	48	5	40	195.35	197.35	1550	1000	40
32.7	34.7	218	13	40	117.5	120	45	5	40	197.35	199.35	140	650	40
34.7	36.7	219	270	40	120	120.5	62	5	40	199.35	201.35	25	160	40
36.7	38.7	227	370	40	120.5	122.5	52	5	40	201.35	203.35	25	12	40
38.7	40.7	250	110	40	122.5	124.5	43	5	40	203.35	205.35	100	8	40
40.7	42.7	340	76	40	124.5	126.5	25	5	40	205.35	207.35	52	12	40
42.7	44.4	178	470	40	126.5	128.5	30	5	40	207.35	209.35	35	11	40
44.4	46.4	252	360	40	128.5	130.25	28	5	40	209.35	211.35	106	9	40
46.4	48.4	179	850	40	130.25	132.55	43	5	40	211.35	213.35	62	27	40
48.4	49.3	510	193	40	132.55	133.55	20	5	40	213.35	215.35	40	5	40
49.3	50.6	360	210	40	133.55	134.6	43	5	40	215.35	217.35	37	5	40
50.6	52.6	153	215	40	134.6	136.6	16	5	40	217.35	219.35	79	5	40
52.6	54.6	362	150	40	136.6	138	72	5	40	219.35	221.35	80	11	40
54.6	56.6	500	85	40	138	140	12	5	40	221.35	223.35	125	5	40
56.6	58.7	442	350	40	140	142	14	5	40	223.35	225.35	42	54	40
58.7	61.2	176	21	40	142	144	27	5	40	225.35	227.35	26	18	40
61.2	64.4	236	8	40	144	146	18	5	40	227.35	230.25	97	5	40

Table C.5(Continue) Data of borehole 5 for Cu-Mo-Au from MTA 2006.

64.4	66.2	70	5	40	146	147.7	27	5	40	230.25	233.3	185	5	40
66.2	68.4	110	5	40	147.7	149.95	380	7	40	233.3	235.55	30	11	40
68.4	70.4	110	5	40	149.95	150.85	105	8	40	235.55	237.35	37	5	40
70.4	72.4	147	16	40	150.85	154	26	5	40	237.35	240.75	191	5	40
72.4	73.75	70	5	40	154	155.25	17	5	40	240.75	242.3	545	5	40
73.75	75.75	115	9	40	155.25	160.1	15	5	40	242.3	244.3	34	290	40
75.75	78.4	226	17	40	160.1	161.3	31	5	40	244.3	246.3	28	5	40
78.4	80.4	130	13	40	161.3	164.15	15	5	40	246.3	248.3	56	14	40
80.4	82.4	390	27	40	164.15	165.7	14	5	40	248.3	250.7	30	13	40
82.4	84.75	760	20	40	165.7	167	17	5	40	250.7	253.1	93	11	40

Table C.6 Data for borehole 6 from MTA 2006.

From (m)	To (m)	Cu (ppm)	Mo (ppm)	Au (ppm)	From (m)	To (m)	Cu (ppm)	Mo (ppm)	Au (ppm)
0	2	125	5	40	73.3	75.3	255	5	40
2	3.05	65	5	40	75.3	77.3	82	5	40
3.05	6.2	85	5	40	77.3	78.75	600	40	40
6.2	8.6	105	5	40	78.75	80.8	160	32	40
8.6	11.1	69	5	40	80.8	82.8	440	5	40
11.1	14.95	43	5	40	82.8	84.8	350	5	40
14.95	17.6	62	5	40	84.8	86.8	415	5	40
17.6	19.6	32	5	40	86.8	88.3	500	5	40
19.6	21.55	22	5	40	88.3	90.3	310	5	40
21.55	23.5	20	5	40	90.3	92.3	235	5	40
23.5	26.75	80	5	40	92.3	94.3	200	5	40
26.75	28.75	39	5	40	94.3	96.05	310	5	40
28.75	30.4	72	5	40	96.05	96.5	180	5	40
30.4	31.65	88	5	40	96.5	98.5	310	5	40
31.65	32.75	120	5	40	98.5	99.4	195	5	40
32.75	33.75	380	5	40	99.4	101.4	106	5	40
33.75	35.75	270	5	40	101.4	103.8	49	5	40
35.75	37.5	23	5	40	103.8	105.8	197	5	40
37.5	39.05	37	5	40	105.8	107.85	152	14	40
39.05	41.15	90	5	40	107.85	109.85	365	100	40
41.15	43.15	83	5	40	109.85	111.85	830	13	40
43.15	45.15	63	5	40	111.85	113.85	25	34	40
45.15	47.15	140	5	40	113.85	115.85	22	60	40
47.15	49.15	122	5	40	115.85	117.85	13	110	40
49.15	50.1	52	8	40	117.85	119.85	12	52	40
50.1	52	42	5	40	119.85	121.85	20	12	40
52	53.35	59	5	40	121.85	123.25	14	7	40
53.35	55	380	5	40	123.25	125.5	6	5	40
55	55.45	300	5	40	125.5	126.55	13	5	40
55.45	57	80	5	40	126.55	128.55	15	5	40
57	57.75	135	5	40	128.55	130.55	15	5	40
57.75	59.8	82	5	40	130.55	132.65	10	5	40
59.8	61.2	245	5	40	132.65	134.65	14	5	40

Table C.6(Continue) Data of borehole 6 for Cu-Mo-Au from MTA 2006.									
61.2	63.5	150	18	40	134.65	136.65	11	5	40
63.5	65.5	340	5	40	136.65	138.65	15	5	40
65.5	67.5	850	5	40	138.65	140.65	13	5	40
67.5	68.6	115	5	40	140.65	142.65	15	5	40
68.6	71	187	5	40	142.65	144.65	13	5	40
71	72.5	139	5	40	144.65	145.75	14	5	40
72.5	73.3	258	5	40	145.75	147.4	10	5	40

Table C.7 Data for borehole 7 from MTA 2006.

Tps-7					Tps-7				
From (m)	To (m)	Cu (ppm)	Mo (ppm)	Au (ppm)	From (m)	To (m)	Cu (ppm)	Mo (ppm)	Au (ppm)
0	2	125	5	40	74	76	55	5	40
2	4	187	5	40	76	78	20	5	40
4	6	129	5	40	78	80	15	5	40
6	8	210	5	40	80	82	34	5	40
8	10	200	5	40	82	84.15	40	5	40
10	12	146	5	40	84.15	86.15	25	5	40
12	13	118	5	40	86.15	88.15	37	5	40
13	14.5	38	5	40	88.15	90.15	40	5	40
14.5	16.5	59	5	40	90.15	92.15	30	5	40
16.5	18.5	13	5	40	92.15	94.15	19	5	40
18.5	20.5	16	5	40	94.15	95.2	58	5	40
20.5	21.95	110	5	40	95.2	97.2	21	5	40
21.95	23.95	29	5	40	97.2	99.2	28	5	40
23.95	25.95	28	5	40	99.2	100.2	36	5	40
25.95	27.95	34	5	40	100.2	102.15	45	5	40
27.95	29.95	19	5	40	102.15	104.15	54	5	40
29.95	31.05	20	5	40	104.15	106	48	5	40
31.05	32.5	28	5	40	106	108.25	18	5	40
32.5	34.5	20	5	40	108.25	110.25	13	5	40
34.5	36.25	23	5	40	110.25	112.25	28	5	40
36.25	38.25	16	5	40	112.25	114.25	60	5	40
38.25	40.25	15	5	40	114.25	116.25	51	5	40
40.25	42.25	18	5	40	116.25	118.25	23	5	40
42.25	44.25	16	5	40	118.25	120.25	50	5	40
44.25	26.25	21	5	40	120.25	122.25	13	5	40
26.25	48.25	14	5	40	122.25	124.25	18	5	40
48.25	50.25	13	5	40	124.25	126.25	25	5	40
50.25	52.25	21	5	40	126.25	128.25	23	5	40
52.25	54.25	17	5	40	128.25	130.25	18	33	40
54.25	56.25	38	5	40	130.25	132.25	26	5	40
56.25	58.25	23	5	40	132.25	134.25	40	5	40
58.25	60.25	18	5	40	134.25	136.25	22	6	40
60.25	62.25	22	5	40	136.25	138.25	16	5	40
62.25	64.25	45	5	40	138.25	140.25	17	5	40
64.25	66.25	19	5	40	140.25	142.25	25	5	40
66.25	68.25	17	5	40	142.25	144.25	34	5	40
68.25	70.25	26	5	40	144.25	146.25	50	5	40
70.25	72.25	33	5	40	146.25	148.25	45	5	40

Table C.7(Continue) Data of borehole 7 for Cu-Mo-Au from MTA 2006.									
72.25	74	30	5	40	148.25	150.25	124	5	40
					150.25	151.5	23	5	40

Table C.8 Data of borehole 8 from MTA 2006.

From (m)	To (m)	Cu (ppm)	Mo (ppm)	Au (ppm)	From (m)	To (m)	Cu (ppm)	Mo (ppm)	Au (ppm)	From (m)	To (m)	Cu (ppm)	Mo (ppm)	Au (ppm)
0	4	60	14	40	94	95	300	10	40	184	186	264	5	40
4	6	56	6	40	95	97.3	53	11	40	186	188	165	330	40
6	8.85	32	5	40	97.3	99.3	62	5	40	188	190	425	220	40
8.85	10.85	66	10	40	99.3	101.3	69	5	40	190	192	145	8	40
10.85	12.85	33	7	40	101.3	104	118	8	40	192	194	1850	1000	40
12.85	13.9	125	13	40	104	106	70	10	40	194	196	290	220	40
13.9	14.8	110	9	40	106	108	76	10	40	196	198	210	730	40
14.8	16.8	58	5	40	108	110	123	15	40	198	200	157	30	40
16.8	18.8	60	10	40	110	112	115	17	40	200	202	375	5	40
18.8	20	66	8	40	112	114	268	25	40	202	204	38	5	40
20	21.4	32	5	40	114	116	140	38	40	204	206	116	60	40
21.4	23.4	57	5	40	116	118	637	7	40	206	208	64	5	40
23.4	25.4	78	5	40	118	120	320	10	40	208	210.15	40	5	40
25.4	27.4	84	5	40	120	122	280	12	40	210.15	212.15	50	21	40
27.4	29.4	81	5	40	122	124	290	12	40	212.15	214.15	200	9	40
29.4	31.4	69	5	40	124	126	235	20	40	214.15	216.15	455	5	40
31.4	33.4	40	5	40	126	127.7	225	11	40	216.15	217.4	200	21	40
33.4	35.5	100	6	40	127.7	129	81	500	40	217.4	218.6	19	20	40
35.5	37.75	75	5	40	129	131.5	596	200	40	218.6	220.6	430	60	40
37.75	39.75	20	5	40	131.5	133.05	680	85	40	220.6	222.6	60	8	40
39.75	42.5	21	5	40	133.05	135.05	585	240	40	222.6	224.6	158	5	40
42.5	44.5	100	5	40	135.05	135.9	550	500	40	224.6	227.6	63	5	40
44.5	45.5	33	35	40	135.9	137.9	390	300	40	227.6	229.6	60	5	40
45.5	46.75	104	5	40	137.9	138.35	148	70	40	229.6	231.6	19	5	40
46.75	47.75	105	12	40	138.35	140.6	250	195	40	231.6	233.6	20	5	40
47.75	48.75	59	15	40	140.6	143.6	1950	250	40	233.6	235.6	16	5	40
48.75	50.5	95	13	40	143.6	145.25	725	550	40	235.6	237.6	20	5	40
50.5	53.55	162	19	40	145.25	147.85	49	600	40	237.6	239.6	18	5	40
53.55	55	60	14	40	147.85	150.25	164	45	40	239.6	241.75	24	5	40
55	57.6	35	10	40	150.25	152.25	1000	120	40	241.75	243.75	18	5	40
57.6	59.6	16	13	40	152.25	154.25	1500	70	40	243.75	245.75	25	5	40
59.6	61.6	45	10	40	154.25	156	200	50	40	245.75	247.75	20	5	40

Table C.8(Continue) Data of borehole 8 for Cu-Mo-Au from MTA 2006.

61.6	64	98	8	40	156	158	240	70	40	247.75	249.75	23	5	40
64	66	160	10	40	158	159	90	60	40	249.75	251.75	18	5	40
66	68	76	7	40	159	160	125	13	40	251.75	253.75	19	5	40
68	70	150	5	40	160	161.3	120	30	40	253.75	255.75	12	7	40
70	72	89	5	40	161.3	163.3	100	40	40	255.75	257.75	10	5	40
72	74	130	5	40	163.3	165.3	231	18	40	257.75	259.75	13	5	40
74	76	240	5	40	165.3	166.5	300	48	40	259.75	261.75	22	12	40
76	78	294	5	40	166.5	167.85	365	5	40	261.75	263.75	13	5	40
78	80	80	5	40	167.85	169.85	280	75	40	263.75	265.75	18	10	40
80	82	270	5	40	169.85	171.85	120	110	40	265.75	267.75	14	5	40
82	84	58	5	40	171.85	173.85	290	123	40	267.75	269.75	19	5	40
84	86	92	5	40	173.85	175.85	182	60	40	269.75	271.75	9	5	40
86	88	30	5	40	175.85	177.85	510	11	40	271.75	273.75	20	5	40
88	90	28	5	40	177.85	179.85	120	67	40	273.75	275.75	10	5	40
90	92	140	8	40	179.85	181.75	284	68	40	275.75	278.5	14	5	40
92	94	58	8	40	181.75	184	242	9	40					

Table C.9 Data for borehole 9 from MTA 2006

From (m)	To (m)	Cu (ppm)	Mo (ppm)	Au (ppm)	From (m)	To (m)	Cu (ppm)	Mo (ppm)	Au (ppm)	From (m)	To (m)	Cu (ppm)	Mo (ppm)	Au (ppm)
0	2	910	5	40	122	124	70	13	40	242	244	950	5	40
2	4	450	5	40	124	126	57	15	40	244	246	141	5	40
4	6	750	5	40	126	128	117	7	40	246	248	57	5	40
6	8	240	21	40	128	130	125	8	40	248	250	62	6	40
8	10	210	5	40	130	132	110	5	40	250	252	70	5	40
10	12	360	10	40	132	134	65	6	40	252	254	71	5	40
12	14	180	10	40	134	136	270	10	40	254	256	33	5	40
14	16	280	10	40	136	138	367	5	40	256	258	67	5	40
16	18	380	5	40	138	140	425	5	40	258	260	75	5	40
18	20	215	5	40	140	142	1300	5	40	260	262	100	5	40
20	22	180	5	40	142	144	260	5	40	262	264	65	5	40
22	24	356	5	40	144	145.25	312	5	40	264	266	50	5	40
24	26	270	5	40	145.25	146.75	133	5	40	266	268	44	5	40
26	28	258	5	40	146.75	148	197	5	40	268	270	52	5	40
28	30	226	5	40	148	150	212	5	40	270	272	95	5	40
30	32	318	5	40	150	152	208	5	40	272	274	92	5	40
32	34	271	5	40	152	154	210	5	40	274	276	67	5	40

Table C.9(Continue) Data of borehole 9 for Cu-Mo-Au from MTA 2006.

34	36	118	5	40	154	156	347	5	40	276	278	65	5	40
36	38	73	5	40	156	158	350	5	40	278	280	55	5	40
38	40	65	5	40	158	160	224	9	40	280	282	78	5	40
40	42	68	11	40	160	162	231	5	40	282	284	72	5	40
42	44	256	8	40	162	164	485	5	40	284	285.55	99	9	40
44	46	217	10	40	164	166	620	5	40	285.55	287.5	34	5	40
46	48	79	5	40	166	168	226	5	40	287.5	289.55	34	7	40
48	50	320	8	40	168	170	265	5	40	289.55	292	57	22	40
50	52	230	8	40	170	172	346	5	40	292	295	61	5	40
52	54	300	5	40	172	174	279	59	40	295	298	55	5	40
54	56	352	38	40	174	176	380	5	40	298	301	150	5	40
56	58	377	21	40	176	178	262	5	40	301	304	88	5	40
58	60	365	8	40	178	180	222	5	40	304	306	131	5	40
60	62	152	82	40	180	182	108	5	40	306	308	70	5	40
62	64	270	70	40	182	184	310	5	40	308	310	55	14	40
64	66	220	16	40	184	186	265	5	40	310	312	86	5	40
66	68	100	14	40	186	188	265	5	40	312	315	49	5	40
68	70	210	21	40	188	190	74	5	40	315	316.55	65	5	40
70	72	160	5	40	190	192	118	5	40	316.55	319	68	18	40
72	74	150	28	40	192	194	93	5	40	319	322	25	5	40
74	76	360	7	40	194	196	215	5	40	322	325	47	5	40
76	78	190	5	40	196	198	120	5	40	325	328.2	14	5	40
78	80	220	7	40	198	200.5	101	5	40	328.2	330	19	5	40
80	82	210	10	40	200.5	202	43	6	40	330	332	77	5	40
82	84	116	47	40	202	204	148	6	40	332	334	19	5	40
84	86	260	14	40	204	206	72	5	40	334	336	32	7	40
86	88	160	8	40	206	207	30	5	40	336	338	212	19	40
88	90	1250	10	40	207	210	55	5	40	338	340	127	8	40
90	92	240	5	40	210	212	58	5	40	340	342	135	5	40
92	94	210	6	40	212	214	149	5	40	342	344	135	6	40
94	96	160	5	40	214	216	93	5	40	344	346	86	5	40
96	98	290	5	40	216	218	175	6	40	346	348	192	5	40
98	100	200	55	40	218	220	68	11	40	348	350	13	5	40
100	102	110	5	40	220	222	57	7	40	350	352	166	5	40
102	104	79	5	40	222	224	86	8	40	352	354	99	5	40
104	106	130	146	40	224	226	104	10	40	354	356	14	5	40
106	108	95	5	40	226	228	88	8	40	356	358	213	5	40
108	110	62	5	40	228	230	99	20	40	358	360	10	5	40
110	112	123	38	40	230	232	54	13	40	360	362	30	5	40

Table C.9(Continue) Data of borehole 9 for Cu-Mo-Au from MTA 2006.

112	115	88	5	40	232	234	79	9	40	362	364	19	5	40
115	116	155	8	40	234	236	54	5	40	364	366	59	5	40
116	118	51	7	40	236	238	68	7	40	366	368	69	5	40
118	120	135	5	40	238	240	64	5	40	368	369	119	5	40
120	122	140	12	40	240	242	240	5	40	369	369.7	49	5	40

Table C.10 Data for borehole 10 from MTA 2006.

From (m)	To (m)	Cu (ppm)	Mo (ppm)	Au (ppm)	From (m)	To (m)	Cu (ppm)	Mo (ppm)	Au (ppm)	From (m)	To (m)	Cu (ppm)	Mo (ppm)	Au (ppm)
0	2	2440	21	40	99.5	101.5	151	5	40	224	226	100	14	40
2	3.85	3200	15	50	101.5	103.5	460	11	40	226	228	95	9	40
3.85	5.4	817	10	40	103.5	105.5	335	11	40	228	230	142	20	40
5.4	7.9	1132	12	40	105.5	107.5	294	9	40	230	232	77	14	40
7.9	8.7	1195	15	40	107.5	109.5	85	11	40	232	234	138	18	40
8.7	10.7	4180	83	80	109.5	111.5	114	6	40	234	236	130	14	40
10.7	12.7	7460	195	100	111.5	113.5	118	8	40	236	238	59	6	40
12.7	14.7	9180	600	330	113.5	115.5	184	5	40	238	240	54	5	40
14.7	15.25	18000	765	240	115.5	117.5	109	9	40	240	242	72	9	40
15.25	15.8	14500	60	840	117.5	119.5	185	11	40	242	244	215	9	40
15.8	16.55	9500	1800	1100	119.5	121.5	158	16	40	244	247.25	140	5	40
16.55	17.05	16800	80	60	121.5	123.5	232	11	40	247.25	250	10	5	40
17.05	18.05	20000	1900	100	123.5	125.5	231	11	40	250	253	160	5	40
18.05	20.1	6920	1400	140	125.5	127.5	184	13	40	253	255	90	5	40
20.1	22.1	7670	180	80	127.5	129.5	76	6	40	255	257.5	280	9	40
22.1	23.15	2890	11	40	129.5	131.5	187	12	40	257.5	260	96	14	40
23.15	25	10400	40	40	131.5	133.5	267	15	40	260	262	58	6	40
25	26	18250	300	40	133.5	135.5	145	10	40	262	264	30	5	40
26	27	28000	281	280	135.5	137.5	257	15	40	264	266	110	18	40
27	28	7115	550	40	137.5	139.5	272	16	40	266	268	86	5	40
28	29	39100	2000	150	139.5	141.5	210	21	40	268	270	64	20	40
29	30	6430	670	40	141.5	143.5	175	24	40	270	272	180	9	40
30	31	5400	31	40	143.5	145.5	328	22	40	272	274	45	6	40
31	31.4	5280	8	40	145.5	147.5	840	20	40	274	276	60	5	40

Table C.10(Continue) Data of borehole 10 for Cu-Mo-Au from MTA 2006.

31.4	32.5	4000	700	40	147.5	149.5	2120	28	40	276	278	53	10	40
32.5	33.5	6115	445	40	149.5	151.5	142	40	40	278	280	97	6	40
33.5	34.5	3140	202	40	151.5	153.5	262	16	40	280	282	50	6	40
34.5	35.5	6440	40	40	153.5	155.5	159	25	40	282	284	63	5	40
35.5	36.5	3000	100	40	155.5	157.5	169	26	40	284	286	78	20	40
36.5	37.5	315	980	40	157.5	159.5	130	58	40	286	288	93	5	40
37.5	38.8	1140	42	40	159.5	161.5	194	26	40	288	291	90	7	40
38.8	39.5	135	35	40	161.5	163.5	114	38	40	291	293	88	58	40
39.5	41.5	275	54	40	163.5	165.5	206	50	40	293	295	280	38	40
41.5	43.5	312	68	40	165.5	167.5	158	20	40	295	297	520	22	40
43.5	45.5	1400	79	40	167.5	169.5	155	20	40	297	300	130	17	40
45.5	47.5	2620	92	40	169.5	171.5	52	28	40	300	302	133	5	40
47.5	49.5	114	92	40	171.5	173.5	55	12	40	302	304	60	7	40
49.5	51.5	823	27	40	173.5	175.5	77	26	40	304	306.8	155	5	40
51.5	53.5	320	41	40	175.5	177.5	119	19	40	306.8	308.8	54	5	40
53.5	55.5	157	72	40	177.5	179.5	136	26	40	308.8	31	92	5	40
55.5	57.5	310	144	40	179.5	181.5	102	14	40	31	313	16	5	40
57.5	59.5	355	29	40	181.5	183.5	85	16	40	313	315	30	5	40
59.5	61.5	213	6	40	183.5	185.5	123	17	40	315	317	32	5	40
61.5	63.5	303	19	40	185.5	187.5	73	145	40	317	319	55	5	40
63.5	65.5	263	8	40	187.5	189.5	158	27	40	319	321.5	43	5	40
65.5	67.5	281	15	40	189.5	191.5	160	32	40	321.5	324	58	5	40
67.5	69.5	210	5	40	191.5	193.5	119	26	40	324	326	600	5	40
69.5	71.6	81	5	40	193.5	195.5	90	31	40	326	328	98	215	40
71.6	73.6	247	12	40	195.5	197.5	145	146	40	328	330	116	5	40
73.6	75.5	146	6	40	197.5	200	70	36	40	330	332.25	78	20	40
75.5	77.5	118	13	40	200	202.5	78	44	40	332.25	335.25	22	5	40
77.5	79.5	221	8	40	202.5	204.5	185	20	40	335.25	341.7	16	5	40
79.5	81.5	175	13	40	204.5	206	135	53	40	341.7	344.7	18	5	40
81.5	83.5	205	27	40	206	208	186	33	40	344.7	348	15	5	40
83.5	85.5	129	8	40	208	210	100	42	40	348	350	62	7	40
85.5	87.5	2160	6	40	210	212	116	24	40	350	354.55	35	8	40
87.5	89.5	132	5	40	212	214	143	80	40	354.55	357.4	13	5	40
89.5	91.5	245	5	40	214	216	153	14	40	357.4	360.45	11	26	40

Table C.10(Continue) Data of borehole 10 for Cu-Mo-Au from MTA 2006.

91.5	93.5	165	24	40	216	218	90	13	40	360.45	363.65	10	14	40
93.5	95.5	292	29	40	218	220	95	11	40	363.65	366	11	5	40
95.5	97.5	212	19	40	220	222	98	11	40	366	370.85	9	5	40
97.5	99.5	126	8	40	222	224	33	7	40					

Table C.11 Data for borehole from MTA 2006.

From (m)	To (m)	Cu (ppm)	Mo (ppm)	Au (ppm)	From (m)	To (m)	Cu (ppm)	Mo (ppm)	Au (ppm)	From (m)	To (m)	Cu (ppm)	Mo (ppm)	Au (ppm)
0	3	2592	52	60	89	91	47	208	40	175	177	87	25	40
3	5	3100	52	40	91	93	64	10	40	177	179	92	14	40
5	7	1211	42	40	93	95	267	19	40	179	181	74	8	40
7	9	501	53	40	95	97	631	8	40	181	183	76	19	40
9	11	3580	17	50	97	99	190	13	40	183	185	53	5	40
11	13	3198	27	40	99	101	249	15	40	185	187	42	7	40
13	15	1791	20	40	101	103	257	220	40	187	189	73	10	40
15	17	3508	205	50	103	105	86	49	40	189	191	19	21	40
17	19	2552	105	40	105	107	105	29	40	191	193	35	44	40
19	21	583	28	40	107	109	138	27	40	193	195	60	9	40
21	23	908	54	40	109	111	185	12	40	195	197	121	6	40
23	25	599	68	40	111	113	180	21	40	197	199	55	10	40
25	27	1359	60	40	113	115	326	25	40	199	201	42	8	40
27	29	745	27	40	115	117	120	10	40	201	203	53	10	40
29	31	995	158	40	117	119	126	17	40	203	205	48	5	40
31	33	300	142	40	119	121	137	18	40	205	207	79	140	40
33	34	189	20	40	121	123	104	32	40	207	209	85	7	40
34	36	178	21	40	123	125	124	38	40	209	209.75	84	10	40
36	38	321	110	40	125	127	133	12	40	209.75	211.5	18	14	40
38	40	344	24	40	127	129	89	15	40	211.5	213.5	13	304	40
40	42	538	26	40	129	131	79	5	40	213.5	215.5	85	416	40
42	44	390	21	40	131	133	124	8	40	215.5	217.5	179	107	40
44	46	1343	21	40	133	135	130	11	40	217.5	219.5	253	112	40
46	48	547	28	40	135	137	86	11	40	219.5	220.75	212	78	40
48	50	268	30	40	137	139	1000	27	40	220.75	222.5	197	87	40
50	52	415	57	40	139	141	86	21	40	222.5	224.5	1080	114	40
52	54	390	92	40	141	141.5	251	6	40	224.5	226.3	480	119	40
54	56	330	42	40	141.5	142.5	690	5	40	226.3	227	1660	58	40
56	58	572	15	40	142.5	144.5	100	5	40	227	229	177	113	40
58	60	62	13	40	144.5	147	125	13	40	229	231	345	231	40
60	62	125	203	40	147	149	76	12	40	231	233	450	200	40

Table C.11(Continue) Data of borehole 11 for Cu-Mo-Au from MTA 2006.

62	64	217	50	40	149	151	179	7	40	233	235	610	125	40
64	66	126	9	40	151	153	184	12	40	235	236	194	130	40
66	68	2155	25	40	153	155	171	19	40	236	238	362	147	40
68	70	166	12	40	155	157	115	7	40	238	239.5	430	135	40
70	72	184	107	40	157	159	101	12	40	239.5	241	495	248	40
72	74	101	81	40	159	161	102	8	40	241	242.5	368	175	40
74	75.5	181	126	40	161	163	344	8	40	242.5	244.5	440	123	40
75.5	77.5	74	5	40	163	165	810	7	40	244.5	246	18	84	40
77.5	79.5	27	5	40	165	167	53	8	40	246	248	12	5	40
79.5	81.5	151	86	40	167	169	21	5	40	248	250	18	5	40
81.5	84	59	7	40	169	171	50	6	40	250	251.25	39	5	40
84	86	221	23	40	171	173	188	5	40					
86	89	247	16	40	173	175	88	5	40					

Table C.12 Data for borehole 12 from MTA 2006.

From (m)	To (m)	Cu (ppm)	Mo (ppm)	Au (ppm)	From (m)	To (m)	Cu (ppm)	Mo (ppm)	Au (ppm)	From (m)	To (m)	Cu (ppm)	Mo (ppm)	Au (ppm)
0	2	324	6	40	74	75	730	16	40	139	140	8875	280	90
2	4	435	6	40	75	76.05	172	29	40	140	141	7050	400	230
4	6	580	5	40	76.05	78	181	15	40	141	142	12000	380	350
6	8	1130	8	40	78	79	1125	195	40	142	143	5400	102	250
8	10	505	5	40	79	81.8	3600	1140	40	143	144	18800	188	750
10	12	304	15	40	81.8	82	3600	90	220	144	145	11800	766	780
12	14	284	5	40	82	83	3320	65	50	145	146	16000	207	12000
14	15	207	5	40	83	84	1620	200	40	146	147	6000	382	380
15	16	274	6	40	84	85	2750	45	60	147	148	8180	258	220
16	17	258	5	40	85	86	1300	53	40	148	149	4400	200	140
17	19	184	5	40	86	87	2500	203	60	149	150	10300	1170	390
19	20	14200	7	40	87	88	2800	68	40	150	151	5000	352	80
20	21	5600	5	40	88	89	5380	337	110	151	152	8700	760	210
21	22	475	27	40	89	90	4360	243	80	152	153	7800	200	350
22	23	815	28	40	90	91	3000	1000	80	153	154	17700	140	650
23	24	358	12	40	91	92	3500	1000	100	154	155	12000	26	680
24	25	343	20	40	92	93	3200	2400	70	155	156	5500	313	130
25	26	410	27	40	93	94	5750	1730	150	156	157	3100	425	110
26	27	404	11	40	94	95	3430	463	30	157	158	820	43	40
27	27.85	213	5	40	95	96	1400	530	50	158	159	570	19	40

Table C.12(Continue) Data of borehole 12 for Cu-Mo-Au from MTA 2006.

27.85	29	137	13	40	96	97	1250	600	60	159	160	820	15	40
29	30	220	30	40	97	98	1276	460	40	160	161	1250	51	70
30	31	381	44	40	98	99.15	770	337	40	161	162	1450	52	40
31	32	482	65	40	99.15	99.75	865	1800	40	162	163	710	83	40
32	33	365	23	40	99.75	101	865	1800	40	163	164	2420	118	80
33	34	267	26	40	101	102	522	98	40	164	165	1950	66	80
34	35	810	41	40	102	103	1000	880	100	165	166	5100	14	140
35	37	1000	58	40	103	103.3	2000	3000	80	166	167	2840	630	80
37	39	317	55	40	103.3	104	2220	218	20	167	168	2390	65	230
39	41	960	16	40	104	105	27200	1300	420	168	169	518	62	40
41	42	318	102	40	105	106	18800	2130	550	169	170	83	15	40
42	43	127	86	40	106	108	14200	200	480	170	172	80	5	40
43	44	140	32	40	108	109	21350	157	450	172	174	382	13	40
44	45	112	35	40	109	110	8400	180	370	174	176	78	5	40
45	46	1350	77	40	110	111	3220	115	80	176	178	260	27	40
46	47	294	175	40	111	112	3850	1000	100	178	180	1600	7	40
47	48	98	1840	40	112	113	13800	1430	400	180	182	152	21	40
48	49	180	71	40	113	114	23500	1700	640	182	184	810	128	40
49	50	128	91	40	114	115	23200	1480	180	184	186	1200	23	40
50	51	161	21	40	115	116	16500	441	150	186	188	2500	105	40
51	52	508	63	40	116	117	25100	3200	410	188	190	178	27	40
52	53	107	78	40	117	118	14880	1400	200	190	192	126	9	40
53	54	160	65	40	118	119	12150	550	180	192	194	93	8	40
54	55	390	130	40	119	120	12980	1200	400	194	196	58	5	40
55	56	118	114	40	120	121	8830	800	150	196	198	88	14	40
56	57	147	80	40	121	122	8400	727	180	198	200	204	8	40
57	58	614	363	40	122	123	8000	455	180	200	202	386	11	40
58	59	180	25	40	123	124	7110	400	200	202	203.25	128	15	40
59	60	408	42	40	124	125	3180	632	250	203.25	206	8	5	40
60	61	80	23	40	125	126	3840	300	130	206	207.25	28	5	40
61	62	58	17	40	126	127	3275	100	210	207.25	209.2	200	9	40
62	63	4000	150	40	127	128	3320	1400	170	209.2	211	67	5	40
63	64	5780	135	40	128	129	3280	620	110	211	212	68	6	40
64	65	950	75	40	129	130	3150	235	100	212	213	14	5	40
65	66	284	67	40	130	132	3375	100	280	213	215	32	5	40
66	67	285	33	40	132	133	18850	285	350	215	217	7	5	40

Table C.12(Continue) Data of borehole 12 for Cu-Mo-Au from MTA 2006.

67	68	531	30	40	133	134	13880	3300	280	217	219	88	5	40
68	69	410	27	40	134	135	13575	1100	300	219	221	482	5	40
69	70	106	21	40	135	136	10000	1880	250	221	223.15	93	5	40
70	71	1000	41	40	136	137	8000	680	150	223.15	225.25	181	5	40
71	72	203	59	40	137	138	12200	1200	280	225.25	227.4	25	48	40
72	73	188	27	40	138	139	14400	355	380					
73	74	288	17	40										

Table C.13 Data of borehole 13 from MTA 2006.

From (m)	To (m)	Cu (ppm)	Mo (ppm)	Au (ppm)	From (m)	To (m)	Cu (ppm)	Mo (ppm)	Au (ppm)	From (m)	To (m)	Cu (ppm)	Mo (ppm)	Au (ppm)
0	3	220	5	40	61	62	1180	55	40	142.6	144	130	20	40
3	5	190	5	40	73	75	358	16	40	144	146	170	16	40
5	7	380	5	40	75	77	128	63	40	146	148	88	56	40
7	9	400	5	40	77	79	225	325	40	148	150	600	59	40
9	11	240	5	40	79	81	180	325	40	150	150.75	850	36	40
11	13	500	5	40	81	83	300	65	40	150.75	152	75	5	40
13	15	265	5	40	83	85	195	12	40	152	153	85	37	40
15	17	300	5	40	85	87	277	7	40	153	153.5	43	6	40
17	19	320	5	40	87	89	283	13	40	153.5	155	137	8	40
19	21	380	5	40	89	91	100	25	40	155	157	340	82	40
21	23	280	5	40	91	93	63	12	40	157	158	108	388	80
23	25	570	5	40	93	95	172	24	40	158	161	123	20	40
25	27	480	5	40	95	97	112	30	40	161	163	97	480	40
27	29	280	5	40	97	99	154	60	40	163	165	105	34	40
29	31	100	5	40	99	101	189	38	40	165	167	38	54	40
31	33	168	5	90	101	103	127	15	40	167	169	220	240	40
33	35	445	36	40	103	104.5	200	10	40	169	171	225	19	40
35	37.4	120	5	40	104.5	106	325	62	40	171	173	450	37	40
37.4	40	85	7	10	106	108	90	23	40	173	175	225	80	40
40	42	1140	150	40	108	110	155	11	40	175	177	85	130	40
42	44	225	7	40	110	112	108	16	40	177	179	143	53	40
44	46	210	8	40	112	114	172	25	40	179	181	430	22	40
46	47	2800	245	40	114	116	211	18	40	181	183	144	13	40
47	48	5700	488	40	116	118	130	25	40	183	185	146	25	40
48	49	2800	250	40	118	120	190	25	40	185	187	125	80	40
49	50	1550	5	40	120	122	120	21	40	187	189	285	5	40
50	51	810	70	40	122	124	110	18	40	189	191	185	8	40
51	52	5600	840	80	124	126	96	11	40	191	193	205	7	40
52	53	1200	20	40	126	128	80	7	40	193	195	100	10	40

Table C.13(Continue) Data of borehole 13 for Cu-Mo-Au from MTA 2006.

53	54	1170	15	40	128	130	140	6	40	195	197	110	8	40
54	55	3200	120	40	130	132	215	36	40	197	199	225	10	40
55	56	350	35	40	132	134	120	30	40	199	201	27	5	40
56	57	1080	75	40	134	136	400	78	40	201	203	72	8	40
57	58	485	60	40	136	138	88	23	40	203	204	95	5	40
58	59	375	350	40	138	140	230	10	40	204	205.7	120	10	40
59	60	1300	10	40	140	142	112	12	40					
60	61	1350	180	40	142	142.6	20		40					

Table C.14 Data for borehole 14 from MTA 2006.

From (m)	To (m)	Cu (ppm)	Mo (ppm)	Au (ppm)	From (m)	To (m)	Cu (ppm)	Mo (ppm)	Au (ppm)	From (m)	To (m)	Cu (ppm)	Mo (ppm)	Au (ppm)
0	2	2950	9	40	85.7	86.5	58	1300	40	143	145	17	5	40
2	4	2000	7	40	86.5	87.5	68	305	40	145	147	22	34	40
4	6	1565	18	40	87.5	89.25	20	1000	40	147	149	44	62	40
6	8	1885	850	40	89.25	90.15	1100	23	40	149	151	51	80	40
8	10	1610	700	40	90.15	92	132	405	40	151	153	116	40	40
10	10.75	325	980	40	92	93	446	1400	40	153	155	96	55	40
10.75	12.85				93	94	97	380	40	155	157	12	18	40
12.85	14.85	510	190	40	94	95	18	10	40	157	159	9	5	40
14.85	16.8				95	96	20	32	40	159	161	120	7	40
16.8	17.55	510	130	40	96	97	120	1900	40	161	163	173	60	40
17.55	20.6				97	98	70	2500	40	163	165	52	28	40
20.6	22	150	5	40	98	99	65	2000	40	165	167	23	5	40
22	24	140	5	40	99	100	100	2000	40	167	170	75	15	40
24	26	310	5	40	100	101	700	1700	40	170	174	22	8	40
26	28	208	8	40	101	102	75	2300	40	174	176	58	22	40
28	30	248	5	40	102	103	3850	150	40	176	178	44	12	40
30	32	247	5	40	103	104	1350	1880	40	178	180	61	58	40
32	34	408	5	40	104	105	118	1740	40	180	182	7	20	40
34	36	227	16	40	105	106	35	1800	40	182	184	7	5	40
36	38	270	24	40	106	107	55	5780	40	184	186	8	5	40
38	40	158	29	40	107	108	182	240	40	186	188	33	5	40
40	42	480	45	40	108	109	18	1000	40	188	190	22	5	40
42	44	200	30	40	109	110	8	1100	40	190	192	10	5	40
44	46	480	62	40	110	111	84	1250	40	192	194	9	5	40
46	48	480	22	40	111	112	1600	480	40	194	196	10	5	40
48	50	240	18	40	112	113	2800	100	40	196	198	8	6	40
50	52	240	18	40	113	114	4400	130	40	198	200	10	13	40
52	54	280	35	40	114	115	4800	610	40	200	202	35	14	40

Table C.14(Continue) Data of borehole 14 for Cu-Mo-Au from MTA 2006.

54	55	315	40	40	115	116	7500	885	40	202	205	12	5	40
55	57	314	32	40	116	117	12600	445	40	205	208	13	5	40
57	59	260	600	40	117	118	1190	1080	40	208	211	8	5	40
59	61	134	5	40	118	119	850	970	40	211	213	5	5	40
61	63	880	5	40	119	120	580	740	40	213	214	9	5	40
63	66	130	5	40	120	121	485	580	40	214	217	5	5	40
66	67	180	5	40	121	124	825	675	40	217	220	5	5	40
67	69	44	5	40	124	126	180	30	40	220	223	5	5	40
69	71	168	5	40	126	128	69	435	40	223	226	5	5	40
71	73	30	5	40	128	130	53	1230	40	226	229.55	5	5	40
73	75	488	6	40	130	131	43	930	40	229.55	232	5	5	40
75	77	510	14	40	131	132	170	1480	40	232	235	5	5	40
77	79	92	5	40	132	133	116	1370	40	235	238	17	5	40
79	81	125	5	40	133	134	50	980	40	238	241	10	300	40
81	83	280	5	40	134	137	20	240	40	241	246.5	8	13	40
83	84.5	35	5	40	137	139	162	50	40					
84.5	85.7	167	89	40	139	143	97	64	40					

Table C.15 Data of borehole 15 from MTA 2006.

From (m)	To (m)	Cu (ppm)	Mo (ppm)	Au (ppm)	From (m)	To (m)	Cu (ppm)	Mo (ppm)	Au (ppm)	From (m)	To (m)	Cu (ppm)	Mo (ppm)	Au (ppm)
0	2	184	5	40	81.65	83	27000	15	40	156.7	158.7	84	5	40
2	4	205	5	40	83	83.5	710	100	40	158.7	161.5	7	5	40
4	6	310	5	40	83.5	85	721	121	40	161.5	163.5	26	5	40
6	8	286	5	40	85	87	2200	230	40	163.5	167	19	35	40
8	10	211	5	40	87	89	115	15	40	167	170.25	24	3122	40
10	12	610	7	40	89	91	1075	148	40	170.25	172	50	16	40
12	13.25	320	5	40	91	93	1230	149	40	172	173.5	448	38	40
13.25	15.5	232	38	40	93	95	3720	435	40	173.5	175	19	20	40
15.5	17	22	5	40	95	96.5	165	114	40	175	177	56	10	40
17	19	470	15	40	96.5	97.75	30	17	40	177	179	76	9	40
19	21	428	5	40	97.75	98.75	236	400	40	179	181	275	8	40
21	22	250	6	40	98.75	101.75	500	46	40	181	183	17	15	40
22	23.5	300	21	40	101.75	103.75	100	36	40	183	185	16	67	40
23.5	25	343	11	40	103.75	105.5	350	10	40	185	187	98	113	40
25	27	580	13	40	105.5	107	227	27	40	187	189	56	37	40
27	29	542	16	40	107	109	51	5	40	189	191	275	67	40
29	31	350	7	40	109	109.5	228	66	40	191	193	368	52	40
31	33	815	18	40	109.5	111	127	23	40	193	195	85	78	40
33	35	180	5	40	111	113	470	200	40	195	197	16	7	40

Table C.15(Continue) Data of borehole 15 for Cu-Mo-Au from MTA 2006.

35	37	317	7	40	113	115	226	685	40	197	199	12	5	40
37	39	538	9	40	115	116.6	148	33	40	199	201	18	5	40
39	41	430	6	40	116.6	119.4	47	5	40	201	203	57	5	40
41	43	398	40	40	119.4	119.65	269	38	40	203	205	19	5	40
43	45	1270	44	40	119.65	121	90	12	40	205	207	140	5	40
45	47	520	5	40	121	122.5	159	31	40	207	209	15	5	40
47	49	451	18	40	122.5	124	306	20	40	209	211	25	5	40
49	51	544	8	40	124	126	128	80	40	211	213	69	5	40
51	53	640	13	40	126	128.2	77	515	40	213	215	8	5	40
53	55	184	5	40	128.2	130	63	845	40	215	217	9	11	40
55	57	268	5	40	130	132	57	940	40	217	219	140	5	40
57	59	236	5	40	132	134	44	24	40	219	221	85	5	40
59	61	2380	8	40	134	136	40	5	40	221	223	19	5	40
61	63	850	33	40	136	138	37	69	40	223	225	31	5	40
63	65	286	5	40	138	140.45	8	198	40	225	227	19	5	40
65	67	177	7	40	140.45	141.5	55	200	40	227	229	63	5	40
67	69	200	6	40	141.5	142.5	173	465	40	229	231	6	5	40
69	71	258	24	40	142.5	144	85	5	40	231	233	10	5	40
71	73	1100	56	40	144	145.8	230	134	40	233	236.15	34	5	40
73	75	181	26	40	145.8	146.25	195	111	40	236.15	240	12	6	40
75	77	700	102	40	146.25	148	836	308	40	240	243	33	11	40
77	78.5	4850	600	40	148	150	100	122	40	243	245.3	5	5	40
78.5	78.8		85	40	150	152	1400	107	40	245.3	248	5	5	40
78.8	79.3	3500	67	40	152	154	885	148	40	248	250.5	13	5	40
79.3	80.65	1275	120	40	154	156	71	520	40	250.5	253	8	5	40
80.65	81.65	280	15	40	156	156.7	16	220	40	253	256	12	5	40
										256	259	9	5	40

Table C.16 Data of borehole 16 from MTA 2006.

From (m)	To (m)	Cu (ppm)	Mo (ppm)	Au (ppm)	From (m)	To (m)	Cu (ppm)	Mo (ppm)	Au (ppm)	From (m)	To (m)	Cu (ppm)	Mo (ppm)	Au (ppm)
0	2	86	8	40	98	100	145	5	50	193.2	195.2	140	5	40
2	4	56	5	40	100	101	275	5	40	195.2	196.5	145	14	40
4	6	51	5	40	101	103	1300	340	40	196.5	198.5	34	780	40
6	8	65	6	40	103	105	795	375	40	198.5	200.5	55	6	40
8	10	290	8	40	105	106.15	1050	332	40	200.5	203	125	270	40
10	12.85	126	6	40	106.15	107	1400	42	40	203	205	18	78	40
12.85	14	198	6	40	107	109	390	30	40	205	207	10	32	40
14	16	103	7	40	109	111	970	130	40	207	209	19	7	40
16	18	182	5	40	111	113	360	47	40	209	211	12	7	40

Table C.16(Continue) Data of borehole 16 for Cu-Mo-Au from MTA 2006.

18	20	102	5	40	113	115	780	29	40	211	213	12	13	40
20	22	152	5	40	115	117	630	41	40	213	215	14	9	40
22	24	172	5	40	117	119	1100	275	40	215	217	31	5	40
24	26	172	24	40	119	121	1300	129	40	217	218	55	5	40
26	28	174	5	40	121	123	1500	102	40	218	220	10	5	40
28	30	250	9	40	123	125	1780	190	40	220	223.35	39	10	40
30	32	250	7	40	125	127	880	91	40	223.35	225	64	7	40
32	34	370	13	40	127	129	930	155	40	225	227	46	5	40
34	36	340	21	40	129	131	1700	200	40	227	230.45	38	5	40
36	38	135	7	40	131	133	2360	105	80	230.45	233	41	10	40
38	40	175	20	40	133	135	2440	37	90	233	235	46	5	40
40	42	580	100	40	135	137	1230	200	40	235	237.75	80	5	40
42	44	475	55	40	137	139	830	145	40	237.75	240	40	5	40
44	46	500	70	40	139	1419	1330	245	40	240	242	57	6	40
46	48	345	75	40	1419	143	1400	150	40	242	244	40	5	40
48	50	240	22	40	143	145	860	145	40	244	246	175	6	40
50	52	86	15	40	145	147	1100	155	40	246	248	40	5	40
52	54	310	38	40	147	147.75	310	140	40	248	250	70	5	40
54	55.8	286	15	40	147.75	150	425	190	40	250	252	54	10	40
55.8	58	645	48	40	150	152	220	48	40	252	254	250	5	40
58	60	340	52	40	152	154	175	25	40	254	256	47	5	40
60	62	470	45	40	154	156	150	140	40	256	258	27	5	40
62	64	3200	255	40	156	158	210	40	40	258	259.5	42	5	40
64	66	1080	105	40	158	160	135	84	40	259.5	260.5	2750	5	40
66	67	710	66	40	160	162	350	160	40	260.5	262.5	235	5	40
67	69	1300	46	40	162	164	190	38	40	262.5	264	37	5	40
69	71	1850	57	40	164	166	185	125	40	264	266	120	5	40
71	73	190	108	40	166	168	205	135	40	266	268	65	5	40
73	75	2300	8	40	168	170	430	85	40	268	270	215	5	40
75	77	2070	15	40	170	172	180	95	40	270	272	110	5	40
77	79	490	22	40	172	174	580	170	40	272	274	830	5	40
79	81	330	40	40	174	176	142	68	40	274	276.1	250	7	40
81	83	240	33	40	176	178	305	112	40	276.1	279.15	15	5	40
83	85	82	8	40	178	180	470	34	40	279.15	281	6	5	40
85	86.5	112	9	40	180	182	210	39	40	281	283	9	5	40
86.5	88	76	7	40	182	184	45	90	40	283	285	32	34	40
88	90	120	5	40	184	186	43	5	40	285	287	9	5	40
90	92	340	40	40	186	188	32	5	40	287	289	18	5	40
92	94	2100	5	4000	188	190	39	5	40	289	291	31	5	40
94	96	460	5	40	190	192.2	50	50	40	291	294	15	5	40
96	98	175	5	40	192.2	193.2	30	5	40					

Table C.17 Data of borehole 17 from MTA 2006.

From (m)	To (m)	Cu (ppm)	Mo (ppm)	Au (ppm)	From (m)	To (m)	Cu (ppm)	Mo (ppm)	Au (ppm)	From (m)	To (m)	Cu (ppm)	Mo (ppm)	Au (ppm)
0	3	98	9	40	86	88	65	5	40	169	171	175	12	40
3	5	70	10	40	88	90	62	8	40	171	173	193	14	40
5	6	74	10	40	90	92	195	20	40	173	175	170	12	40
6	8	83	14	40	92	94	132	14	40	175	177	53	12	40
8	10	69	15	40	94	96	143	5	40	177	179	133	19	40
10	12	63	10	40	96	98	184	21	40	179	181	122	12	40
12	14	60	7	14000	98	100	460	194	40	181	182	140	6	40
14	16	56	5	100	100	102	1020	300	40	182	184	56	5	40
16	18	46	96	40	102	104	102	10	40	184	186	78	9	40
18	20	68	11	40	104	106	41	6	40	186	188	60	25	40
20	22	503	12	40	106	108	36	5	40	188	190	55	11	40
22	24	33	15	40	108	110	42	6	40	190	192	71	17	40
24	26	44	14	40	110	112	53	5	40	192	193.75	185	8	40
26	28	26	6	40	112	114	23	14	40	193.75	195	95	5	40
28	30	100	13	40	114	116	35	5	40	195	197	38	18	40
30	32	43	22	40	116	118	62	5	40	197	199	19	275	40
32	34	76	8	40	118	120	36	5	40	199	201	132	75	40
34	36	69	13	40	120	122	15	5	40	201	203	68	93	40
36	38	86	12	40	122	124	21	5	40	203	205	50	11	40
38	40	28	8	40	124	126	63	5	40	205	207	43	5	40
40	42	204	11	40	126	128	48	5	40	207	209	37	5	40
42	44	65	34	360	128	130	20	5	40	209	211	14	7	40
44	46	57	7	40	130	132	210	5	40	211	213	107	6	40
46	48	314	10	40	132	134	205	5	40	213	215	251	5	40
48	50	95	7	40	134	136	475	7	40	215	217	64	5	40
50	52	62	25	40	136	138	130	9	40	217	219	53	5	40
52	54	109	30	40	138	140	102	5	40	219	221	61	5	40
54	56	65	5	40	140	141.5	78	8	40	221	223	104	5	40
56	58	66	5	40	141.5	143	130	5	40	223	224.5	22	5	40
58	60	38	5	40	143	145	115	7	40	224.5	226	15	5	40
60	62	36	5	40	145	147	95	5	40	226	228	25	38	40
62	64	27	10	40	147	149	690	5	40	228	230	30	5	40
64	66	51	5	40	149	150.05	1000	5	40	230	231.1	32	5	40
66	68	47	5	40	150.05	152	55	5	40	231.1	233	31	5	40
68	70	33	5	40	152	154	44	5	40	233	235	30	5	40
70	72	131	5	40	154	156	90	9	40	235	237	26	5	40
72	74	49	5	40	156	158	70	5	40	237	239	28	5	40
74	76	75	6	40	158	160	50	155	40	239	242	11	5	40
76	78	55	5	40	160	162	230	14	40	242	245	59	5	40

Table C.17(Continue) Data of borehole 17 for Cu-Mo-Au from MTA 2006.

78	80	34	5	40	162	164	205	25	40	245	248	37	5	40
80	82	13	5	40	164	166	150	24	40	248	251.7	152	5	40
82	84	77	5	40	166	167.05	24	5	40					
84	86	57	5	40	167.05	169	210	11	40					

Table C.18 Data of borehole 18 from MTA 2006.

From (m)	To (m)	Cu (ppm)	Mo (ppm)	Au (ppm)	From (m)	To (m)	Cu (ppm)	Mo (ppm)	Au (ppm)	From (m)	To (m)	Cu (ppm)	Mo (ppm)	Au (ppm)
0	1	51	5	40	76	78	66	5	40	153	155	8	5	40
1	3	37	5	40	78	80	120	5	40	155	156	65	5	40
3	6	104	7	40	80	82	137	5	40	156	158	124	5	40
6	7	135	10	40	82	84	64	5	40	158	158.85	43	55	40
7	9	81	6	40	84	86	172	5	40	158.85	160	13	30	40
9	11	83	6	40	86	88	77	5	40	160	161	23	8	40
11	13	71	5	40	88	90	49	5	40	161	161.4	80	5	40
13	15	96	10	40	90	92	164	5	40	161.4	163	19	13	40
15	17	49	6	40	92	94	134	5	40	163	165	23	32	40
17	19	116	5	40	94	96	131	5	40	165	167	28	14	40
19	21	69	5	40	96	98	121	5	40	167	168.75	82	5	40
21	23	177	15	40	98	100	33	5	40	168.75	170.75	48	5	40
23	25	53	5	40	100	102	16	5	40	170.75	172	12	5	40
25	27	33	5	40	102	104	17	5	40	172	172.5	81	5	40
27	29	55	5	40	104	106	10	10	40	172.5	174	11	5	40
29	31	64	5	40	106	108	14	5	40	174	176	8	5	40
31	33	1850	150	40	108	110	19	5	40	176	178	11	5	40
33	34	201	14	40	110	112	12	5	40	178	179.25	17	7	40
34	36	31	5	40	112	114	11	5	40	179.25	179.75	6	18100	40
36	38	12	5	40	114	116	8	5	40	179.75	181	7	54	40
38	40	51	5	40	116	118	8	5	40	181	182.5	9	7	40
40	42	15	5	40	118	120	6	5	40	182.5	182.5			40
42	44	121	11	40	120	122	12	5	40	182.5	184	8	132	40
44	46	71	10	40	122	124	7	5	40	184	186	10	27	40
46	48	65	5	40	124	126	7	5	40	186	188	16	12	40
48	50	14	5	40	126	128	7	5	40	188	190	14	6	40
50	52	11	58	40	128	130	7	5	40	190	192	14	38	40
52	54	8	5	40	130	132	12	6	40	192	194	10	44	40
54	56	83	6	40	132	134	11	29	40	194	197	14	5	40
56	58	18	6	40	134	136	35	185	40	197	200	9	10	40
58	60	26	5	40	136	138	12	8	40	200	203	9	22	40

Table C.18(Continue) Data of borehole 18 for Cu-Mo-Au from MTA 2006.

60	62	21	8	40	138	140	126	20	40	203	206	11	5	40
62	64	30	5	40	140	142	37	16	40	206	209	9	75	40
64	66	63	6	40	142	144	13	10	40	209	212	20	10	40
66	68	101	270	40	144	145.85	88	25	40	212	214	50	5	40
68	70	83	41	40	145.85	146.6	11	71	40	214	216.3	15	5	40
70	72	19	6	40	146.6	148.85	12	5	40	216.3	217.55	12	5	40
72	74	67	6	40	148.85	150.5	8	5	40					
74	76	185	5	40	150.5	153	9	5	40					

Table C.19 Data of borehole 19 from MTA 2006.

From (m)	To (m)	Cu (ppm)	Mo (ppm)	Au (ppm)	From (m)	To (m)	Cu (ppm)	Mo (ppm)	Au (ppm)	From (m)	To (m)	Cu (ppm)	Mo (ppm)	Au (ppm)
0	3	53	11	40	108	110	220	12	40	214	216	301	11	40
3	5	63	16	40	110	112	384	10	40	216	218	187	30	40
5	7	85	15	40	112	114	148	10	40	218	220	62	5	40
7	9	80	7	40	114	116	217	23	40	220	222	109	7	40
9	10.65	442	5	40	116	118	1556	14	40	222	224	84	14	40
10.65	12	214	31	40	118	120	615	14	40	224	226	67	5	40
12	14	136	27	40	120	122	153	29	40	226	228	91	5	40
14	16	126	25	40	122	124	161	14	40	228	230	85	7	40
16	18	81	24	40	124	126	122	16	40	230	232	58	9	40
18	20	117	25	40	126	128	110	13	40	232	234	64	8	40
20	22	236	34	40	128	130	215	8	40	234	236	47	5	40
22	24	254	64	40	130	132	326	25	40	236	238	64	5	40
24	26	577	32	40	132	134	190	15	40	238	240	58	5	40
26	28	374	23	40	134	136	187	5	40	240	242	283	30	40
28	30	149	38	40	136	138	242	19	40	242	244	205	40	40
30	32	116	39	40	138	140	183	5	40	244	246	270	30	40
32	34	95	78	40	140	142	130	8	40	246	248	160	42	40
34	36	84	17	40	142	144	133	12	40	248	250	185	15	40
36	38	31	5	40	144	146	99	5	40	250	252	135	9	40
38	40	100	15	40	146	148	107	5	40	252	254	108	13	40
40	42	80	5	40	148	150	201	5	40	254	255	39	102	40
42	44	68	6	40	150	152	43	5	40	255	258	250	75	40
44	46	365	294	40	152	154	82	5	40	258	260.75	165	28	40
46	48	118	54	40	154	156	90	7	40	260.75	263	21	600	40
48	50	356	91	40	156	158	130	13	40	263	265	61	14	40
50	52	438	35	40	158	160	104	9	40	265	267	322	102	40
52	54	185	13	40	160	162	205	7	40	267	269	32	28	40

Table C.19(Continue) Data of borehole 19 for Cu-Mo-Au from MTA 2006.

54	56	277	11	40	162	164	53	6	40	269	271	46	18	40
56	58	226	15	40	164	166	243	5	40	271	273	36	9	40
58	60	207	35	40	166	168	208	5	50	273	275	810	113	40
60	62	202	14	40	168	170	222	21	50	275	277	463	20	40
62	64	291	15	40	170	172	230	5	100	277	279	62	50	40
64	66	117	21	40	172	174.24	134	5	40	279	281	34	28	40
66	68	185	19	40	174.24	176	61	16	40	281	283	116	23	40
68	70	780	20	40	176	178	47	6	40	283	285	1093	140	40
70	72	204	13	40	178	180	37	5	40	285	287	83	21	40
72	74	224	15	40	180	181.5	30	5	40	287	289	36	34	40
74	76	164	9	40	181.5	183.5	44	5	40	289	291	99	80	40
76	78	666	63	40	183.5	185	84	10	40	291	293	113	12	40
78	80	182	22	40	185	187	63	20	40	293	300	77	15	40
80	82	275	19	40	187	189	111	6	40	300	302	25	5	40
82	84	183	21	40	189	191	103	6	40	302	303	10	5	40
84	86	95	24	40	191	193	206	9	40	303	304.1	530	5	40
86	88	183	52	40	193	195	86	6	40	304.1	306	20	5	40
88	90	159	28	40	195	197	77	5	40	306	307	45	5	40
90	92	181	23	40	197	199	65	5	40	307	309	8	12	40
92	94	174	25	40	199	201	68	8	60	309	311	6	5	40
94	96	525	40	40	201	203	146	5	40	311	313	19	5	40
96	98	147	13	40	203	205	186	32	40	313	315	11	5	40
98	100	430	22	40	205	206	124	92	40	315	317	13	5	40
100	102	211	22	40	206	208	41	5	40	317	319	17	5	40
102	104	276	28	40	208	210	27	5	40	319	321.75	13	5	40
104	106	408	11	40	210	212	102	75	40					
106	108	13	13	40	212	214	126	15	40					

Table C.20 Data of borehole 20 from MTA 2006.

From (m)	To (m)	Cu (ppm)	Mo (ppm)	Au (ppm)	From (m)	To (m)	Cu (ppm)	Mo (ppm)	Au (ppm)	From (m)	To (m)	Cu (ppm)	Mo (ppm)	Au (ppm)
0	2	2080	57	40	74	76	200	5	40	146	148	283	36	40
2	4	2480	125	40	76	78	600	8	40	148	150	260	12	40
4	6	2460	17	40	78	80	830	5	40	150	153	120	12	40
6	8	2840	39	40	80	82	1640	5	40	153	156	160	8	40
8	10	3400	270	70	82	84	1360	5	40	156	159	168	38	40
10	12	6280	668	100	84	86	1320	23	40	159	162	74	5	40
12	14	6980	400	100	86	88	1460	26	40	162	166	132	6	40
14	16	6520	160	110	88	90	2180	5	40	166	168	180	8	40
16	18	9420	420	60	90	92	1540	5	40	168	171	214	5	40
18	20	5500	550	100	92	94	1420	43	40	171	174	177	9	40
20	22	6260	700	50	94	96	660	230	40	174	180.5	435	10	40

Table C.20(Continue) Data of borehole 20 for Cu-Mo-Au from MTA 2006.

22	24	18600	280	150	96	98	1460	14	40	180.5	183	120	25	40
24	26	5780	450	40	98	100	570	18	40	183	186	80	6	40
26	28	6120	530	40	100	100.9	116	36	40	186	189.4	265	7	40
28	30	4520	180	60	100.9	103	700	15	40	189.4	193.5	77	12	40
30	32	4740	560	230	103	104.25	238	38	40	193.5	197	108	5	40
32	34	3000	450	40	104.25	106	7	5	40	197	200	100	5	40
34	36	17120	153	300	106	108	7	5	40	200	203	47	5	40
36	38	10600	85	90	108	110	7	22	40	203	206	90	20	40
38	40	12800	400	130	110	110.5	57	5	40	206	209	155	10	40
40	42	2280	78	40	110.5	112	430	6	40	209	211	95	11	40
42	44	150	20	40	112	114	680	5	40	211	212.25	600	12	40
44	46	147	15	40	114	116	720	8	40	212.25	215	30	5	40
46	47.75	167	10	40	116	118	665	10	40	215	218	20	5	40
47.75	50.3	95	5	40	118	120	1000	15	40	218	221	10	5	40
50.3	52	318	95	40	120	122	940	9	40	221	224	23	5	40
52	54	237	47	40	122	124	485	6	40	224	227	10	5	40
54	56	285	38	40	124	126	840	16	40	227	230	27	5	40
56	58	350	43	40	126	127.25	310	33	40	230	233	16	5	40
58	60	60	5	40	127.25	129	530	17	40	233	236	50	5	40
60	62	113	37	40	129	130	300	30	40	236	239	22	5	40
62	63.5	240	97	40	130	132	1680	19	40	239	242	22	5	40
63.5	65	785	28	40	132	134	740	72	40	242	245	18	5	40
65	66.9	435	5	40	134	136	270	30	40	245	248	30	5	40
66.9	67.5	105	5	40	136	138	227	18	40	248	250.75	9	5	40
67.5	69.5	90	27	40	138	140	355	13	40	250.75	251.75	5	5	40
69.5	70.5	128	9	40	140	142	190	11	40	251.75	254	20	5	40
70.5	72.5	250	5	40	142	144	230	78	40	254	257	7	5	40
72.5	74	7	5	40	144	146	255	10	40	257	260.1	6	5	40

Table C.21 Data of borehole 21 from MTA 2006.

From (m)	To (m)	Cu (ppm)	Mo (ppm)	Au (ppm)	From (m)	To (m)	Cu (ppm)	Mo (ppm)	Au (ppm)	From (m)	To (m)	Cu (ppm)	Mo (ppm)	Au (ppm)
0	2	113	9	40	76	78	106	38	40	156	158	198	8	40
2	4	97	10	40	78	80	191	9	40	158	160	680	29	40
4	5.5	111	8	40	80	82	33	5	40	160	162	105	115	40
5.5	7	64	5	40	82	84	75	6	40	162	164	56	50	40
7	9	77	10	40	84	85	44	5	40	164	166	70	65	40
9	11	92	14	40	85	87	77	16	40	166	167.2	53	8	40
11	13	112	5	40	87	89	100	11	40	167	170	145	94	40

Table C.21(Continue) Data of borehole 21 for Cu-Mo-Au from MTA 2006.

13	15	110	11	40	89	91	155	15	40	170	172	155	5	40
15	17	238	11	40	91	93.3	430	23	40	172	172.5	480	5	40
17	19	115	10	40	93.3	95	103	9	40	172.5	173.5	48	5	40
19	21	92	10	40	95	97	97	19	40	173.5	175	520	5	40
21	23	86	8	40	97	99	106	16	40	175	177	2050	95	40
23	25	103	11	40	99	101	125	10	40	177	179	5300	1300	40
25	27	75	6	40	101	103	78	58	40	179	181	67000	510	40
27	29	71	9	40	103	105	280	11	40	181	182	48000	985	40
29	31	95	16	40	105	107	380	11	40	182	184	2500	330	40
31	33	59	12	40	107	109	37	20	40	184	185.5	630	52	40
33	35	56	7	40	109	111	117	10	40	185.5	187	46	5	40
35	37	94	12	40	111	113.15	63	15	40	187	189	25	5	40
37	39	167	5	40	113.15	115	79	6	40	189	191	41	5	40
39	41	114	5	40	115	117	126	7	40	191	193	31	5	40
41	43	138	18	40	117	119	45	16	40	193	196	100	5	40
43	45	27	13	40	119	121	124	7	40	196	199	31	5	40
45	47	39	9	40	121	123	100	29	40	199	202	552	5	40
47	49	28	22	40	123	125	70	5	40	202	204	16	5	40
49	51	28	5	40	125	127	37	5	40	204	206	1800	5	40
51	53	74	6	40	127	128	58	5	40	206	208	230	24	40
53	55	35	13	40	128	130	45	93	40	208	210	215	14	40
55	57	93	6	40	130	132	110	15	40	210	212	496	5	40
57	57.9	106	5	40	132	134.2	90	10	40	212	214	295	550	40
57.9	28.95	107	5	40	134.2	136	41	5	40	214	216	330	40	40
28.95	59.5	88	68	40	136	138	84	12	40	216	218	160	67	40
59.5	60.75	88	45	40	138	140	43	7	40	218	220	215	18	40
60.75	62.75	61	48	40	140	142	215	16	40	220	223	390	66	40
62.75	64.5	60	5	40	142	144	92	12	40	223	226	11	5	40
64.5	66.5	100	28	40	144	146	430	5	40	226	229	9	5	40
66.5	68.5	153	15	40	146	148	53	8	40	229	232	9	5	40
68.5	70	134	32	40	148	150	61	8	40	232	235	10	5	40
70	72	84	18	40	150	152	150	22	40	235	238	8	5	40
72	74	86	28	40	152	154	90	15	40	238	241	7	5	40
74	76	90	11	40	154	156	78	12	40	241	242.75	8	5	40

Table C.22 Data of borehole 22 from MTA 2006.

From (m)	To (m)	Cu (ppm)	Mo (ppm)	Au (ppm)	From (m)	To (m)	Cu (ppm)	Mo (ppm)	Au (ppm)	From (m)	To (m)	Cu (ppm)	Mo (ppm)	Au (ppm)
0	4	252	5	40	100	102	2593	82	30	233	236	239	21	40
4	6	201	9	40	102	104	1820	46	40	236	239	114	21	40
6	8	89	5	40	104	106	1200	74	70	239	242	114	21	40
8	10	92	5	40	106	108	1858	72	40	242	245	58	21	40
10	12	119	5	40	108	110	1250	142	40	245	248	67	21	40
12	14	279	5	40	110	112	1920	144	40	248	251	80	21	40
14	16	144	7	120	112	114	2824	135	60	251	254	52	21	40
16	18	294	5	40	114	116	6400	100	100	254	257	70	21	40
18	20	138	12	40	116	118	1500	113	40	257	260	50	21	40
20	22	182	10	40	118	119.5	410	20	40	260	263	53	21	40
22	24	191	7	120	119.5	122	619	46	40	263	266	57	21	40
24	26	304	5	40	122	124	825	12	40	266	269	43	21	40
26	28	242	5	40	124	125	1741	23	40	269	272	88	21	40
28	30	533	6	40	125	126	1638	38	40	272	275	149	21	40
30	32	450	6	40	126	128	184	7	80	275	277	29	21	40
32	34	539	6	40	128	130	105	24	40	277	279	11	21	40
34	36	291	6	40	130	133	121	13	70	279	281	78	21	40
36	37	420	16	40	133	136	475	21	40	281	283.5	85	21	40
37	38	1917	5	40	136	139	88	24	40	283.5	285.5	123	21	40
38	40	771	24	40	139	142	91	17	40	285.5	287.5	116	21	40
40	42	867	135	40	142	145	73	51	40	287.5	289.5	101	21	40
42	44	660	8	40	145	148	104	30	40	289.5	291.5	110	21	40
44	46	731	13	40	148	151	71	8	40	291.5	293.5	123	21	40
46	48	1180	27	40	151	154	114	12	40	293.5	294.1	1122	21	40
48	50	1310	43	40	154	157	78	9	40	294.1	296	47	21	40
50	52	2519	26	40	157	160	38	5	40	296	298	340	21	40
52	54	1580	26	40	160	163	69	5	40	298	300	51	21	40
54	56	665	145	40	163	166	138	5	40	300	302	131	21	40
56	58	524	1951	40	166	169	38	33	40	302	304	83	21	40
58	6	1146	712	40	169	172	95	5	40	304	306	326	21	40
6	62	698	153	40	172	175	146	25	40	306	308	435	21	40
62	64	723	43	40	175	178	172	24	40	308	310	102	21	40
64	66	600	38	40	178	181	414	6	40	310	312	173	21	40
66	68	570	51	40	181	184	580	5	40	312	314	475	21	40
68	70	372	17	40	184	187	108	5	40	314	316	151	21	40
70	72	4096	12	40	187	190	225	5	40	316	318	237	21	40
72	72.5	1004	6	40	190	193	110	21	40	318	320	395	21	40
72.5	73.2	17	5	40	193	196	80	21	40	320	324.6	6	21	40
73.2	75	2282	46	40	196	199	79	21	40	324.6	328.15	59	21	40
75	77	2181	49	40	199	202	73	21	40	328.15	330	19	21	40

Table C.22(Continue) Data of borehole 22 for Cu-Mo-Au from MTA 2006.

77	79	1093	37	40	202	205	132	21	40	330	333	14	21	40
79	81	1930	24	40	205	208	275	21	40	333	336	9	5	40
81	83	680	17	40	208	211	119	21	40	336	339	13	21	40
83	85	589	34	40	211	214	144	21	40	339	342	9	21	40
85	87	1613	330	40	214	217	172	21	40	342	345	26	33	40
87	89	1858	36	40	217	220	712	21	40	345	348	16	6	40
89	91	1300	60	40	220	223	102	21	40	348	351	8	26	40
91	93	950	32	40	223	226	83	21	40	351	354	17	24	40
93	95	1253	79	40	226	227	169	21	40	354	357	11	66	40
95	95.8	1217	970	40	227	228	591	21	40	357	360	6	5	40
95.8	96.8	2010	43	40	228	230.4	62	21	40	360	363	5	5	40
96.8	98	1638	506	40	230.4	231	19	21	40	363	367.8	5	5	40
98	100	2000	440	40	231	233	118	21	40					

Table C.23 Data of borehole 23 from MTA 2006.

From (m)	To (m)	Cu (ppm)	Mo (ppm)	Au (ppm)	From (m)	To (m)	Cu (ppm)	Mo (ppm)	Au (ppm)	From (m)	To (m)	Cu (ppm)	Mo (ppm)	Au (ppm)
0	2	3200	6	40	76	78	42	5	40	152	154	65	5	40
2	4	3100	8	40	78	80	130	90	40	154	156	62	5	40
4	6	4700	35	40	80	82	220	800	40	156	158	62	8	40
6	8	5360	13	40	82	84	88	10	40	158	160	250	8	40
8	10	4500	8	4	84	86	43	5	40	160	162	145	7	40
10	12	3350	60	40	86	88	120	10	40	162	164	64	10	40
12	14	1200	20	50	88	90	136	5	40	164	166	77	15	40
14	16	1270	9	40	90	92	370	5	40	166	168	100	8	40
16	18	550	9	40	92	94	800	5	40	168	170	66	19	40
18	20	2500	13	40	94	96	70	90	40	170	172	65	5	40
20	22	650	9	40	96	98	185	20	40	172	174	630	5	40
22	24	190	11	40	98	100	45	6	40	174	176	82	5	40
24	26	800	13	40	100	102	40	210	40	176	178	67	8	40
26	28	360	5	40	102	104	12	5	40	178	180	4000	5	40
28	30	2600	7	40	104	106	68	5	40	180	182	130	5	40
30	32	3150	5	40	106	108	250	5	40	182	184	35	5	40
32	34	6500	10	40	108	110	690	5	40	184	186	280	5	40
34	36	3000	9	40	110	112	240	9	40	186	188	145	5	40
36	38	4150	14	40	112	114	120	9	40	188	190	135	5	40
38	40	3270	10	40	114	116	130	5	40	190	192	68	5	40
40	42	5200	8	40	116	118	150	6	40	192	194	120	8	40
42	44	2350	5	40	118	120	130	18	40	194	196	110	5	40
44	46	6900	5	40	120	122	150	11	40	196	198	190	5	40
46	48	1300	7	40	122	124	180	19	40	198	200	93	5	40

Table C.23(Continue) Data of borehole 23 for Cu-Mo-Au from MTA 2006.

48	50	92	15	40	124	126	70	5	40	200	202	95	5	40
50	52	140	6	40	126	128	140	6	40	202	204	72	5	40
52	54	140	5	40	128	130	78	10	40	204	206	10	5	40
54	56	130	5	40	130	132	110	6	40	206	208	18	5	40
56	58	80	5	40	132	134	95	5	40	208	210	13	5	40
58	60	83	35	40	134	136	130	18	40	210	212	16	5	40
60	62	520	8	40	136	138	210	85	40	212	214	160	5	40
62	64	59	5	40	138	140	130	38	40	214	216	15	5	40
64	66	160	5	40	140	142	65	12	40	216	218	58	5	40
66	68	175	22	40	142	144	50	15	40	218	220	52	5	40
68	70	54	29	40	144	146	100	15	40	220	222	25	5	40
70	72	72	5	40	146	148	96	290	40	222	225	15	5	40
72	74	85	12	40	148	150	48	12	40	225	227	145	6	40
74	76	170	130	40	150	152	47	11	40					

Table C.24 Data of borehole 24 from MTA 2006.

From (m)	To (m)	Cu (ppm)	Mo (ppm)	Au (ppm)	From (m)	To (m)	Cu (ppm)	Mo (ppm)	Au (ppm)	From (m)	To (m)	Cu (ppm)	Mo (ppm)	Au (ppm)
0	4.2	132	7	40	118	121	26	5	40	238	241	58	5	40
4.2	6.2	83	7	40	121	123	36	5	40	241	243.2	63	15	40
6.2	7.25	51	5	40	123	127	63	5	40	243.2	243.8	27	5	40
7.25	8.5	49	6	40	127	129	92	5	40	243.8	247	50	8	40
8.5	10	94	12	40	129	131	104	15	40	247	250	89	16	40
10	14	121	18	40	131	134	67	19	40	250	252	80	8	40
14	16	193	53	40	134	137	79	19	40	252	255	19	5	40
16	18	340	23	40	137	140	76	9	40	255	257	17	5	40
18	20	158	28	40	140	143	120	25	40	257	261	187	9	40
20	22	155	26	40	143	146	106	27	40	261	264	66	5	40
22	24	400	22	40	146	149	42	24	40	264	267	81	5	40
24	26	57	6	40	149	152	84	63	40	267	270	70	5	40
26	28	58	12	40	152	155	70	22	40	270	274	46	5	40
28	30	139	8	40	155	158	85	80	40	274	277	45	5	40
30	32	118	5	40	158	161	170	9	40	277	279	117	5	40
32	34	66	5	40	161	164	84	12	40	279	281	1332	7	40
34	36	69	12	40	164	167	69	9	40	281	283	918	9	40
36	38	47	8	40	167	170	133	73	40	283	285	124	6	40
38	40	105	5	40	170	172	123	6	40	285	287	120	17	40
40	42	88	5	40	172	174	138	7	40	287	290	70	175	40
42	44	22	6	40	174	176	78	27	40	290	293	86	18	40
44	46	121	8	40	176	180.5	80	23	40	293	296	300	40	40
46	47	8	5	40	180.5	182.5	123	25	40	296	299	247	8	40

Table C.24(Continue) Data of borehole 24 for Cu-Mo-Au from MTA 2006.

47	49	44	5	40	182.5	184	157	61	40	299	302	182	100	40
49	52	54	6	40	184	186	152	20	40	302	305	18	5	40
52	55	84	16	40	186	188	200	13	40	305	308	29	5	40
55	58	81	10	40	188	190	401	17	40	308	311	28	230	40
58	61	77	7	40	190	192	526	20	40	311	314	12	80	40
61	64	45	9	40	192	194	504	18	40	314	317	20	5	40
64	67	81	9	40	194	196	481	28	40	317	320	100	8	40
67	70	70	14	40	196	198	370	28	40	320	323	34	37	40
70	73	45	17	40	198	200	265	58	40	323	326	42	5	40
73	76	77	5	40	200	202	810	40	80	326	329	38	6	40
76	79	80	7	40	202	204	672	74	40	329	332	12	5	40
79	82	59	11	40	204	206	1125	31	40	332	335	20	5	40
82	85	46	6	40	206	20	870	24	40	335	338	14	5	40
85	88	100	5	40	20	210	136	230	40	338	341	31	5	40
88	91	48	7	40	210	212	40	6	40	341	344	16	5	40
91	94	60	8	40	212	215	27	18	40	344	347	9	5	40
94	97	44	5	40	215	217	108	19	40	347	350	32	5	40
97	100	47	5	40	217	220	138	17	40	350	354	65	5	40
100	103	30	5	40	220	223	90	14	40	354	358	11	5	40
103	108	107	5	40	223	228	52	11	40	358	362	12	5	40
108	109	37	5	40	228	229	47	25	40	362	366	16	5	40
109	112	30	5	40	229	232	40	5	40	366	370	52	5	40
112	115	35	5	40	232	235	62	13	40	370	373	26	5	40
115	118	24	5	160	235	238	123	11	40					

Table C.25 Data of borehole 25 from MTA 2006.

From (m)	To (m)	Cu (ppm)	Mo (ppm)	Au (ppm)	From (m)	To (m)	Cu (ppm)	Mo (ppm)	Au (ppm)	From (m)	To (m)	Cu (ppm)	Mo (ppm)	Au (ppm)
0	1.8	465	5	40	83	85	16300	1258	120	178	178.55	113	230	40
1.8	4	683	14	40	85	87	11500	500	280	178.55	179	79	22	40
4	6	380	7	40	87	89	14500	135	380	179	181	160	13	40
6	8	380	5	40	89	91	20300	1000	210	181	184	72	23	40
8	10	184	17	40	91	93	18400	910	880	184	187	79	10	40
10	12	496	30	40	93	95	14200	550	380	187	190	78	10	40
12	14	265	54	40	95	97	2300	230	40	190	193.15	66	35	40
14	16	990	45	40	97	99	1720	138	40	193.15	194.35	27	75	40
16	18	615	32	40	99	100	240	6	40	194.35	197	202	11	40
18	20	117	58	40	100	101.65	1000	35	40	197	200	136	7	40
20	22	85	133	40	101.65	103	525	5	40	200	203	48	6	40

Table C.25(Continue) Data of borehole 25 for Cu-Mo-Au from MTA 2006.

22	24	96	64	40	103	105	184	6	40	203	208	130	12	40
24	26	150	80	40	105	104	340	16	40	208	208.75	228	5	40
26	28	272	115	40	104	109.5	378	10	40	208.75	210	91	47	40
28	29.5	358	480	40	109.5	110	6	5	40	210	211	85	76	40
29.5	32	1301	520	40	110	112	158	7	40	211	214	88	15	40
32	34	510	1470	40	112	114	157	32	40	214	217	220	10	40
34	36	490	590	40	114	116.8	205	11	40	217	220	102	5	40
36	38	935	640	40	116.8	117	94	5	40	220	223	135	21	40
38	40.15	1500	600	40	117	118.15	160	6	40	223	225	101	5	40
40.15	42	1030	670	40	118.15	118.65	86	5	40	225	226	88	6	40
42	43.5	1100	610	40	118.65	120	157	20	40	226	227	219	28	40
43.5	45	2480	254	40	120	123	148	8	40	227	228	149	5	40
45	47	1072	90	40	123	126	215	12	40	228	230	197	82	40
47	48	375	20	40	126	129	130	9	40	230	232	705	500	40
48	51	720	15	40	129	131.3	1080	12	40	232	234	600	170	40
51	53	5063	1000	70	131.3	132.2	116	5	40	234	236	153	160	40
53	55	17500	2750	180	132.2	135	445	6	40	236	238	167	480	40
55	57	10500	1500	120	135	138	230	27	40	238	240	111	56	40
57	59	6200	600	110	138	141	142	6	40	240	242	212	300	40
59	61	3354	382	80	141	144	410	14	40	242	244	245	202	40
61	63	13100	1600	410	144	147	201	10	40	244	246	214	291	40
63	65	8700	1610	80	147	150	160	11	40	246	248	225	600	40
65	67	14700	550	80	150	153	115	7	40	250	250	1100	366	40
67	69	15000	600	120	153	156	102	14	40	248	251	485	400	40
69	71	15200	970	270	156	159	204	14	40	251	253	182	300	40
71	73	19800	1643	320	159	162	86	41	40	253	255	247	191	40
73	75	13100	682	140	162	165	150	13	40	255	257	435	286	40
75	77	7900	540	110	165	168	157	29	40	257	259	88	126	40
77	79	10100	150	250	168	171	130	16	40	259	261	107	145	40
79	81	7900	25	100	171	174	112	19	40	261	263	18	18	40
81	83	13700	154	140	174	178	155	57	40	263	265.35	10	5	40

CURRICULUM VITAE

Name Surname: Torkan TAHERI BONAB

Place and Date of Birth: IRAN-ORUMIYEH 16.05.1988

E-Mail: torkan.taheri88@gmail.com

B.Sc.: Iran-Azad University of Orumiyeh, 2006

M.Sc. : Istanbul Technical University Faculty Of Mining Geology Engineering